

# **Prediction and Computation of Phase Equilibria in Polar and Polarizable Mixtures Using Theory-based Equations of State**

by

Nayef Masned Al-Saifi

B.Sc., King Fahd University of Petroleum & Minerals, Saudi Arabia (1999)

M.Sc., King Fahd University of Petroleum & Minerals, Saudi Arabia (2004)

A THESIS SUBMITTED IN PARTIAL FULFILLMENT OF THE  
REQUIREMENTS FOR THE DEGREE OF

DOCTOR OF PHILOSOPHY

in

THE FACULTY OF GRADUATE STUDIES

(Chemical and Biological Engineering)

THE UNIVERSITY OF BRITISH COLUMBIA  
(Vancouver)

November 2011

© Nayef Masned Al-Saifi, 2011

## ABSTRACT

The purpose of this dissertation is to contribute to the development of the predictive theory-based equation of state. The specific objectives are threefold: first, to improve the predictive capability of theory-based EOS in studying multiphase equilibrium in water-alcohol-hydrocarbon mixtures by taking into account long-ranged electrostatic interactions. The second objective is to develop a general treatment of polar-polarizable mixtures for any theory-based equation of state; and the third is to develop robust and reliable computational methods that conduct and simplify multiphase and stability calculations for theory-based equations of state.

The long-ranged electrostatic interactions considered in this thesis are dipole-dipole, quadrupole-quadrupole and polarization. The electrostatic interactions are incorporated into the statistical association fluid theory (SAFT) using different polar approaches. The polar SAFT is utilized to predict multiphase equilibrium of water-alcohol-hydrocarbon mixtures. The results are compared to experimental data. Excellent prediction of multiphase equilibrium is obtained without adjusting experimental data including difficult mixtures such as water-hydrocarbons.

This dissertation also presents a general treatment of polar-polarizable systems for theory-based equation of state for non-spherical molecules by the use of the self-consistent mean field theory proposed originally by Carnie and Patey (1982). The treatment is applicable for any kind of polarization arising from polar molecules including ions induced interactions. The theory is tested against simulation data and is applied to the statistical association fluid theory. The general theory is compared to simulation data and is shown to give excellent agreement.

The developments in this dissertation also contribute to the subject of theory-based equations of state by developing a reliable and robust multiphase and stability testing method. The developed algorithm computes multiphase and stability simultaneously. The new algorithm is tested extensively on complex mixtures including water-hydrocarbon mixtures. Furthermore, the calculations of phase equilibrium from theory-based equations of state are significantly simplified by the use of the complex-step derivative approximation which computes derivatives numerically.

# Table of Contents

ABSTRACT.....	ii
LIST OF TABLES .....	vii
LIST OF FIGURES .....	ix
NOMENCLATURE .....	xiv
ACKNOWLEDGEMENTS.....	xvi
DEDICATION.....	xvii
CHAPTER 1 INTRODUCTION .....	1
1.1 Motivation .....	1
1.2 Theory-based equations of state.....	3
1.3 Research objectives .....	4
1.3.1 System of interest.....	4
1.3.2 Model development objectives .....	5
1.3.3 Computational objectives.....	6
1.4 Thesis organization .....	7
CHAPTER 2 STATISTICAL ASSOCIATION FLUID THEORY .....	8
2.1 Introduction .....	8
2.2 Association effect on fluid behavior .....	10
2.3 Molecular shape in SAFT .....	11
2.4 SAFT interactions and parameters .....	12
2.5 SAFT terms derived from Wertheim’s theory .....	13
2.5.1 Association term .....	13
2.5.2 Chain term.....	19
2.6 SAFT versions.....	19
2.6.1 CK-SAFT .....	19
2.6.2 Simplified SAFT.....	21
2.6.3 Perturbed-Chain SAFT .....	21
2.7 Conclusions.....	22
CHAPTER 3 PREDICTION OF VAPOR-LIQUID EQUILIBRIUM IN WATER- ALCOHOL-HYDROCARBON SYSTEMS .....	23
3.1 Introduction .....	23
3.2 Survey of the dipole-dipole interactions in SAFT .....	24
3.3 Dipolar terms.....	27
3.3.1 Jog and Chapman’s dipolar term (JC) .....	27

3.3.2	Gross and Vrabec's dipolar term .....	28
3.3.3	Economou's term .....	29
3.4	Model parameter estimation.....	29
3.5	Results .....	31
3.5.1	Pure parameter values .....	31
3.5.2	Dipole-dipole contribution.....	35
3.5.3	Prediction of VLE for binary systems .....	36
3.5.3.1	Alcohol-hydrocarbon systems.....	36
3.5.3.2	Alcohol-alcohol systems.....	46
3.5.3.3	Water-alcohol and water-hydrocarbon systems.....	52
3.6	Discussion .....	57
3.7	Conclusions .....	58
<b>CHAPTER 4 MULTIPHASE EQUILIBRIUM AND SIMULTANEOUS TESTING OF PHASE STABILITY .....</b>		<b>59</b>
4.1	Introduction .....	59
4.2	Multiphase equilibrium calculations .....	60
4.2.1	The Gibbs energy minimization method.....	60
4.2.2	Equation-solving technique .....	61
4.3	Challenge of the multiphase equilibrium calculations .....	62
4.4	Gupta et al.'s method .....	62
4.4.1	Governing equations of the Gupta et al. method .....	62
4.4.2	Gupta et al. algorithm .....	64
4.5	The proposed algorithm .....	65
4.6	Evaluation of the proposed algorithm .....	67
4.6.1	Water/octane/hexane/pentane/butane/propane mixture .....	67
4.6.1.1	One phase region (vapour only).....	68
4.6.1.2	Incipient hydrocarbon-rich liquid and vapour-liquid phase region.....	70
4.6.1.3	Incipient water-rich liquid and vapour-liquid-liquid phase region.....	73
4.6.1.4	Liquid-liquid phase.....	75
4.6.2	Ethylene glycol/water/propane/methane.....	77
4.6.3	Ethylene glycol/ water/hexane/propane/CO <sub>2</sub> /methane .....	79
4.6.4	Water-hydrocarbon and other systems.....	81
4.7	Conclusions .....	82
<b>CHAPTER 5 EVALUATING THE PREDICTIVE CAPABILITY OF POLAR AND POLARIZABLE SAFT TO MULTIPHASE SYSTEMS.....</b>		<b>83</b>
5.1	Introduction .....	83
5.2	Polar and polarizable terms .....	84

5.2.1	Quadrupole-quadrupole term .....	84
5.2.2	The renormalized perturbation theory .....	85
5.3	Model parameter estimation.....	86
5.4	The role of induced dipole-dipole and quadrupole-quadrupole interactions in VLE .....	88
5.5	Liquid-liquid equilibrium systems .....	89
5.5.1	Alcohol-hydrocarbon mixtures .....	89
5.5.1.1	Prediction of dipolar simplified SAFT.....	95
5.5.2	Water-hydrocarbon mixtures .....	99
5.6	Vapour-liquid-liquid equilibrium systems .....	103
5.6.1	Water-ethylene glycol-hydrocarbon mixtures .....	103
5.7	Conclusions .....	105
<b>CHAPTER 6 ACCURATE PHASE EQUILIBRIUM CALCULATION WITHOUT ANALYTICAL DERIVATIVES .....</b>		<b>106</b>
6.1	Introduction .....	106
6.2	Complex-step derivative approximation .....	108
6.3	Evaluation of simplex-step derivatives in phase equilibrium calculations .....	109
6.3.1	Binary system.....	109
6.3.2	Hydrocarbon mixture .....	111
6.4	Conclusions .....	113
<b>CHAPTER 7 A GENERAL TREATMENT OF POLAR-POLARIZABLE SYSTEMS FOR AN EQUATION OF STATE.....</b>		<b>114</b>
7.1	Introduction .....	114
7.2	Self-consistent mean field theory.....	115
7.3	The free energy of the SCMF.....	117
7.4	Extension of SCMF to mixtures.....	118
7.5	Extension of the scalar dependent functions .....	121
7.6	Comparison with molecular simulation data.....	122
7.6.1	Comparison with phase coexistence simulation data.....	122
7.6.2	Comparison with energy and effective dipole moment .....	128
7.7	Application to real systems .....	130
7.8	Conclusions .....	132
<b>CHAPTER 8 CONCLUSIONS AND RECOMMENDATIONS .....</b>		<b>133</b>
8.1	Conclusions .....	133
8.2	Recommendations for future work.....	136

REFERENCES .....	138
APPENDIX A ADJUSTABLE PARAMETERS OF PC-SAFT .....	153
APPENDIX B PHASE EQUILIBRIUM CALCULATIONS .....	154

## List of Tables

Table 2.1	Comparison between van der Waals and associating interactions. ....	10
Table 2.2	Summary of some theories that describe the non-idealities of associating system. ....	16
Table 3.1	Estimated parameters for pure fluids. ....	33
Table 3.2	Predicted VLE results for alcohol-hydrocarbon systems by the PC-SAFT-JC and PC-SAFT- GV. ....	37
Table 3.3	Predicted VLE results for methanol containing systems by PC-SAFT-JC, PC-SAFT-GV and PC-SAFT-KSE. ....	43
Table 3.4	Predicted VLE results for short chain alcohol-alcohol system by PC-SAFT-JC, PC-SAFT-GV, PC-SAFT-KSE and non-polar SAFT. ....	48
Table 3.5	Predicted VLE results for alcohol-alcohol system by PC-SAFT-JC, PC-SAFT-GV and PC-SAFT-KSE. ....	49
Table 3.6	Predicted VLE results for water-alcohol system by PC-SAFT-JC. ....	54
Table 4.1	State of Phase k in equations 4-8 and 4-9. ....	64
Table 4.2	Phase fractions and stability variables of Water-Paraffin mixture at 24.1 bar. ....	71
Table 4.3	Equilibrium phase composition (mole fraction) of methane-propane-water-ethylene glycol system. ....	78
Table 4.4	Equilibrium phase composition (mole fraction) for ethylene glycol-water-hexane-propane-carbon dioxide-methane. ....	81
Table 5.1	Pure parameter values. ....	87
Table 5.2	Water-ethylene glycol-hydrocarbon mixtures. ....	103

Table 5.3	Predicted mole fractions of ethylene glycol-water-methylcyclohexane-methane by PC-SAFT-JC2, PC-SAFT-JC1, PC-SAFT-GV and PR.....	104
Table 6.1	Examples of molecular models.....	107
Table 6.2	Maximum relative error of pressure and vapour mole fractions. ....	110
Table 6.3	Calculated Pressure at 149.45 °C and $x_{\text{ethanol}}=0.69$ with the change of step size. .....	111
Table 6.4	A comparison between the calculated mole fractions obtained by numerical and analytical derivatives. ....	112
Table A.1	PC-SAFT Parameters.....	153

## List of Figures

Figure 2.1	General frame of perturbation theory.....	8
Figure 2.2	Molecular shape in SAFT. ....	11
Figure 2.3	Representation of SAFT molecules for a) Alkane b) Alcohol c) Acids.....	12
Figure 2.4	Procedure to form a molecule in SAFT (adapted from Prausnitz et al. (1999)) .....	12
Figure 3.1	A schematic representation of molecular approach and segment approach.....	25
Figure 3.2	Reduced Chemical potential of 1-propanol at 250 K and 450 K from the dipolar PC-SAFT for a) repulsion contribution, b) hydrogen bonding contribution, c) dispersion contribution and d) dipole-dipole contribution. ....	35
Figure 3.3	Predicted results of vapor-liquid equilibrium ( $k_{ij} = 0$ ) by the PC-SAFT-JC, PC-SAFT-GV and PC-SAFT-KSE for the ethanol (1)/octane (2) system at 40 °C, 65 °C and 75 °C. ....	41
Figure 3.4	Predicted results of vapor-liquid equilibrium ( $k_{ij} = 0$ ) by the PC-SAFT-JC and PC-SAFT-GV for the 1-propanol(1)/hexane (2) system at 25 °C, 60 °C, 65 °C and 75 °C .....	41
Figure 3.5	Predicted results of vapor-liquid equilibrium ( $k_{ij} = 0$ ) by the PC-SAFT-JC, PC-SAFT-GV and PC-SAFT-KSE for the ethanol (1)/pentane (2) system at 30 °C, 50 °C, 99.55 °C, 124.55 °C, 149.45 °C and 192.25 °C. ....	42
Figure 3.6	Predicted results of vapor-liquid equilibrium ( $k_{ij} = 0$ ) by the PC-SAFT-JC, PC-SAFT-GV and PC-SAFT-KSE for the 2-propanol (1)/heptane (2) system at 30 °C, 45 °C, and 60 °C .....	44
Figure 3.7	Predicted results of vapor-liquid equilibrium ( $k_{ij} = 0$ ) by the PC-SAFT-JC, PC-SAFT-GV and PC-SAFT-KSE for the methanol (1)/hexane (2) system at 60 °C, 70 °C, and 75 °C. ....	45
Figure 3.8	Predicted results of vapor-liquid equilibrium ( $k_{ij} = 0$ ) by the PC-SAFT-JC and PC-SAFT-GV for the 2-butanol (1)/propane (2) system at 55 °C, 75 °C, and 95 °C. ....	46
Figure 3.9	Predicted results of vapor-liquid equilibrium ( $k_{ij} = 0$ ) by the PC-SAFT-JC, PC-SAFT-GV and PC-SAFT-KSE for the 1-decanol (1)/ethanol (2) system at 20 °C, 25 °C, 30 °C, 35 °C, 40 °C and 50 °C.....	47
Figure 3.10	Predicted results of vapor-liquid equilibrium ( $k_{ij} = 0$ ) by the PC-SAFT-JC, PC-SAFT-GV and PC-SAFT-KSE for the methanol (1)/octanol (2) system at 1.013 bar.....	50

Figure 3.11	Predicted results of vapor-liquid equilibrium ( $k_{ij} = 0$ ) by the PC-SAFT-JC, PC-SAFT-GV and PC-SAFT-KSE for the ethanol (1)/pentanol(2) system at 75 °C. ....	50
Figure 3.12	Predicted excess enthalpy ( $k_{ij} = 0$ ) by the PC-SAFT-JC for the ethylene glycol(1)/methanol (2)/ethanol(2)/propanol(2)/2-propanol(2) systems at 35 °C....	51
Figure 3.13	Predicted excess enthalpy ( $k_{ij} = 0$ ) by the PC-SAFT-JC for the ethylene glycol(1)/methanol(2)/ethanol(2)/propanol(2)/2-propanol systems at 25 °C. ....	52
Figure 3.14	Predicted results of vapor-liquid equilibrium ( $k_{ij} = 0$ ) by the PC-SAFT-JC for 2-propanol (1)/water(2) system at 150 °C, 200 °C, 250 °C and 275 °C .....	55
Figure 3.15	Predicted results of vapor-liquid equilibrium ( $k_{ij} = 0$ ) by the PC-SAFT-JC for ethylene glycol (1)/water(2) system at 98 °C, 110 °C and 122 °C.....	55
Figure 3.16	Predicted results of vapor-liquid equilibrium ( $k_{ij} = 0$ ) by the PC-SAFT-JC for propylene glycol (1)/water(2) system at 98 °C, 110 °C and 122 °C. ....	56
Figure 3.17	Predicted results of vapor-liquid equilibrium ( $k_{ij} = 0$ ) by the PC-SAFT-JC and PC-SAFT-GV for water (1)/propane(2) system at 65.5 °C, 110 °C and 148.9 °C.....	57
Figure 4.1	Phase composition of water-paraffin mixture at 24.1 bar predicted by dipolar PC-SAFT.....	68
Figure 4.2	Phase fraction ( $\alpha$ ) and stability variable ( $\theta$ ) vs. iteration number for water-paraffin mixture at 24.1 bar and 460 K for: a) Vapour (stable); b) Water-rich liquid phase (unstable); c) Hydrocarbon-rich liquid phase (unstable) .....	70
Figure 4.3	Phase fraction ( $\alpha$ ) and stability variable ( $\theta$ ) vs. iteration number for water-paraffin mixture at 24.1 bar and 454.513 K for: a) Vapour (stable); b) Water-rich liquid phase (unstable); c) Hydrocarbon-rich liquid phase (incipient).....	72
Figure 4.4	Phase fraction ( $\alpha$ ) and stability variable ( $\theta$ ) vs. iteration number for water-paraffin mixture at 24.1 bar and 450 K for: a) Vapour (stable); b) Water-rich liquid phase (unstable); c) Hydrocarbon-rich liquid phase (stable). ....	73
Figure 4.5	Phase fraction ( $\alpha$ ) and stability variable ( $\theta$ ) vs. iteration number for water-paraffin mixture at 24.1 bar and 441.53 K for: a) Vapour (stable); b) Water-rich liquid phase (incipient); c) Hydrocarbon-rich liquid phase (stable).....	74
Figure 4.6	Phase fraction ( $\alpha$ ) and stability variable ( $\theta$ ) vs. iteration number for water-paraffin mixture at 24.1 bar and 420 K for: a) Vapour (stable); b) Water-rich liquid phase (stable); c) Hydrocarbon-rich liquid phase (stable). ....	75
Figure 4.7	Phase fraction ( $\alpha$ ) and stability variable ( $\theta$ ) vs. iteration number for water-paraffin mixture at 24.1 bar and 406.981 K for: a) Vapour (incipient); b) Water-rich liquid phase (stable); c) Hydrocarbon-rich liquid phase (stable). ....	76
Figure 4.8	Phase fraction ( $\alpha$ ) and stability variable ( $\theta$ ) vs. iteration number for water-paraffin mixture at 24.1 bar and 390 K for: a) Vapour (unstable); b) Water-rich liquid phase (stable); c) Hydrocarbon-rich liquid phase (stable). ....	77

Figure 4.9	Mole phase fraction vs. Pressure of methane-propane-water-ethylene glycol at 283.15 K predicted by dipolar PC-SAFT .....	79
Figure 4.10	Phase fraction ( $\alpha$ ) and stability variable ( $\theta$ ) vs. iteration number for ethylene glycol-water-hexane-carbon dioxide-methane mixture at 68 bar and 283.15 K for: a) Vapour (stable); b) Water-rich liquid phase (stable); c) Hydrocarbon-rich liquid phase (stable).....	80
Figure 5.1	Predicted results of vapor-liquid equilibrium ( $k_{ij} = 0$ ) by the PC-SAFT-GV, PC-SAFT-GV-I and PC-SAFT-GV-I-QQ for the ethanol (1)/pentane (2) system at 30 °C, 50 °C, 99.55 °C, 124.55 °C, and 149.55 °C.....	88
Figure 5.2	Predicted results of vapor-liquid equilibrium ( $k_{ij} = 0$ ) by the PC-SAFT-GV and PC-SAFT-GV-I-QQ for the n-propanol (1)/heptane (2) system at 30 °C and 40 °C.....	89
Figure 5.3	Predicted results of liquid-liquid equilibrium ( $k_{ij} = 0$ ) by the PC-SAFT-JC and PC-SAFT-GV for the methanol (1)/n-decane (2) system. Experimental data were taken from Matsuda and Ochi (2004).....	90
Figure 5.4	Predicted results of liquid-liquid equilibrium ( $k_{ij} = 0$ ) by the PC-SAFT-JC and PC-SAFT-GV for the methanol (1)/hexane (2) system. Experimental data were taken from Hradetzky and Lempe (1991).....	91
Figure 5.5	Predicted results of liquid-liquid equilibrium ( $k_{ij} = 0$ ) by the PC-SAFT-GV for the methanol (1)/octane (2) system. Experimental data were taken from Orge et al. (1997).....	92
Figure 5.6	Predicted results of liquid-liquid equilibrium ( $k_{ij} = 0$ ) by the PC-SAFT-GV and PC-SAFT-JC for the methanol (1)/octane (2) system. Experimental data were taken from Orge et al. (1997).....	93
Figure 5.7	Predicted results of liquid-liquid equilibrium ( $k_{ij} = 0$ ) by the PC-SAFT-GV and PC-SAFT-JC for the ethanol (1)/tetradecane (2) system. Experimental data were taken from Matsuda and Ochi (2004).....	94
Figure 5.8	Predicted results of liquid-liquid equilibrium ( $k_{ij} = 0$ ) by the PC-SAFT-GV and PC-SAFT-JC for the ethanol (1)/hexadecane (2) system. Experimental data were taken from Matsuda and Ochi (2004).....	94
Figure 5.9	Predicted results of liquid-liquid equilibrium ( $k_{ij} = 0$ ) by the PC-SAFT-JC for the ethanol (1)/hexadecane (2) system. Experimental data were taken from Matsuda and Ochi (2004).....	95
Figure 5.10	Predicted results of liquid-liquid equilibrium ( $k_{ij} = 0$ ) by the SSAFT-JC for the methanol (1)/pentane (2) system. Experimental data were taken from Orge et al. (1997).....	96
Figure 5.11	Predicted results of liquid-liquid equilibrium ( $k_{ij} = 0$ ) by the SSAFT-JC for the methanol (1)/hexane (2) system. Experimental data were taken from Hradetzky and Lempe (1991).....	96

Figure 5.12	Predicted results of liquid-liquid equilibrium ( $k_{ij} = 0$ ) by the SSAFT-JC for the methanol (1)/heptane (2) system. Experimental data were taken from Orge et al. (1997).	97
Figure 5.13	Predicted results of liquid-liquid equilibrium ( $k_{ij} = 0$ ) by the SSAFT-JC for the methanol (1)/octane (2) system. Experimental data were taken from Orge et al. (1997).	97
Figure 5.14	Predicted results of liquid-liquid equilibrium ( $k_{ij} = 0$ ) by the SSAFT-JC for the methanol (1)/decane (2) system. Experimental data were taken from Matsuda and Ochi (2004).	98
Figure 5.15	Predicted results of liquid-liquid equilibrium ( $k_{ij} = 0$ ) by the SSAFT-JC for the ethanol (1)/tetradecane (2) system. Experimental data were taken from Matsuda and Ochi (2004).	98
Figure 5.16	Predicted mole fractions of liquid-liquid equilibrium ( $k_{ij} = 0$ ) by the SSAFT-JC and PC-SAFT-GV for the water (1)/hexane (2) system.	99
Figure 5.17	Predicted mole fractions of liquid-liquid equilibrium ( $k_{ij} = 0$ ) by the PC-SAFT-JC and PC-SAFT-GV for the water (1)/heptane (2) system.	100
Figure 5.18	Predicted mole fractions of liquid-liquid equilibrium ( $k_{ij} = 0$ ) by the PC-SAFT-JC and PC-SAFT-GV for the water (1)/octane (2) system.	100
Figure 5.19	Predicted mole fractions of liquid-liquid equilibrium ( $k_{ij} = 0$ ) by the PC-SAFT-JC for the water (1)/hexane (2) system.	102
Figure 5.20	Predicted mole fractions of liquid-liquid equilibrium ( $k_{ij} = 0$ ) by the PC-SAFT-JC for the water (1)/octane (2) system.	102
Figure 5.21	Predicted mole fractions of liquid-liquid equilibrium ( $k_{ij} = 0$ ) by the PC-SAFT-JC for the water (1)/cyclohexane (2) system.	103
Figure 6.1	P-T envelop of methane, ethane, n-propane, n-pentane, n-heptane and n-decane mixture predicted by PC-SAFT.	113
Figure 7.1	Reduced temperature vs. coexistence densities for the non-polarizable Stockmayer fluids with $\mu^*=1$ and $\alpha^*=0$ .	123
Figure 7.2	Reduced temperature vs. coexistence densities for the non-polarizable Stockmayer fluids with $\mu^*=2$ and $\alpha^*=0$ .	124
Figure 7.3	Reduced temperature vs. coexistence densities for the non-polarizable Stockmayer fluids with $\mu^*=1$ and $\alpha^*=0.03$ .	124
Figure 7.4	Reduced temperature vs. coexistence densities for the non-polarizable Stockmayer fluids with $\mu^*=1$ and $\alpha^*=0.06$ .	125

Figure 7.5	Vapour pressure vs. temperature for the polarizable Stockmayer fluids with $\mu^*=1$ and $\mu^*=2$ .	126
Figure 7.6	Reduced temperature vs. coexistence densities for the non- polarizable Stockmayer fluids with $\mu^*=2$ and $\alpha^*=0.06$ .	127
Figure 7.7	Reduced temperature vs. coexistence densities for the non- polarizable Stockmayer fluids with $\mu^*=2$ and $\alpha^*=0.06$ . (Figure taken from Kiyohara et al. (1996)).	128
Figure 7.8	Residual internal energy as a function of density for different polarizable Stockmayer fluids for $T^*=3$ .	129
Figure 7.9	Effective dipole moment of different polarizable Stockmayer fluids versus density for $T^*=3$ .	129
Figure 7.10	Prediction ( $k_{ij}=0$ ) of VLE of 1-butanol-heptane system at 40 °C and 60 °C.	131
Figure 7.11	Prediction ( $k_{ij}=0$ ) of VLE of butyraldehyde-heptane system at 45 °C and 70 °C. Experimental data were taken from Eng & Sandler (1984).	132

## NOMENCLATURE

A	Helmholtz free energy
AAD	average absolute deviation (% AAD = $\sum  (X_{cal} - X_{exp}) / X_{exp}  \times 100 / \# \text{data points}$ )
$C(\bar{\mu})$	scalar dependent function
$d_{ij}$	average diameter of segments $i$ and $j$ .
$f$	fugacity
$I_{2ij}$	angular pair and triplet correlation function
$I_{3ijk}$	angular triplet correlation function
$J_{2,ij}$	integral over the reference-fluid pair-correlation function
$J_{3,ijk}$	integral over three-body correlation function
$k$	Boltzmann constant (J/K)
$k_{ij}$	binary interaction parameter
m	segment number
M	weight-average molar mass (g/mol)
N	number of particles
$n_{\mu i}$	number of dipole moments in component $i$
n. a.	not available
p	induced dipole moment
P	pressure
T	absolute temperature (K)
u	pair-potential energy
U	total average energy
V	volume
$v^{00}$	segment volume (mL/mol)
$v^{dd}$	the characteristic segment volume of dipole– dipole interactions (mL/mol)
$x_p$	fraction of dipolar segment in a molecule
$x_{pi}$	fraction of dipolar segment in a molecule $i$
<i>Greek letters</i>	
$\alpha$	polarizability
$\bar{\alpha}$	renormalized polarizability
$\theta$	stability variable
$\varphi$	fugacity coefficient
$\varepsilon_{ii}$	segment energy parameter of component $i$
$\varepsilon/k$	segment dispersion energy
$\varepsilon^{AB}/k$	energy parameter of association between sites $A$ and $B$ (K)
$\kappa^{AB}$	bonding volume
$\mu$	permanent dipole moment
$\bar{\mu}$	average total molecular dipole moment
$\mu_e$	effective permanent dipole moment
$\mu_i$	dipole moment for component $i$

$\mu_i^{*2}$	dimensionless squared dipole moment
$\tilde{\mu}$	reduced chemical potential
$\rho$	number density
$\sigma$	segment diameter
$\sigma_{ii}$	segment size parameter of component $i$ (Å)

### *Subscripts*

ijk	components
cal.	calculated
e	effective
exp.	experimental

### *Superscripts*

assoc	association term
chain	chain term
DD	dipole-dipole
DO	dipole- octupole
disp	dispersion term
ID	Ion-Dipole
hs	hard sphere
polz	polarizable
QQ	quadrupole-quadrupole

## ACKNOWLEDGEMENTS

I would like to express my utmost gratitude and appreciation to my supervisor Professor Peter Englezos for guiding me throughout my PhD work, for being very understanding, patient, encouraging and supportive, and for giving me opportunities to present my research work at conferences.

My sincere gratitude also goes to Professor Gren Patey, who was very helpful and supportive during my PhD work. I am immensely grateful for his valuable discussion and helpful ideas.

I am particularly indebted to Professor Esam Hamad for being a very positive influence in my understanding of statistical thermodynamics.

I also want to give special thanks to all friends and members of my research group: Praveen Linga, Rajnish Kumar, Shivamurthy Modgi, Robin Susilo, Adebola Adeyemo, Cef Haligva, Jeffry Yoslim, Nagu Daraboina, Yizhou Sang, Alireza Bagherzadeh, Babak Amir-Sardary, Mehrnegar Mirvakili, Sima Motiee, Nabeel Abo-Ghander and Ghassan Mousa.

I am grateful to the King Fahd University of Petroleum & Minerals and the Saudi Cultural Bureau for their generous support in funding my graduate scholarship. I'd also like to acknowledge the financial support I received from the Natural Sciences and Engineering Research Council of Canada (NSERC). Finally, I wish to express my sincere thanks to Benedetta Morini and Margherita Porcelli for their assistance in making the TRESNEI code available for public use.

## DEDICATION

*Dedicated to my parents  
and  
To my wife*

# CHAPTER 1

## INTRODUCTION

### 1.1 Motivation

The study of phase behavior of fluids and fluid mixtures is of special interest to chemical engineers due to industrial needs for designing and developing chemical processes. It also plays a major role in widespread applications for the gas industry, petrochemical industry, polymer manufacturing processes (Chen, 2002), aqueous electrolyte (Chen, 1986) and synthetic fuels (Gallier et al., 1981). For efficient development and design of process in these applications, the acquisition of accurate and reliable equilibrium data is crucial. The lack of accurate data leads to incorrect results and significant deviations from potential optimal process configurations (Carlson, 1996). For instance, based on a survey conducted to identify the main sources of discrepancies between plant data and simulation data, it was found that poor prediction of vapour-liquid equilibrium caused two-thirds of the reported cases; particularly for those involving close-boiling molecules (Kister, 2002).

Experimental measurements are a reliable potential source that provide accurate data for multicomponent mixtures for chemical process design. However, these experimental measurements are costly and time-consuming to acquire. In some cases such as the measurements of high-pressure of vapour-liquid equilibrium, it is extraordinarily difficult to acquire accurate data (Raal & Muhlbauer, 1997). Furthermore, the rapid increase of industrial applications of a tremendous number of chemical systems makes it unlikely that a database could be provided that would be sufficient to cover the mixtures of interest for many applications. These difficulties have motivated physical chemists and chemical engineers to develop thermodynamic models to describe and predict phase equilibrium.

Chemical engineers have traditionally approached the problem of determining phase equilibrium behavior of mixtures by using either semi-empirical equations of state or activity coefficient models. Both approaches have shown noticeable success and they are still widely utilized in many applications. Their success however relies on the availability of experimental

data for mixtures which are barely available at the required conditions of temperature, pressure, or composition. Thus, the development of accurate predictive models that would limit the use of mixture experimental data is always desirable and remains an ultimate target for researchers.

Although tremendous effort has been made for decades to develop accurate models, the progress is still far from being close to achieving a predictive model. Most recent effort has mainly focused on either quantum mechanics calculations or statistical mechanics models, particularly those with development based on statistical perturbation theories which have produced theory-based equations of state. Irrespective of which route has been followed in developing predictive models, a key issue that concerns chemical engineers is whether they can actually be used to carry out quick, robust and accurate calculations. The method of calculations should also be fairly straightforward for chemical engineers to use. These considerations limit the use and wide acceptance of quantum mechanics calculations for such a purpose at the current time, since their long execution time makes their implementation impractical in simulators such as ASPEN PLUS, ChemCAD III, HYSIM, PRO II, and SPEEDUP.

On the other hand, theory-based equations of state appear to be more convenient to implement in simulators and to be simpler to use. Their success as predictive models is, however, still limited to a few studies in literature. For instance, accurate prediction of VLE of binary systems was successfully conducted using the Perturbed-Anisotropic-Chain Theory (PACT) EOS for a few systems such as hydrogen sulfide-pentane and methyl iodide-acetone (Vimalchand et al., 1985). Another success with accurate prediction of VLE was achieved using statistical association fluid theory (SAFT) EOS for dipolar-nonpolar systems (Jog et al., 2001; Sauer & Chapman, 2003; Dominik et al., 2005). The success of these and other similar studies in the literature has contributed to an increased interest in employing concepts from molecular physics rather than improving models empirically. The present thesis follows the footsteps of similar studies to improve thermodynamic models based on the increased interest in molecular physics. Therefore, the motivation of this thesis is driven by the increasing demand for accurate and computationally efficient predictive models that are based on molecular physics principles.

Before describing the thesis objectives and organization, it is necessary to devote the next section to a brief introduction of the theory-based equation of state and why the common semi-empirical EOSs fail to be a suitable foundation for further improvement toward a predictive model. The section is not intended to give a complete literature review of theory-based equations

of state. The objective is to justify the choice of the equation of state in this thesis and to establish the base on which the theoretical equation of state can be developed for further discussion in the subsequent chapters. For a complete literature review about equations of state, the reader could refer to Sengers et al. (2000) and Sandler (1994).

## 1.2 Theory-based equations of state

The study of the equilibrium behavior of fluids and fluid mixtures with an equation of state (EOS) has been a subject of active research since van der Waals proposed his celebrated equation of state in 1873. Van der Waals approximated real fluid behavior using a semi-empirical equation by paying attention to the fact that the fluid's constituent particles have nonzero sizes as well as attraction forces. This led to reasonable success in describing fluid behavior at low density. Many semi-empirical equations of state appeared later in the literature as a modification of the van der Waals EOS, such as Soave (Soave, 1972), Peng-Robinson (Peng & Robinson, 1976), Patel and Teja (Patel & Teja, 1982) and Trebble-Bishnoi (Trebble & Bishnoi, 1988). These equations correlate reasonably well the vapor pressure, saturated vapor densities and thermal physical properties of some molecules of industrial interest. Their success is clearly evident with regard to fluids in which the major intermolecular forces are repulsion and dispersion; for example, low molecular weight hydrocarbons, natural gas constituents, simple organic molecules and simple inorganic molecules. This is why these equations of state have found widespread use in chemical process simulation.

Although these equations have gained acceptance and widespread use in the industrial field and the scientific community, they have certain limitations which must be taken into account when using them. For instance, these equations fail to accurately predict the fluid properties of some fluids such as polar solvents and hydrogen bonded fluids. Moreover, their foundation is based on the availability of a large experimental database over a wide range of temperature and pressure, and unfortunately extrapolation is not safe beyond that range. Furthermore, they sometimes fail to reproduce the available experimental data with the required accuracy (Churakov & Gottschalk, 2003). The reason for these failures and limitations is related to the formulation of the equations without taking into consideration the concepts of molecular thermodynamics other than splitting the pressure into attractive and repulsive terms.

Molecular thermodynamics provides insight into the behavior at a molecular level of solutions (Prausnitz et al., 1999). Significant efforts have been directed toward applying molecular theories in order to propose or develop an equation of state. Remarkable success has been achieved in this field and has resulted in the creation of many theoretical equations of state. One of these equations that was based on Wertheim's perturbation theory (Wertheim, 1984a; Wertheim, 1984b; Wertheim, 1986a; Wertheim, 1986b) and that gained special attention over the others in the literature is the statistical association fluid theory (SAFT) EOS. The SAFT and its main terms are described in detail in **Chapter 2**. Several versions of SAFT have been proposed. The main contribution of SAFT is its ability to deal with association and chain contributions as well as its ability to add more contributions in a straightforward manner. The SAFT EOS has been proven to be successful for both small molecules and macromolecules, and has been extensively tested in the literature. As a result, this EOS is utilized as a platform for the work in this thesis, although any theory-based EOS would benefit from the established developments in this thesis.

## 1.3 Research objectives

The overall objective of the work in this thesis is to improve the theory-based equation of state and to facilitate its use in order to predict phase equilibrium of mixtures; particularly vapour-liquid equilibrium (VLE), liquid-liquid equilibrium (LLE) and vapour-liquid-liquid equilibrium (VLLE). To accomplish this goal, the overall plan falls into two categories: *model development* and *computational tools*. Model development concerns the extension of the SAFT either by adding properly accurate terms that describe specific molecular interactions or by developing new terms. The computational tools concern new schemes to facilitate the application of any difficult theory based equation of state to multiphase equilibrium. Before giving more details about the objectives of these two categories, it is important to start with the system of interest in this study; which is the water-alcohol-hydrocarbon system.

### 1.3.1 System of interest

It is not possible at the current stage to develop a universal predictive thermodynamic model for all classes of mixtures. In fact, even the development of non-predictive models to be applied to many classes of mixtures still faces serious challenges. Thus, our focus in the study is mainly on water-alcohol-hydrocarbon mixtures. This system is selected because of its industrial

importance as well as its complex phase behavior which is difficult to capture mathematically. Water-alcohol-hydrocarbon mixtures show highly non-ideal behavior (e.g. alcohol-hydrocarbon systems). There are also interactions that are difficult to describe such as hydrogen bonding and polar interactions. As far as our knowledge goes, all utilized thermodynamics models are unable to give accurate phase equilibrium of these mixtures unless the models are correlated to experimental data.

### **1.3.2 Model development objectives**

The model development first requires assessment and evaluation of the predictive capability of the original SAFT for the system of interest. The proposed SAFT versions incorporate expressions for dispersion, repulsion, chain and association. Depending on what kind of mixtures are studied, the prediction of phase equilibrium using only these four terms gives only qualitative results except for mixtures of small chain hydrocarbon systems. Other attractive forces like dipole-dipole interactions and other slowly varying interactions have not been considered originally in the proposed version of SAFT. However, since these interactions play a minor role in the structure, and since the SAFT is nothing more than a perturbation theory, these interactions could be incorporated as perturbation terms to improve the predictive capability of SAFT. In this thesis, attention is paid to electrostatic interactions; dipole-dipole, quadrupole-quadrupole and polarization interactions. The influence of these interactions is not by any means negligible; they play a significant role in the phase behavior. Therefore, the objectives of the model development can be summarized as follows:

To incorporate and compare three different dipole-dipole theories into the SAFT model to improve the prediction of vapour-liquid equilibria of alcohol-alcohol, water-alcohol, alcohol-hydrocarbon and water-hydrocarbon systems. The three theories are those proposed by Jog and Chapman (1999), Gross and Vrabec (2006) and Karakatsani et al. (2005).

To develop a general strategy to obtain the adjustable parameters of the dipolar SAFT based solely on pure experimental data.

To assess how capable the dipolar SAFT is to represent multiphase equilibria such as LLE and VLLE.

To determine the role of other electrostatic interactions such as quadrupole-quadrupole and polarization interactions with the SAFT for water-alcohol-hydrocarbon mixtures.

To develop a general polarizable theory that is applicable to theory-based equations of state to take account of polarization interactions arising from dipole-dipole, dipole-quadrupole, dipole-octupole, ion-dipole etc.

### **1.3.3 Computational objectives**

The application of the proposed development in the previous section to real systems faces major obstacles. The first one is related to the computation of multiphase equilibria which cannot be conducted without an efficient computational tool. This is because phase stability testing must be carried out as well. In addition, the increased mathematical complexity of SAFT when several perturbation terms are added is another factor. For instance, the SAFT could consist of the following terms: hard sphere, dispersion, chain, association, dipole-dipole, quadrupole-quadrupole and polarization. To compute phase equilibrium, the first derivatives of these terms with respect to mole fraction, density, etc. is necessary. The determination of the analytical derivatives of these terms is very complex. Therefore, in this section, two other objectives are included:

To develop a new scheme to conduct multiphase equilibrium calculation and stability testing.

To utilize a simple and very accurate numerical method called complex-step approximation to compute the first derivatives of the SAFT terms.

## 1.4 Thesis organization

In **Chapter 2** a detailed description of SAFT and some of its versions are presented since it is the theory-based equation of state that is used in this thesis.

**Chapter 3** presents a study of the prediction of VLE of water-alcohol-hydrocarbon systems using the SAFT EOS with the inclusion of three dipolar terms, namely, Chapman's term, Gross's term and Economou's term. A comparison of the three dipolar terms is also given.

**Chapter 4** presents a new scheme for multicomponent multiphase equilibrium calculations and stability testing. Various molecular interactions are incorporated into the SAFT. The proposed scheme is tested on difficult multi-component mixtures.

**Chapter 5** presents a study of multiphase systems of water-alcohol-hydrocarbons using perturbed chain-SAFT with the incorporation of dipole-dipole, quadrupole-quadrupole and polarization interactions. Another version of the SAFT, which is the simplified SAFT, is extended to take account of the dipolar interactions. Polarization interactions are also considered.

**Chapter 6** is devoted to the complex-step approximation method which is used to compute the required first derivatives to conduct phase equilibrium calculations.

**Chapter 7** presents a study employing the self-consistent mean field theory (SCMF) in theoretical based equation of state to take account of induction effects. The study presents a general approach to including polarizable multipole effect in the equation of state in a straightforward manner.

In **Chapter 8**, the obtained results in this thesis are summarized, and research directions for future work are then recommended, for further improvement of predictive theory-based equations of state.

## CHAPTER 2

# STATISTICAL ASSOCIATION FLUID THEORY

### 2.1 Introduction

Much of our current understanding of real fluid behavior can be traced back to the remarkable developments that started in the last century in several topic areas, including virial expansion, cell and lattice theories of liquid, integral equation theories, perturbation theories and atomistic simulation. Some of these topics contributed directly or indirectly to the development of the statistical association fluid theory (SAFT). As indicated in **Chapter 1**, the SAFT is a perturbation theory. The general frame of perturbation theory involves the combination of two main components; namely, fluid structure and intermolecular forces as shown in Figure 2.1.

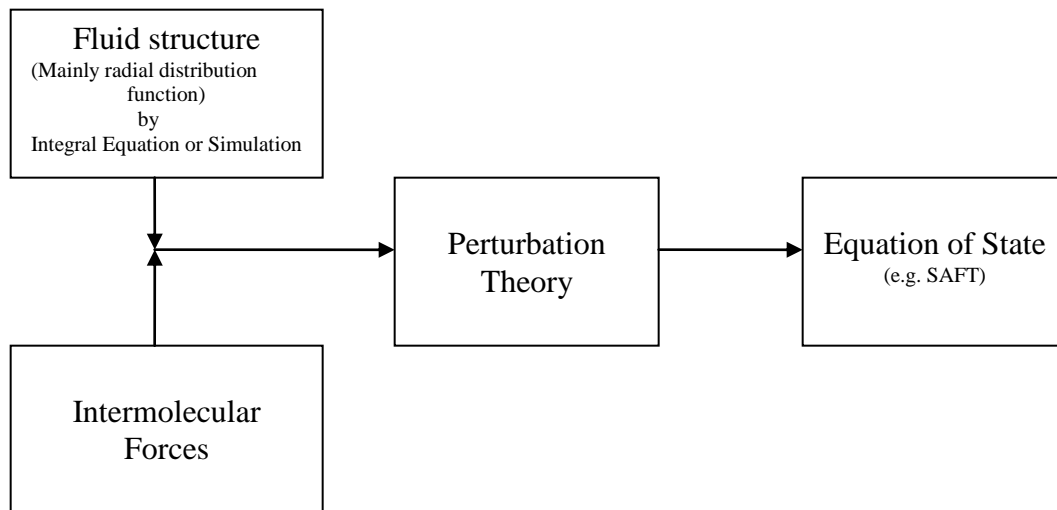


Figure 2.1 General frame of perturbation theory.

The general idea of perturbation theory is to expand the Helmholtz free energy of real fluid behavior around the free energy of a known reference such as the hard sphere by Taylor series expansion. Several perturbation theories have been proposed over the past years such Zwanzig (1954), Barker-Henderson perturbation theory (1967), Weeks-Chandler-Anderson perturbation

theory (1971) and Wertheim perturbation theory (Wertheim, 1984a; Wertheim, 1984b; Wertheim, 1986a; Wertheim, 1986b).

Wertheim perturbation theory is explained in section 2.5.1. One of the most attractive features of Wertheim perturbation theory is the development of an association term which was not considered in the previous perturbation theories. The theory is also flexible in the definition of the reference term (not necessarily a hard sphere reference). In addition, its formulation makes it possible to include various intermolecular interactions in terms of the Helmholtz free energy in a straightforward manner. These features have been exploited by Chapman et al. (1989) and they extended the association term to mixture. They also inspired by Wertheim's theory and developed a term to account for the non-spherical shape of molecules (Chapman et al., 1988). The name of the resulted equation of state was called "statistical association fluid theory". After that, the equation of state was applied to real mixture (Chapman et al., 1990; Huang & Radosz, 1990; Huang & Radosz, 1991). Since that time, the SAFT has been dramatically improved and various versions have appeared.

The increasing interest in SAFT is reflected in the tremendous number of publications as well as the appearance of many SAFT versions such as HS-SAFT (Chapman et al., 1988), CK-SAFT (Huang & Radosz, 1990; Huang & Radosz, 1991), simplified-SAFT (Fu & Sandler, 1995), soft-SAFT (Blas & Vega, 1997), Variable-Range SAFT (Gil-Villegas et al., 1997), Perturbed Chain SAFT (PC-SAFT) (Gross & Sadowski, 2001; Gross & Sadowski, 2002). Due to the highly computational and mathematical complexity of these versions, it is a cumbersome task to give a detailed comparison of them. However, CK-SAFT, PC-SAFT, soft-SAFT and SAFT-VR have gained noticeable attention over the others in the literature. It is necessary to emphasize that the main success behind the SAFT theory is essentially related to its ability to deal with strongly associating fluids such as hydrogen bonding fluids as well as its ability to add additional intermolecular forces easily.

The purpose of this chapter is twofold; first to give a detailed description of the SAFT and its development. Second, the mathematical formulation of some SAFT versions is summarized for further use in subsequent chapters. In this chapter, we start by defining association and describing its effect on phase behavior (section 2.2). Then, the description of non-spherical molecular shape in SAFT is given in section 2.3. Section 2.4 shows how molecular interactions are considered in SAFT and how SAFT adjustable parameters are defined. Section

2.5 is devoted to SAFT terms which are given as explicit forms in terms of the Helmholtz free energy. Finally, section 2.6 covers various SAFT versions that are utilized in this thesis.

## 2.2 Association effect on fluid behavior

Association can arbitrarily be defined as strong attractive forces that act between specific types of molecules to form complexes that exist for a time of the order of  $10^{-13}$  seconds (Muller & Gubbins, 2001). The intermolecular forces are strong enough to be measured experimentally from spectroscopic studies (Elliott & Lira, 1999). Such interactions exist in hydrogen bonding fluids. The effect of association on physical properties of compounds is obvious if the intermolecular forces of association are compared to those of van der Waals attraction forces as shown in Table 2.1 (Sengers et al., 2000b).

Table 2.1 Comparison between van der Waals and associating interactions.

	Bond	Energy/ kJ mol <sup>-1</sup>
<b>Simple Fluids (van der Waals attraction)</b>		
	Ne...Ne	0.14
	Ar...Ar	0.5
	CH <sub>4</sub> ...CH <sub>4</sub>	0.6
	CO <sub>2</sub> ...CO <sub>2</sub>	0.9
	N <sub>2</sub> ...N <sub>2</sub>	1.2
	C <sub>6</sub> H <sub>6</sub> ...C <sub>6</sub> H <sub>6</sub>	1.6
<b>Associating Fluids</b>		
	NH <sub>3</sub> ...NH <sub>3</sub>	15.9
	HF...HF	21.1
	H <sub>2</sub> O...H <sub>2</sub> O	22.3
	HCl...CH <sub>3</sub> CHO	28
	H <sub>2</sub> O...NH <sub>3</sub>	31
	BH <sub>3</sub> ...BH <sub>3</sub>	163.7
	LiH...LiH	199
	TiNi <sub>3</sub> ...TiNi <sub>3</sub>	246

Moreover, association is responsible for the high boiling points of compounds that contain hydrogen bonding. For instance, the normal boiling point of ethyl alcohol (C<sub>2</sub>H<sub>6</sub>O) is 78.5 °C. However, methyl ether (C<sub>2</sub>H<sub>6</sub>O), which is not an associating compound, has a normal boiling of -25 °C although it has the same chemical formula.

## 2.3 Molecular shape in SAFT

In the SAFT EOS, non-spherical molecules are represented by a chain of hard sphere segments joint together by covalent-like bonds as shown in Figure 2.2. The idea of considering a molecule as a chain of segments is not new; it appeared in the literature a long time ago (Huggins, 1941; Flory, 1941). The segments could be atoms, functional groups or complete molecules such as argon or methane (Muller & Gubbins, 2001).



Figure 2.2 Molecular shape in SAFT.

The segment ( $m$ ) is not necessarily an integer number since it is finally a fitting parameter and can be determined by fitting the SAFT EOS to vapor pressure and liquid density data for a pure component. Association is represented as sites located at the perimeter of the molecules (black points in Figure 2.3 b & c), through which molecules can associate. According to Wertheim's theory, the number of association sites on segments is not limited, although in practice it is difficult to justify more than four sites on a segment. Therefore, one might arbitrarily select one, two, three or four sites depending on the type of molecules. For instance, based on spectroscopic data, acids associate to form dimers. Therefore, one might assume that acids contain only one association site. For alcohol, one might assume two sites: one at the hydrogen atom and the second at the unbounded electron pair on the oxygen as shown in Figure 2.3. For water, four sites are normally assumed: two at the unbounded electron pairs and two at the hydrogen atoms. Two and three association sites have also been used for water (Gross & Sadowski, 2002; Fu & Sandler, 1995). Association occurs in pure components as well as in mixtures. In mixtures, association between different components is called solvation or cross-association.

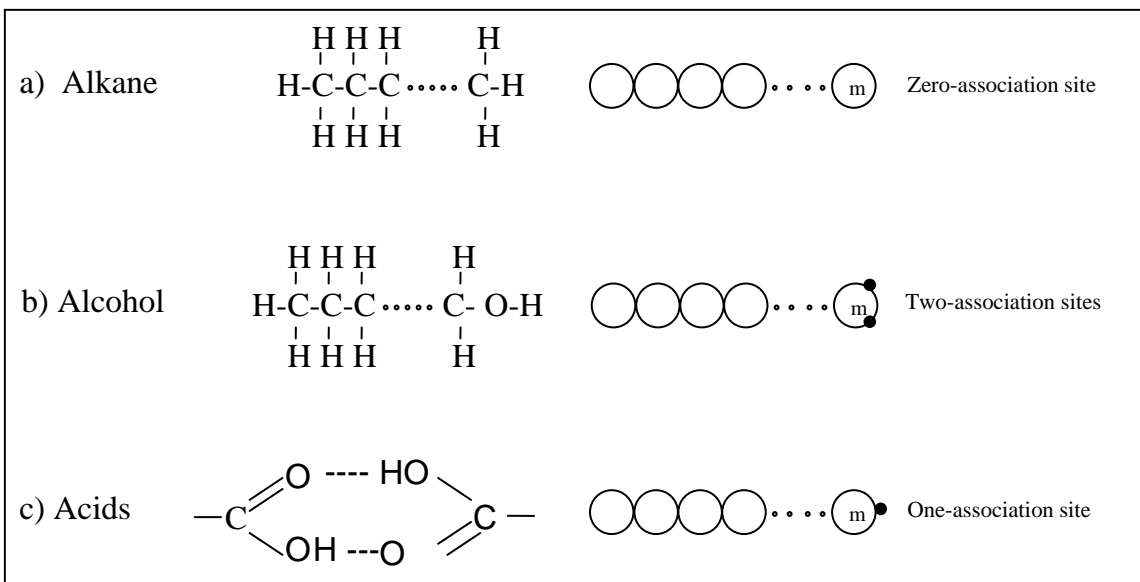


Figure 2.3 Representation of SAFT molecules for a) Alkane b) Alcohol c) Acids.

## 2.4 SAFT interactions and parameters

The question that is raised at this stage is how to take account of all contributions including attraction, repulsion, chain formation and association. The procedure to form a molecule for a pure fluid in SAFT is shown in Figure 2.4. Initially, the fluid consists of non-bonded hard sphere segments. Then, attractive forces are added and after that chain molecules appear by joining segments at chain sites. Finally, if the molecules are associating compounds such as acids or alcohols, molecules form association complexes through association sites. Each one of these steps adds to the free energy.

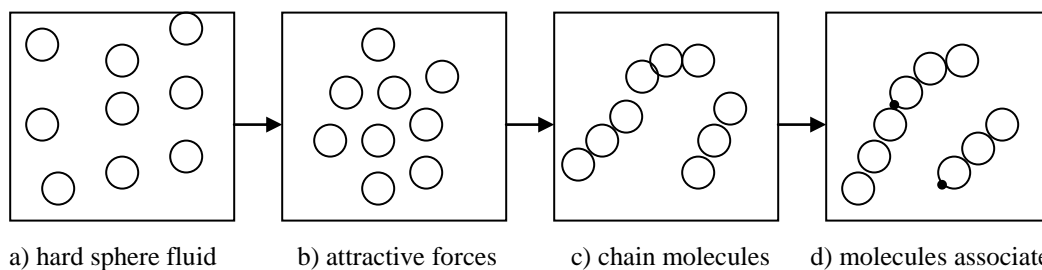


Figure 2.4 Procedure to form a molecule in SAFT (adapted from Prausnitz et al. (1999)).

The total Helmholtz free energy of the system which has a constant number of particles (N), temperature (T), and volume (V) is separated into various contributions as (Chapman et al., 1990):

$$\frac{A}{NkT} - \frac{A^{ideal}}{NkT} = \frac{A^{hs}}{NkT} + \frac{A^{chain}}{NkT} + \frac{A^{disp}}{NkT} + \frac{A^{assoc}}{NkT} \quad 2-1$$

where hs, assoc and disp stands for hard sphere, association and dispersion, respectively.

A pair potential model such as Lennard-Jones is required to account for both repulsion (hard sphere) and dispersion between segments. The Lennard-Jones potential is a function of two parameters: well-depth ( $\epsilon$ ) and diameter ( $\sigma$ ), which differ from one substance to another. Further, chain length of molecules, which is represented by the number of segments ( $m$ ), is not the same for all molecules. Therefore, the well-depth ( $\epsilon$ ), the diameter ( $\sigma$ ), and number of segments ( $m$ ) are three adjustable parameters in SAFT for non-associating compounds. In associating compounds, there are two more parameters, namely, bonding volume ( $\kappa^{AA}$ ) and interaction energy ( $\epsilon^{AA}$ ). To understand what these two parameters represent, one needs to be aware of how Wertheim considers the association interaction. Wertheim assumed that associating molecules contain attraction sites through which molecules associate with other molecules via square-well potential. Therefore, two parameters are required to represent the square potential: the well-depth and the well-width ( $r^{AA}$ ). The interaction energy ( $\epsilon^{AA}$ ) represents the well-depth while bonding volume ( $\kappa^{AA}$ ) characterizes the volume of association corresponding to the well-width ( $r^{AA}$ ). The five SAFT parameters are determined by fitting SAFT EOS to liquid density and vapor pressure data for pure components.

## 2.5 SAFT terms derived from Wertheim's theory

### 2.5.1 Association term

For years, researchers have worked to establish a theory for describing the association effect on fluid behavior. Some theories such as chemical theory, lattice theory and Anderson's theory are summarized in Table 2.2. Wertheim (1984a; 1984b; 1986a; 1986b) was inspired by Anderson's approach and, like Anderson, he introduced geometry at an early stage. Wertheim's cluster expansion however is not only based on the total number density but also on the monomer density, to guarantee the correct low density limit of the second virial coefficient as well as to

provide an accurate representation of the extent of dimerization for liquid-like densities. Wertheim defined the intermolecular-pair potential as the sum of a repulsive reference potential (e.g a hard sphere potential) and a number of short-ranged attraction sites (each interacts via a potential  $u^A$ ):

$$u_{ij}(12) = u_{ij}^{ref}(12) + \sum_{a \in \Gamma^{(i)}} \sum_{b \in \Gamma^{(j)}} u_{ij}^{Aab}(12) \quad 2-2$$

where  $\Gamma^{(i)}$  corresponds to all attraction sites (labeled a, b, c,...) located on the perimeter of molecule. Wertheim did not specify the actual nature of the potential. As a result, the segment interactions can be investigated from a simple potential model such as square-well to a more realistic potential model such as Lennard-Jones. The diversity of choosing the potential model is one reason for the appearance of various versions of the SAFT EOS.

Wertheim derived a relation between the Helmholtz energy due to association ( $A^{assoc}$ ) and the fraction of molecules which are not bonded at association site ( $X^A$ ):

$$A^{assoc} = RT \left( \sum_{i=A}^M \left( \ln X^A - \frac{X^A}{2} \right) + \frac{M}{2} \right) \quad 2-3$$

$$X^A = \frac{1}{1 + N_{Av} \sum_B \rho X^B \Delta^{AB}} \quad 2-4$$

where  $R$ ,  $T$ ,  $M$ ,  $\rho$  and  $N_{Av}$  are the ideal gas constant, temperature, the number of association sites, the molar density of molecules and Avogadro number, respectively. The association strength ( $\Delta^{AB}$ ) is given by:

$$\Delta^{AB} = \int g_R(12) f_{AB}(12) d(12) \quad 2-5$$

where  $g_R(12)$  is the reference fluid pair correlation function and  $f_{AB}(12)$  is Mayer f-function. This equation can be further simplified to:

$$\Delta^{AB} = d^3 g(d)^{seg} \kappa^{AB} \left[ \exp\left(\frac{\mathcal{E}^{AB}}{kT}\right) - 1 \right] \quad 2-6$$

where  $d$ ,  $g(d)^{\text{seg}}$ ,  $\varepsilon^{AB}$  and  $\kappa^{AB}$  are the segment diameter, the segment RDF at contact, association energy and volume for the interaction between association sites A and B, respectively. The volume for the interaction between association sites ( $\kappa^{AB}$ ) and association energy ( $\varepsilon^{AB}$ ), which were defined previously, are determined by fitting liquid density and vapor pressure for compounds; these are the only two association parameters that are obtained from fitting.

Table 2.2 Summary of some theories that describe the non-idealities of associating system.

Theory	Summary	Disadvantages
<p><b>Chemical Theory</b> (Dolezalek (1908))</p>	<ul style="list-style-type: none"> <li>• The chemical theory treats the association phenomena as chemical reactions which cause formation of distinct molecular species in solution.</li> <li>• The molecular species are assumed to be at chemical equilibrium and each chemical reaction is characterized by an equilibrium constant.</li> <li>• It has been successful in describing the solution properties for real system.</li> </ul>	<ul style="list-style-type: none"> <li>• The procedure that one follows is sometimes cumbersome.</li> <li>• Due to the empirical determination of equilibrium constants, the use of the chemical theory as a predictive tool is limited.</li> <li>• The main drawback of the chemical theory is related to the fact that the distinct probable species must be determined <i>a priori</i>.</li> </ul>
<p><b>Lattice Theory</b> (Guggenheim, 1952, Wheeler, J. C., 1975 and Walker, 1980) (Wilson, 1964 &amp; Abrams and Prausnitz, 1975).</p>	<ul style="list-style-type: none"> <li>• The liquid structure is described as a solid-like lattice structure, lattice theories.</li> <li>• Based on lattice theories, several excess Gibb's free energy models were developed such as the Wilson model.</li> </ul>	<ul style="list-style-type: none"> <li>• The description of the liquid structure by lattice theory is undoubtedly an oversimplification and mainly limited to predicting the qualitative properties of the associating fluids.</li> </ul>

Table 2.2 Summary of some theories that describe the non-idealities of associating system (continued).

Theory	Summary	Disadvantages
<p style="text-align: center;"><b>Anderson's Theory</b> Anderson (1973, 1974)</p>	<ul style="list-style-type: none"> <li>• Anderson's theory is based on statistical mechanics.</li> <li>• Anderson introduced the geometry of the interaction of highly directional hydrogen bonding fluids at an early stage in his theoretical development.</li> <li>• A cluster expansion (McQuarrie, 2000) in terms of the total number density was developed by assuming only one bond per attraction site could be formed.</li> <li>• Because Anderson assumed that the attractive site is short-ranged and highly directional, the repulsive cores restrict the system to single bonds at each attractive site. This makes many graphs negligible.</li> </ul>	<ul style="list-style-type: none"> <li>• Because Anderson proposed the cluster expansion in terms of the total number density, the expansion is cumbersome as with the conventional starting point for simple fluids.</li> </ul>

Since segments are approximated as hard spheres, the radial distribution function of hard sphere such as (Carnahan & Starling, 1969) is utilized for the segment RDF:

$$g(d)^{seg} \approx g(d)^{hs} = \frac{2-\eta}{2(1-\eta)^3} \quad 2-7$$

where  $\eta$  is the reduced density defined as:

$$\eta = \frac{\pi N_{Av}}{6} \rho d^3 m \quad 2-8$$

The association term is extended to mixtures and tested with Monte Carlo simulation by Chapman et al. (1988) and Jackson et al. (1988). The mathematical representation of the association term for mixture is given by:

$$\frac{A^{assoc}}{RT} = \sum_i X_i \left[ \sum_{A_i} \left[ \ln X^{A_i} - \frac{X^{A_i}}{2} \right] + \frac{1}{2} M_i \right] \quad 2-9$$

$$X^{A_i} = \left[ 1 + N_{A_i} \sum_i \sum_{B_j} \rho_j X^{B_j} \Delta^{A_i B_j} \right]^{-1} \quad 2-10$$

$$\rho_j = X_j \rho_{mixture} \quad 2-11$$

$$\Delta^{A_i B_j} = g_{ij}(d_{ij})^{seg} \left[ \exp(\varepsilon^{A_i B_j} / kT) - 1 \right] (\sigma_{ij})^3 \kappa^{A_i B_j} \quad 2-12$$

$$\sigma_{ij} = (\sigma_{ii} + \sigma_{jj}) / 2 \quad 2-13$$

Writing  $X^A$  as an explicit expression from 2-10 is not always possible. It is only possible when the mixture has a maximum of one associating compound. As a result, involved expressions and calculations are expected when the mixture has more than one associating compound. For pure components, based on simplifying assumptions, Huang and Radosz (1990) provided analytical expressions of  $X^A$  for some substances.

If the structure of the reference fluid is modified, the association term is also modified by using RDF of the reference fluid since the association strength ( $\Delta$ ) is a function of radial distribution function as shown in equation 2-5.

### 2.5.2 Chain term

To take account of change of energy in SAFT due to bonding, Chapman et al. (1988) derived a term of the chain in terms of the compressibility factor:

$$Z^{chain} = -\sum_{i=1} \frac{\rho_c^{(i)}}{\rho} (m_i - 1) \left\{ 1 + \rho \left( \frac{\partial \ln \Delta^{(ii)}}{\partial \rho} \right) \right\} \quad 2-14$$

where  $\rho_c$  is the number density of chain. The previous equation contains the association strength which is a function of RDF of the reference system. Therefore, the chain term can be derived based on the RDF of the reference. In the case of hard sphere reference, the previous equation can be written for Helmholtz energy as:

$$\frac{A^{chain}}{RT} = \sum_i x_i (1 - m_i) \ln(g_{ii}^{hs}) \quad 2-15$$

## 2.6 SAFT versions

The success of Wertheim's theory in describing association interactions and derivation of chain term has motivated researchers to complete the equation of state. The first appearances of a complete SAFT equation were those by Huang & Radosz (1990), (CK-SAFT), and another by Chapman et al. (1990). Later, other versions have appeared. In this section, we give a brief description of CK-SAFT (Huang & Radosz, 1990), simplified SAFT (Fu & Sandler, 1995) and PC-SAFT (Gross & Sadowski, 2001). These versions are utilized throughout this thesis.

### 2.6.1 CK-SAFT

Huang and Radosz (1990; 1991) introduced the first SAFT version (CK-SAFT) which is sometimes called the original SAFT. The Helmholtz energy terms in equation 2-1 were given by equation 2-9 for association term and by equation 2-15 for chain term. The hard sphere term was given by Mansoori et al. (1971):

$$\frac{A^{hs}}{RT} = \frac{6}{\pi\rho} \left[ \frac{\xi_2^3 + 3\xi_1\xi_2\xi_3 - 3\xi_1\xi_2\xi_3^2}{\xi_3(1-\xi_3)^2} - \left[ \xi_0 - \frac{\xi_2^3}{\xi_3^2} \right] \ln(1-\xi_3) \right] \quad 2-16$$

where  $\xi_k$  is a function of molar density:

$$\xi_k = \left( \frac{\pi N_{Av}}{6} \right) \rho \sum_i x_i m_i d_{ii}^k \quad 2-17$$

The dispersion term is represented by a power series term fitted by Alder et al. (1972) to molecular dynamics data for square-well fluid:

$$\frac{A^{disp}}{RT} = \sum_i \sum_j D_{ij} \left[ \frac{\varepsilon}{kT} \right]^i \left[ \frac{\eta}{\tau} \right]^j \quad 2-18$$

where  $\tau$  is a constant equal to 0.74048.  $D_{ij}$  are universal constants proposed by Chen and Kreglewski (1977). The universal constants were determined by fitting equation 2-18 to argon physical properties. Equation 2-18 is normally extended to mixtures by the use of conformal van der Waals one fluid theory:

$$\frac{\varepsilon}{kT} = \frac{\sum_i \sum_j x_i x_j m_i m_j \left[ \frac{\varepsilon_{ij}}{kT} \right] (v_{ij}^0)}{\sum_i \sum_j x_i x_j m_i m_j (v_{ij}^0)} \quad 2-19$$

where the well depth ( $\varepsilon_{ij}$ ) and the segment molar volume ( $v_{ij}^0$ ) are given by:

$$\varepsilon_{ij} = (1 - k_{ij}) \sqrt{\varepsilon_{ii} \varepsilon_{jj}} \quad 2-20$$

And

$$(v^0)_{ij} = \left[ \frac{1}{2} \left[ (v^0)_i^{1/3} + (v^0)_j^{1/3} \right] \right]^3 \quad 2-21$$

$k_{ij}$  is an empirical binary interaction parameter which will be set to zero in this thesis. The pure adjustable parameters of CK-SAFT were tabulated by Huang and Radosz (1990) for more than

130 components including hydrocarbons, alkanols, amines, ethers, ketones, carboxylic acids and polymers, having molar mass up to 100,000.

### 2.6.2 Simplified SAFT

Because the dispersion term in CK-SAFT is complicated, Fu and Sandler (1995) suggested a simplified dispersion term that was originally developed by Lee et al. (1985). The dispersion term was developed based on the generalized van der Waals partition function. With the aid of molecular simulation data of square-well fluid, it was possible to show how the coordination number varies with temperature and density. The dispersion term was given by:

$$\frac{A^{disp}}{RT} = mZ_m \ln \left( \frac{v_s}{v_s + \langle v^*Y \rangle} \right) \quad 2-22$$

where  $Z_m$  is the maximum coordination number which is 36,  $v^*$  is the close-packed molar volume of a segment,  $v_s$  is the molar volume of a segment and

$$Y = \exp \left( \frac{\varepsilon}{2kT} \right) - 1 \quad 2-23$$

The dispersion term was extended to mixtures by extending  $m$  and  $\langle v^*Y \rangle$  to mixtures as follows:

$$m = \sum_i x_i m_i \quad 2-24$$

$$\langle v^*Y \rangle = \frac{N_{Av} \sum_i \sum_j x_i x_j m_i m_j \left( \frac{d_{ij}^3}{\sqrt{2}} \right) \left[ \exp \left( \frac{\varepsilon_{ij}}{2kT} \right) - 1 \right]}{\sum_i \sum_j x_i x_j m_i m_j} \quad 2-25$$

### 2.6.3 Perturbed-Chain SAFT

PC-SAFT, which was developed by Gross and Sadowski (2001; 2002), is extensively utilized in the literature because it is in general more accurate than CK-SAFT and it differs only in the dispersion term. The dispersion term is developed based on the second order Barker-Henderson perturbation theory (Barker & Henderson, 1967) where the non-bonded RDF is

replaced by RDF for chain molecules. In doing so, the effect of chain connectivity on dispersion term is accounted for and the reference is now hard chain. The dispersion term was given by:

$$A^{disp} = A_1^{disp} + A_2^{disp} \quad 2-26$$

$$A_1^{disp} = -2\pi\rho \sum_{i=0}^6 a_i(m) (\xi_3)^i \sum_i \sum_j x_i x_j m_i m_j \left(\frac{\varepsilon_{ij}}{kT}\right) \sigma_{ij}^3 \quad 2-27$$

$$A_2^{disp} = -\pi\rho m kT \left(\frac{\partial\rho}{\partial P}\right) \sum_i \sum_j x_i x_j m_i m_j \left(\frac{\varepsilon_{ij}}{kT}\right)^2 \sigma_{ij}^3 \sum_{i=0}^6 b_i(m) (\xi_3)^i \quad 2-28$$

The  $a_i(m)$  and  $b_i(m)$  are functions consisting of 42 adjustable parameters obtained by adjusting the dispersion term to alkane physical properties.

## 2.7 Conclusions

In this chapter, a detailed description of the statistical association fluid theory was given. Various SAFT versions were described and their mathematical formulations were given in terms of the Helmholtz free energy. We have emphasized that the success behind the SAFT is mainly due to its association term that presented an acceptable solution to hydrogen bonding. The mathematical formulation of SAFT makes it an adequate theory-based equation of state for our objective in this thesis since various terms will be incorporated to describe various intermolecular forces.

## CHAPTER 3

# PREDICTION OF VAPOR-LIQUID EQUILIBRIUM IN WATER- ALCOHOL-HYDROCARBON SYSTEMS

### 3.1 Introduction

It has become customary to measure the success of any proposed equation of state for mixtures by its ability to correlate accurately experimental data of mixtures; particularly VLE data. Indeed, even the recent developed EOSs including the SAFT EOS are still widely evaluated on this basis. The progress that has recently been made in the SAFT EOS is substantial. Consequently, we speculate that it is now possible with a little effort to improve the SAFT to capture the quantitative behavior of VLE mixtures without using mixture experimental data. This goal is attainable through a proper employment of accurate explicit models that are capable of describing any type of intermolecular interactions. For instance, electrostatic interactions such as dipole-dipole, dipole-quadrupole and quadrupole-quadrupole, which may play a significant role in many systems, have been ignored in the original SAFT development. A proper employment of such interactions may significantly improve the predictive capability of the SAFT. It is conceptually correct to add any term that describes specific interactions to any perturbation theory as a perturbation term provided that the term doesn't play a significant role in the structure.

As discussed in **Chapter 2**, the main reason for the SAFT success and acceptance is essentially related to its ability to deal with hydrogen bonding interactions and also to its formulation which makes it possible to include additional intermolecular forces. These advantages make the SAFT an adequate model to tackle difficult systems such as water–alcohol–hydrocarbon systems which are the systems of interest in our work. Water–alcohol–hydrocarbon systems are interesting systems from both industrial and theoretical perspectives. The thermodynamic properties of these systems are required, for example, in the inhibition of gas hydrate formation in the oil and gas industry. Various attractive forces play a role in these systems such as hydrogen bonding interactions, permanent dipole–dipole interactions, induced dipole–permanent dipole interactions and London dispersion interactions arising from interaction between the instantaneous dipole moments. Among these interactions which may profoundly

influence the phase behavior and which have not been considered in the original form of the SAFT are the dipole-dipole interactions. Although the effect of dipole-dipole interactions is less than that from hydrogen bonding, both give rise to the association phenomena (Moelwyn-Hughes & Thorpe, 1964). Principally, all associating fluids such as water and alcohols have permanent dipole moments and hence the dipolar interactions must be taken into account to improve the predictive capability of the SAFT.

However, incorporating the dipolar term or other electrostatic interactions in the SAFT for associating compounds is not trivial, due to three closely related issues. The first issue is that hydrogen bonding is electrostatic in its nature in real molecules, but the association term is non-electrostatic in the SAFT. That makes it difficult to accurately quantify the magnitude of electrostatic interactions if any electrostatic term is added. The second issue is computational and arises from the need to determine adjustable parameters. When one adds association and dipolar terms, the number of adjustable parameters could reach 6 parameters. To obtain a good set of pure compound parameters, several authors have suggested adjusting the pure SAFT parameters with the aid of mixture data to guarantee that the SAFT gives good results. The use of mixture data as input to the EOS violates our objective in this thesis and it doesn't guarantee a realistic evaluation of SAFT. The last issue is that there are several complex dipolar models in the literature, developed by several groups. It is not easy to decide which one is more accurate. Each group has developed a dipolar model in a different manner with a distinctive perspective, and a systematic comparison of the performance of these models is not available.

The above raised issues are illustrated in more detail in subsequent sections. In section 3.2, a survey on the ongoing development of the incorporation of electrostatic interactions into the SAFT with emphasis on dipole-dipole interactions is presented. In section 3.3, the mathematical formulation of three dipolar terms is presented; Section 3.4 is devoted to model parameter estimation which is based solely on pure component data. Finally, the results, discussion and conclusion are presented in sections 3.5, 3.6 and 3.7, respectively.

## **3.2 Survey of the dipole-dipole interactions in SAFT**

Much of the current effort in SAFT focuses on the consideration of dipolar interactions (Jog & Chapman, 1999; Jog et al., 2001; Sauer & Chapman, 2003; Dominik et al., 2005;

Karakatsani et al., 2005; Gross & Vrabec, 2006; Honggang & McCabe, 2006; Karakatsani & Economou, 2006; Karakatsani & Economou, 2007; NguyenHuynh et al., 2008), quadrupolar interactions (Gross, 2005; Karakatsani & Economou, 2006; Karakatsani & Economou, 2007; NguyenHuynh et al., 2008) and the effect of polarizability of molecules and the resulting induction of dipolar interactions (Kleiner & Gross, 2006). Because the influence of the dipolar interactions on phase behavior is substantial, many authors have been motivated to incorporate these interactions into the SAFT either by developing new approaches (Jog & Chapman, 1999; Karakatsani et al., 2005; Gross & Vrabec, 2006; Honggang & McCabe, 2006) or by modifying old theories (Karakatsani & Economou, 2006; Karakatsani & Economou, 2007; NguyenHuynh et al., 2008). The progress in the field of developing dipolar theories and performing simulations is noticeable since the works of Larsen et al (1977), Gubbins and Twu (1978a; 1978b) and Saager and Fischer (1992; 1991) which all have been recently incorporated into the SAFT (Muller & Gubbins, 2001; Dominik et al., 2005; Karakatsani & Economou, 2006; NguyenHuynh et al., 2008).

However, such progress has not had as much influence as it should until recently when Jog and Chapman developed a successful chain dipolar approach (Jog & Chapman, 1999; Jog et al., 2001; Sauer & Chapman, 2003; Dominik et al., 2005). The approach takes into account multipolar interactions where the dipole moment is located on certain segments and oriented perpendicular to the molecular axis. This approach has been called “segment approach” and its advantage over the classical “molecular approach”, which treats non-spherical dipolar molecules as spherical, has been elaborated by Jog et al (2001) and Tumakaka and Sadowski (2004). A schematic representation of ethylene glycol, which has two dipolar functional groups, is illustrated for both approaches in Figure 3.1.

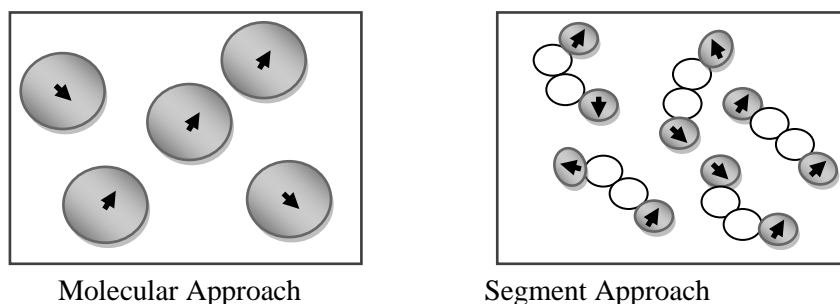


Figure 3.1 A schematic representation of molecular approach and segment approach.

The conclusion that has been drawn from the comparison of the molecular approach and the segment approach is that the molecular approach could handle only a single polar group on a molecule and it underestimates the dipolar interactions effect.

Following the segment approach but with axial alignment of the dipole moment, Gross and Vrabec (2006) proposed another dipolar term that takes into account the multipolar interactions and shape effects based on a third-order perturbation theory. The success of the “segment approach” motivated others to upgrade old “molecular approach” theories to “segment approach” as done recently by NguyenHuynh et al. (2008). More specifically, they extended the Gubbins and Twu work to segment approach and incorporated it into three versions of Group Contribution SAFT. Another successful dipolar model is the one that was developed by Economou’s group (Karakatsani et al., 2005). This model was developed by exploiting the fact that hydrogen bonding and dipole-dipole interactions are short and long-ranged interactions; respectively. Therefore, since the hydrogen bonding operates only at very short distance from the molecule, a short-range cut-off was utilized for the dipole-dipole interactions.

All the above dipolar models have been incorporated into the SAFT and have shown fairly good results when applied to VLE of dipolar mixtures. However, they were limited to non-associative polar mixtures with the exception of Economou’s model which was applied to alcohols; nevertheless, quantitative prediction of VLE was not achieved by the incorporation of Economou’s model.

Before we close this section, it is important to realize that it is not possible to evaluate the performance of the various dipolar terms unless they are compared at the same circumstances and conditions in one study. For this reason, three dipolar models were considered in this chapter; namely, Gross and Vrabec, Jog and Chapman and Economou’s models and incorporated into the perturbed-chain SAFT (PC-SAFT). These three terms are chosen among others in the literature for two reasons. First, they were developed for non-spherical molecules and consistent with the general framework of SAFT. Second, the three terms showed fairly good results and their uses are growing; however, it is not clear which one is the most accurate. In the original papers of these three dipolar terms, when these three approaches have been utilized, they were incorporated into PC-SAFT and have all been named Polar PC-SAFT. In order to distinguish them, the initials of their authors are added to the PC-SAFT as follows: PC-SAFT-JC for that by Jog and Chapman, PC-SAFT-GV for that by Gross and Vrabec and PC-SAFT-KSE for that by Karakatsani et al., (Economou term) respectively.

### 3.3 Dipolar terms

In this section, the three dipolar terms are described in more detail and their mathematical formulation is given in terms of Helmholtz free energy.

#### 3.3.1 Jog and Chapman's dipolar term (JC)

The dipolar term of Jog and Chapman was developed based on Wertheim's perturbation theory of first order which has been proven to be successful in describing associating systems. The contribution of the dipolar interactions to the change in free energy has been obtained by dissolving all of the bonds in a chain and forming a mixture of non-bonded segments of both polar and non-polar segments. The u-expansion was then applied to the mixture and the resulting equations of the dipolar terms were written in the Pade approximate form of Rushbrooke et al. (1973) in terms of reduced Helmholtz Energy ( $a = A/NkT$ ):

$$a^{polar} = \frac{a_2^{polar}}{1 - a_3^{polar} / a_2^{polar}} \quad 3-1$$

where

$$a_2^{polar} = -\frac{2\pi}{9} \frac{\rho}{(kT)^2} \sum_i \sum_j x_i x_j m_i m_j x_{pi} x_{pj} \frac{\mu_i^2 \mu_j^2}{d_{ij}^3} I_{2,ij} \quad 3-2$$

$$a_3^{polar} = \frac{5}{162} \pi^2 \frac{\rho^2}{(kT)^3} \sum_i \sum_j \sum_k x_i x_j x_k m_i m_j m_k x_{pi} x_{pj} x_{pk} \frac{\mu_i^2 \mu_j^2 \mu_k^2}{d_{ij} d_{jk} d_{ik}} I_{3,ijk} \quad 3-3$$

In the above equations,  $\rho$  is number density,  $k$  is Boltzmann constant,  $T$  is temperature,  $x_{pi}$  is the fraction of dipolar segment in a molecule  $i$ ,  $x_{pj}$  is the fraction of dipolar segment in a molecule  $j$ ,  $\mu_i$  is the dipole moment for component  $i$  and  $d_{ij}$  is the average diameter of segments  $i$  and  $j$ . In equations 3.2 and 3.3,  $I_{2,ij}$  and  $I_{3,ijk}$  are the angular pair and triplet correlation functions and given respectively by:

$$I_{2,ij} = \frac{3d_{ij}^3}{4\pi} \int g_{HS_{ij}}(r, \rho^*) r^{-6} dr = 3 \int_1^\infty g_{HS_{ij}}(r_{ij}^*, \rho^*) r_{ij}^{*-4} dr_{ij}^* \quad 3-4$$

$$I_{3,ijk} = \frac{192}{5} \pi \left( \frac{14\pi}{5} \right)^{1/2} \int_0^\infty dr_{12}^* r_{12}^{*-2} \int_0^\infty dr_{13}^* r_{13}^{*-2} \\ \times \int_{|(\sigma_{ij}/\sigma_{jk})r_{12}^* - (\sigma_{ij}/\sigma_{jk})r_{13}^*|}^{(\sigma_{ij}/\sigma_{jk})r_{12}^* + (\sigma_{ij}/\sigma_{jk})r_{13}^*} dr_{23}^* r_{23}^{*-2} g_{ijk}(r_{12}^*, r_{23}^*, r_{13}^*) \psi_{222}(\alpha_1, \alpha_2, \alpha_3) \quad 3-5$$

In the last two equations,  $r^*$  is the dimensionless radius and  $\psi_{222}$  is a function in terms of  $\alpha_1$ ,  $\alpha_2$  and  $\alpha_3$ , which are the angles of the triangle that connects the centers of three molecules.

### 3.3.2 Gross and Vrabec's dipolar term

The Gross and Vrabec term was developed based on a third order perturbation theory. They utilized simulation data of two-center Lennard-Jones plus point dipole fluid to determine the model constants by defining some parameters to translate between two-center Lennard-Jones and spherical segments. The resulting model was compared to simulation data of pure dipolar non-spherical molecules and their mixtures. Excellent agreement was found. The equations were also written in the Pade approximate form of Rushbrooke et al. (1973):

$$a_2^{polar} = -\pi\rho \sum_i \sum_j x_i x_j \frac{\varepsilon_{ii}}{kT} \frac{\varepsilon_{jj}}{kT} \frac{\sigma_{ii}^3 \sigma_{jj}^3}{\sigma_{ij}^3} n_{\mu,i} n_{\mu,j} \mu_i^{*2} \mu_j^{*2} J_{2,ij}^{DD} \quad 3-6$$

$$a_3^{polar} = -\frac{4\pi^2}{3} \rho^2 \sum_i \sum_j \sum_k x_i x_j x_k \frac{\varepsilon_{ii}}{kT} \frac{\varepsilon_{jj}}{kT} \frac{\varepsilon_{kk}}{kT} \frac{\sigma_{ii}^3 \sigma_{jj}^3 \sigma_{kk}^3}{\sigma_{ij} \sigma_{ik} \sigma_{jk}} n_{\mu,i} n_{\mu,j} n_{\mu,k} \mu_i^{*2} \mu_j^{*2} \mu_k^{*2} J_{3,ijk}^{DD} \quad 3-7$$

where  $\varepsilon_{ii}$  is segment energy parameter of component  $i$ ,  $\sigma_{ii}$  is segment size parameter of component  $i$ ,  $n_{\mu i}$  is number of dipole moments in component  $i$  and  $\mu_i^{*2}$  is dimensionless squared dipole moment.  $J_{2,ij}$  and  $J_{3,ijk}$  denote integrals over the reference-fluid pair-correlation function and over three-body correlation functions. These integrals are approximated by power series functions in which the constants are adjusted to simulation data.

### 3.3.3 Economou's term

The Economou dipolar term is developed based on modifying a simple model suggested originally by Nezbeda and Pavlicek (1996). The model is also written in the Pade approximate form:

$$a^{polar} = m \frac{a_2^{polar}}{1 - a_3^{polar} / a_2^{polar}} \quad 3-8$$

where

$$a_2^{polar} = -\frac{4}{3} \left( \frac{\varepsilon}{kT} \right)^2 \tilde{\mu}^4 \tilde{F}_2 \quad 3-9$$

$$a_3^{polar} = \frac{10}{9} \left( \frac{\varepsilon}{kT} \right)^3 \tilde{\mu}^6 \tilde{F}_3 \quad 3-10$$

In the above equations,  $\tilde{\mu}$  is the reduced chemical potential,  $\tilde{F}_2$  equals to  $\eta / K^3$  and  $\tilde{F}_3$  equals to  $\eta^2 / K^3$  where  $\eta$  is reduced density. The functions  $\tilde{F}_2$  and  $\tilde{F}_3$  are obtained by the mean spherical approximation. They are defined to ensure a smooth transition between the short range hydrogen bonding and the long range dipolar interactions. For that reason, a short-range cut-off is introduced for the dipolar interactions ( $\sigma_d$  and  $K = \sigma_d / \sigma$ ). Equations 3-8, 3-9 and 3-10 are extended to mixtures in a simple straightforward manner (Karakatsani et al., 2005).

## 3.4 Model parameter estimation

As discussed earlier, incorporating the segment approach to SAFT to model associating compounds is expected to improve the prediction of vapor-liquid equilibrium in water-alcohol-hydrocarbon systems due to the noticeable success observed in polar systems including ketones, esters and ethers (Jog et al., 2001). However, employing the dipolar SAFT to model associating systems is complicated due to the increased number of parameters. It has been observed that the inclusion of Jog and Chapman's dipolar term led to pure component parameter value multiplicity (Dominik et al., 2005). The multiplicity of parameters is common in equations of state when the

number of the adjustable parameters exceeds three (Kontogeorgis et al., 1996; Karakatsani et al., 2005; Dominik et al., 2005). Therefore, the exploitation of the power of the segment approach to take account of multipolar interactions in associated components may be influenced by the difficulty in obtaining parameters. In order to obtain a unique set of parameter values, Dominik et al. (2005) suggested including one set of binary mixture data in the regression. NguyenHuynh et al. (2008) also included a binary mixture data set. Although the inclusion of binary data in the estimation of pure component parameters improved the ability of the SAFT to calculate binary vapor-liquid equilibrium, it is obvious that this approach is arbitrary. Thus, one cannot evaluate the SAFT terms correctly in order to improve SAFT as a predictive tool. It also violates the objective in this thesis. Thus, the adjustable pure parameters are obtained based solely on pure data. It will be demonstrated that binary data are not necessarily needed to estimate pure component parameters

The three models of polar behavior require the following five adjustable parameters when considering associating components: the segment number ( $m$ ), the segment diameter ( $\sigma$ ), the segment dispersion energy ( $\varepsilon/k$ ), the energy of association ( $\varepsilon^{AB}/k$ ) and the volume of association ( $\kappa^{AB}$ ). PC-SAFT-JC requires an extra adjustable parameter to represent the fraction of dipolar segment in a molecule ( $x_p$ ). Similarly, PC-SAFT-KSE also requires an extra parameter in the dipolar term (the characteristic segment volume of dipole-dipole interactions,  $v^{dd}$ , which is a function of  $\sigma_d$ ). The PC-SAFT-GV model does not require an adjustable parameter for the dipolar term. This model was developed to accommodate a maximum of two polar functional groups (Gross & Vrabec, 2006). However, when more than two polar functional groups exist, the dipolar term must have an adjustable parameter. The optimum parameter values for alcohols and water are obtained by fitting the dipolar PC-SAFT to pure component vapor pressure and liquid density data. A least squares objective function was formulated and minimized. The estimation of parameter values may encounter two challenges. The first one is related to multiplicity of parameters and the second one is due to convergence of some parameters to unrealistic values.

Since multiple parameter sets represent local minima, a unique solution may be obtained by using a global optimization method. However, for some compounds, using a global technique may lead to unrealistic values of the parameters such as a very large segment number ( $m$ ) for low molecular weight molecules or a value of  $x_p$  greater than one ( $x_p$  is a fraction in PC-SAFT-JC). Of course, this is a result of several factors including the accuracy of the SAFT in representing a particular molecule. On the other hand, using a local optimization technique such as the Gauss Newton method with the Marquardt-Levenberg correction may result in numerous sets of

parameters that produce accurate correlation of the pure data. In order to diminish the number of parameter sets, it is necessary to choose an optimization technique other than the classical Gauss Newton method with the Marquardt-Levenberg correction.. It should be noted, however, that the choice of the minimization method is crucial. In the PC-SAFT-JC, if a unique solution of parameter values of one compound within a specific homologous series is estimated, the parameter estimation for the other compounds is significantly simplified. The reason is that the product of  $mx_p$  is expected to be constant when working on a specific homologous series (Dominik et al., 2005).

For the PC-SAFT-KSE equation of state, the parameters are taken from Karakatsani et al (2005) except the parameters of 2-propanol and 1,2-propylene glycol which were not available. The parameter values of 2-propanol are estimated ( $m=3.4065$ ,  $v^{00}= 12.5$  mL/mol,  $\varepsilon/k = 187.94$  K,  $\kappa^{AB} = 0.042235$ ,  $\varepsilon^{AB}/k = 2324.2$  K,  $v^{dd} = 44.2$  mL/mol,  $\mu = 1.58$  D) and the percent average absolute deviation in pressure and liquid density are 2.28 and 1.36 %, respectively. For 1,2-propylene glycol, the estimated parameters ( $m=4.3166$ ,  $v^{00}= 9.8832$  mL/mol,  $\varepsilon/k = 176.53$  K,  $\kappa^{AB} = 0.15723$ ,  $\varepsilon^{AB}/k = 2048.9$  K,  $v^{dd} = 44.2$  mL/mol,  $\mu = 2.27$  D) are obtained with percent average deviation in pressure and liquid density equal to 2.28 and 0.15%. The parameters  $v^{00}$  and  $v^{dd}$  stand for segment volume and the characteristic segment volume of dipole– dipole interactions, respectively.

## 3.5 Results

### 3.5.1 Pure parameter values

The estimated parameter values are listed in Table 3.1 for the PC-SAFT-JC and PC-SAFT-GV for alcohols having one and two dipolar function groups in the chain. It is found that the simplex technique is much less sensitive to the initial guess than the Gauss Newton method with the Marquardt-Levenberg correction and in many cases unique solutions are obtained.

In the PC-SAFT-JC, as mentioned earlier, the product of  $mx_p$  is expected to be constant for components within a homologous series. In order to specify this product for the series of monohydric alcohols, the regression is first done for the six parameters for 1-propanol based on pure data only and a unique solution is obtained after trying several initial guesses. The product of  $mx_p$  is then fixed for the rest of all other monohydric alcohols including primary and secondary

alcohols. The reason for choosing 1-propanol and not one of the first two members in the series (methanol, ethanol) is to avoid potential complexities arising with short-chain molecules such as methanol. This will be discussed later. For short-chain molecules such as methanol, ethanol and water, regression is separately conducted for the six parameters. For glycols having two dipolar functional groups, ethylene glycol is used as the key component in fixing the product of  $mx_p$  by conducting the regression for the six parameters. It is not always necessary to fix the product of  $mx_p$ . However,  $x_p$  is a sensitive parameter and for some components it diverges to unrealistic values. The dipole moment of the functional group is taken in this study to be consistent with the proposed theories (Jog et al., 2001; Gross & Vrabec, 2006). The dipole moment of the functional group (-C-OH) equals to 1.7 (Gokel, 2004).

Table 3.1 Estimated parameters for pure fluids.

Compound	Model*	M	m	$\sigma$	$\varepsilon/k$	$\kappa^{AB}$	$\varepsilon^{AB}/k$	$x_p$	$\mu$	% AAD		Temp. Range	Data Ref.
Equation of state		[g/mol]		[Å]	[K]		[K]		[D]	$P^{sat}$	$\rho^L$	[K]	
methanol	2B	32.042							1.7				
PC-SAFT-JC			1.7266	3.1369	168.84	0.06311	2585.9	0.35128		0.43	0.47	212-497	(Smith & Srivastava, 1986)
PC-SAFT-GV			1.9708	2.9908	179.06	0.06445	2465.9			0.34	0.47		
ethanol	2B	46.068							1.7				
PC-SAFT-JC			2.2049	3.2774	187.24	0.03363	2652.7	0.29466		0.35	0.49	195-510	(Yaws, 2003)
PC-SAFT-GV			2.4382	3.1477	191.31	0.03481	2599.8			0.36	0.29		
1-propanol	2B	60.096							1.7				
PC-SAFT-JC			2.6268	3.3918	219.13	0.02096	2479.4	0.26625		0.78	0.76	210-500	(Yaws, 2003)
PC-SAFT-GV			2.8428	3.2928	225.70	0.01934	2377.7			1.32	0.67		
1-butanol	2B	74.123							1.7				
PC-SAFT-JC			2.9286	3.5235	239.23	0.01635	2371.8	0.23902		1.13	0.74	223-560	(Yaws, 2003)
PC-SAFT-GV			2.9636	3.5015	243.62	0.01293	2426.9			1.01	0.60		
1-pentanol	2B	88.150							1.7				
PC-SAFT-JC			3.8133	3.3911	239.76	0.01303	2079.4	0.18357		0.60	0.68	240-566	(Yaws, 2003)
PC-SAFT-GV			3.9179	3.3518	240.37	0.01097	2140.2			0.68	0.78		
1-hexanol	2B	102.18							1.7				
PC-SAFT-JC			2.8971	3.9467	267.33	0.00815	2769.4	0.24162		1.58	0.53	250-580	(Yaws, 2003)
PC-SAFT-GV			2.9560	3.9068	265.30	0.00814	2806.0			0.94	0.42		
1-heptanol	2B	116.20							1.7				
PC-SAFT-JC			4.1962	3.6119	254.99	0.00260	2662.7	0.16682		0.82	0.84	290-600	(Yaws, 2003)
PC-SAFT-GV			4.0319	3.6651	261.06	0.00188	2818.9			0.83	0.76		
1-octanol	2B	130.23							1.7				
PC-SAFT-JC			4.3683	3.7078	260.49	0.00282	2660.4	0.16025		0.65	0.58	277-650	(Yaws, 2003)
PC-SAFT-GV			4.4030	3.6943	260.90	0.00261	2700.3			0.61	0.58		
1-decanol	2B	158.28							1.7				
PC-SAFT-JC			4.7826	3.8415	266.50	0.00284	2810.8	0.14636		0.25	0.42	310-670	(Yaws, 2003)

Table 3.1 Estimated parameters for pure fluids (continued).

Compound	Model*	M	m	$\sigma$	$\varepsilon/k$	$\kappa^{AB}$	$\varepsilon^{AB}/k$	$x_p$	$\mu$	% AAD		Temp. Range	Data Ref.
Equation of state		[g/mol]		[Å]	[K]		[K]		[D]	$P^{sat}$	$\rho^L$	[K]	
PC-SAFT-GV			4.8060	3.8329	266.81	0.00271	2838.2			0.27	0.43		
2-propanol	2B	60.096							1.7				
PC-SAFT-JC			2.6856	3.3800	199.10	0.02237	2473.8	0.26065		1.98	1.64	209-507	(Smith & Srivastava, 1986; Yaws, 2003)
PC-SAFT-GV			2.6850	3.3800	212.32	0.01552	2485.3		1.85	1.79			
2-butanol	2B	74.123							1.7				
PC-SAFT-JC			2.8566	3.5543	239.01	0.00798	2314.8	0.24505		1.35	1.08	222-525	(Smith & Srivastava, 1986; Yaws, 2003)
PC-SAFT-GV			2.9302	3.5131	240.74	0.00658	2374.7		1.28	0.88			
water	2B	18.015							1.85				
PC-SAFT-JC			1.0405	2.9657	175.15	0.08924	2706.7	0.66245		3.33	1.54	273.16-634	(Wanger & Prub, 2002)
PC-SAFT-GV			1.2255	2.7920	203.00	0.07172	2406.7		3.47	0.73			
Ethylene glycol	4C								1.7				
PC-SAFT-JC		62.068	2.6653	3.1526	143.29	0.10379	2233.5	0.56335		2.24	0.05	290-530	(Yaws, 2003)
PC-SAFT-GV			3.4038	2.8442	178.37	0.13480	2152.4		2.29	0.15			
1,2-Propylene glycol	4C								1.7				
PC-SAFT-JC		76.090	3.4136	3.1419	147.35	0.12393	2111.6	0.43942		2.28	0.09	290-530	(Yaws, 2003)
PC-SAFT-GV			4.2579	2.8699	173.33	0.15927	2011.7		2.30	0.15			

\* The type of bonding schemes in associating fluid was taken from Huang and Radosz (1990).

### 3.5.2 Dipole-dipole contribution

Before proceeding to the application of the dipolar PC-SAFT to the systems of interest, it is necessary to assess the contribution of the three dipolar terms with the PC-SAFT. The contribution of the reduced chemical potential ( $\mu/NkT$ ) of 1-propanol is depicted in Figure 3.2 a-d for the repulsion, dispersion, hydrogen bonding and dipole-dipole terms at 250 K and 450 K. The contributions from repulsion, dispersion and hydrogen bonding are clearly comparable for the three models. However, Figure 3.2-d shows that the PC-SAFT-JC dipolar interactions have the largest contribution to the reduced chemical potential while the PC-SAFT-KSE has the smallest. The same behavior is observed for other aliphatic alcohols. This indicates that the influence of the Jog and Chapman term on phase behavior of alcohols is expected to be substantial compared to the other dipolar terms. It is also clear that as the temperature increases, the magnitude of the reduced chemical potential decreases. This is expected because as the temperature increases, the average dipole-dipole energy decreases and therefore, the influence of dipole-dipole interactions is less pronounced.

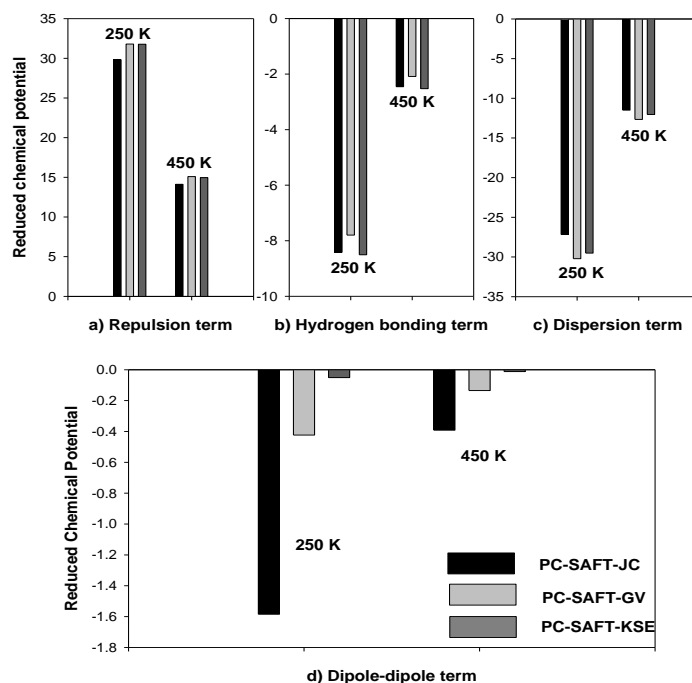


Figure 3.2 Reduced Chemical potential of 1-propanol at 250 K and 450 K from the dipolar PC-SAFT for a) repulsion contribution, b) hydrogen bonding contribution, c) dispersion contribution and d) dipole-dipole contribution.

### 3.5.3 Prediction of VLE for binary systems

In the following three sections, a total of 53 binary systems are considered at different temperatures with the incorporation of the previous three dipolar terms into PC-SAFT. It should be noted that these are pure predictions and no binary data were used in the estimation of pure component parameters.

#### 3.5.3.1 Alcohol-hydrocarbon systems

The non-polar PC-SAFT EOS requires an adjustable binary interaction parameter in order to quantitatively represent the phase behavior of binary alcohol-hydrocarbon systems (Gross & Sadowski, 2002; Yarrison & Chapman, 2004). Inclusion of the dipolar term enables PC-SAFT to improve the prediction of the VLE of these binary systems compared to non-polar PC-SAFT. Table 3.2 lists the binary alcohol-hydrocarbon systems examined and shows the absolute average deviations (AAD) from bubble-point pressure calculations and the comparison with the data.

As seen from the bubble-point pressure calculations, the Jog and Chapman term significantly improves PC-SAFT in most of the tested systems compared to non-polar PC-SAFT except for the toluene-ethanol system. In order to appreciate the magnitude of the AADs, the ethanol-octane and 1-propanol-hexane systems were selected from the alkane-alcohol group. The deviations in this group ranged from 0.47 to 4.01 %. The AADs in pressure for the two chosen systems are 3.71 and 4.01 % respectively. Hence, they are appropriate to gauge the magnitude of the deviations. Figure 3.3 and Figure 3.4 show the phase diagrams of these two systems. It is clear that the predictive capability is very satisfactory. It is also noted that the PC-SAFT-JC is capable of representing the VLE behavior well over a wide temperature range as shown in Figure 3.5.

The PC-SAFT-JC model is also successful for 2-alkanol systems such as the 2-propanol-heptane which is depicted in Figure 3.6. However, when the PC-SAFT-JC was tested for methanol-hydrocarbon systems (methanol with butane, hexane, benzene or toluene) shown in Table 3.3, liquid-liquid splitting was observed at some temperatures.

Table 3.2 Predicted VLE results for alcohol-hydrocarbon systems by the PC-SAFT-JC and PC-SAFT-GV.

system		T (°C)	PC-SAFT-JC		PC-SAFT-GV		non- Polar PC-SAFT		N data pt	Ref.
			AAD P (%)	AAD y x 10 <sup>2</sup>	AAD P (%)	AAD y x 10 <sup>2</sup>	AAD P (%)	AAD y x 10 <sup>2</sup>		
methanol	butane	100	1.89	0.35	5.06	0.29	11.2	0.20	13	(Leu et al., 1990)
	pentane	99.55	2.31	1.14	6.37	0.81	12.5	1.15	11	(Wilsak et al., 1987)
		124.55	2.52	0.74	5.92	0.55	10.9	0.74	11	(Wilsak et al., 1987)
		149.45	2.75	0.45	5.70	0.36	9.53	0.47	11	(Wilsak et al., 1987)
ethanol	hexane	70	1.41	n. a.	5.84	n. a.	14.3	n. a.	25	(Wolff & Hoeppe, 1968)
	butane	75	1.40	n. a.	6.44	n. a.	14.5	n. a.	25	(Wolff & Hoeppe, 1968)
		25.3	4.07	n. a.	5.41	n. a.	12.6	n. a.	24	(Holderbaum et al., 1991)
ethanol	pentane	50.6	2.09	n. a.	5.69	n. a.	12.1	n. a.	24	(Holderbaum et al., 1991)
		72.5	1.16	n. a.	5.71	n. a.	11.3	n. a.	24	(Holderbaum et al., 1991)
		30	3.55	0.58	6.43	0.42	13.4	0.48	26	(Reimers et al., 1992)
	hexane	99.55	1.13	0.02	5.71	0.08	9.31	0.45	10	(Campbell et al., 1987)
		124.55	1.74	0.40	5.28	0.33	8.09	0.13	12	(Campbell et al., 1987)
		149.45	1.67	0.24	4.95	0.20	7.94	0.22	11	(Campbell et al., 1987)
		192.25	0.95	0.13	2.66	0.11	4.45	0.10	15	(Seo et al., 2000)
	hexene	40	2.10	n. a.	6.04	n. a.	11.6	n. a.	15	(Janaszewski et al., 1982)
		45	1.60	0.91	6.75	0.63	11.3	0.65	40	(OShea & Stokes, 1986)
		60	0.86	n. a.	6.40	n. a.	10.8	0.74	26	(Wolff & Goetz, 1976)
heptane	60	2.37	0.02	6.01	0.06	12.0	0.13	8	(Hanson & Van Winkle, 1967)	
	30	2.88	n. a.	6.96	2.56	12.7	n. a.	24	(Ronc & Ratcliff, 1976)	
	50	1.46	n. a.	7.16	n. a.	12.0	n. a.	33	(Van Ness & Abbott, 1997)	
octane	70	1.11	1.62	8.37	1.10	13.3	1.02	35	(Berro & Peneloux, 1984)	
	40	1.83	n. a.	9.09	n. a.	15.8	n. a.	15	(Boublikova & Lu, 1969)	
		65	2.85	8.06	8.38	5.18	12.9	4.64	20	(Goral et al., 2004)

Table 3.2 Predicted VLE results for alcohol-hydrocarbon systems by the PC-SAFT-JC and PC-SAFT-GV (continued).

system		T (°C)	PC-SAFT-JC		PC-SAFT-GV		non- Polar PC-SAFT		N data pt	Ref.
			AAD P (%)	AAD y x 10 <sup>2</sup>	AAD P (%)	AAD y x 10 <sup>2</sup>	AAD P (%)	AAD y x 10 <sup>2</sup>		
		75	3.71	5.98	8.55	3.93	12.6	3.55	21	(Goral et al., 2004)
	nonane	70	1.90	12.9	8.07	8.31	12.0	7.46	27	(Alekseeva & Moiseenko, 1982)
	toluene	35	12.6	n. a.	3.79	n. a.	6.90	n. a.	12	(Zielkiewicz, 1991)
		45	19.4	0.33	7.34	0.18	9.51	0.15	19	(Zielkiewicz, 1991)
		55	8.79	13.7	3.57	7.88	6.76	6.90	12	(Zielkiewicz, 1991)
Propanol	hexane	25	3.72	0.66	4.92	0.31	9.95	0.20	11	(Maciel & Francesconi, 1988)
		40	1.81	0.26	5.45	0.18	10.1	0.18	25	(Van Ness et al., 1967)
		75	4.01	0.02	10.8	0.11	15.0	0.16	10	(Zielkiewicz, 1992)
	heptane	30	2.56	1.06	6.35	0.60	11.5	0.43	21	(Berro, 1987)
		40	1.87	n. a.	6.34	n. a.	11.6	n. a.	26	(Berro et al., 1986)
		60	0.47	0.64	6.23	0.45	10.4	0.37	21	(Berro, 1987)
	octane	40	1.54	n. a.	6.87	n. a.	12.2	n. a.	39	(Berro et al., 1986)
		90	2.06	0.89	8.24	0.57	12.9	0.40	24	(Schmelzer et al., 1983)
	nonane	60	0.47	3.67	7.35	2.04	12.3	1.19	25	(Oracz & Kolasinka, 1987)
		90	2.58	2.20	9.47	1.34	14.6	0.85	22	(Oracz & Kolasinka, 1987)
	undecane	60	1.48	0	11.4	0.01	18.2	0.01	16	(Gracia et al., 1992)
	toluene	40	4.29	n. a.	5.07	n. a.	11.0	0.47	21	(Zielkiewicz, 1991)
	benzene	40	4.66	n. a.	4.50	n. a.	10.4	n. a.	25	(Zielkiewicz, 1991)
		60	4.96	0.1	2.87	0.07	8.37	0.17	34	(Zielkiewicz, 1991)
		75	5.70	0.11	2.10	0.06	7.41	0.13	13	(Zielkiewicz, 1991)
	p-xylene	40	2.65	n. a.	7.10	n. a.	13.7	n. a.	19	(Berro et al., 1982)
butanol	hexane	40	1.27	n. a.	4.77	n. a.	6.73	0.14	15	(Zielkiewicz, 1994)
		60	1.29	0.06	5.19	0.10	7.11	0.13	26	(Berro & Peneloux, 1984)
	heptane	40	1.60	n. a.	5.12	n. a.	7.29	0.20	21	(Gracia et al., 1992)
		60	1.16	0.14	5.79	0.15	7.85	0.16	24	(Gierycz et al., 1988)

Table 3.2 Predicted VLE results for alcohol-hydrocarbon systems by the PC-SAFT-JC and PC-SAFT-GV (continued).

system		T (°C)	PC-SAFT-JC		PC-SAFT-GV		non- Polar PC-SAFT		N data pt	Ref.
			AAD P (%)	AAD <sub>y</sub> x 10 <sup>2</sup>	AAD P (%)	AAD <sub>y</sub> x 10 <sup>2</sup>	AAD P (%)	AAD <sub>y</sub> x 10 <sup>2</sup>		
		90	2.54	0.12	6.01	0.14	7.68	0.15	24	(Gierycz et al., 1988)
	octane	34.94	1.31	n. a.	4.80	n. a.	6.99	0.12	13	(Bernatova et al., 1992)
		50.03	1.03	n. a.	5.64	n. a.	7.58	0.12	13	(Bernatova et al., 1992)
		100	3.07	n. a.	3.07	n. a.	7.77	0.31	14	(Wieczorek & Stecki, 1978)
	decane	85	2.00	2.65	4.51	2.16	5.06	1.81	14	(Geiseler et al., 1967)
		100	2.73	2.03	4.97	1.68	5.21	1.42	14	(Geiseler et al., 1967)
		115	3.23	1.59	5.26	1.33	5.43	1.13	14	(Geiseler et al., 1967)
	benzene	25	5.27	n. a.	4.97	0.27	11.2	0.25	7	(Zielkiewicz, 1991)
		45	2.26	0.16	2.93	0.14	4.25	0.14	11	(Zielkiewicz, 1991)
	toluene	60	1.45	n. a.	3.22	n. a.	4.58	0.23	17	(Zielkiewicz, 1991)
		80	1.61	0.31	3.25	0.23	4.33	0.19	17	(Zielkiewicz, 1991)
		100	2.43	0.36	1.76	0.28	2.77	0.23	11	(Zielkiewicz, 1991)
	p-xylene	40	1.46	n. a.	4.20	n. a.	6.06	n. a.	18	(Berro et al., 1982)
hexanol	hexane	30	1.79	n. a.	4.10	n. a.	5.3	n. a.	9	(Lindberg & Tassios, 1971)
		69.67	1.95	n. a.	3.33	n. a.	6.54	n. a.	11	(Lindberg & Tassios, 1971)
octanol	heptane	20	3.96	n. a.	2.36	n. a.	2.73	n. a.	24	(Gros et al., 1996)
		40	2.28	n. a.	4.77	n. a.	5.81	n. a.	24	(Gros et al., 1996)
2-propanol	heptane	30	1.48	2.1	5.75	1.31	10.9	0.82	13	(Gmehling et al., 1977)
		45	0.88	1.58	6.08	1.03	10.9	0.69	20	(Gmehling et al., 1977)
		60	1.44	1.21	6.37	0.83	10.9	0.59	20	(Gmehling et al., 1977)
	benzene	45	4.92	n. a.	2.55	n. a.	7.91	n. a.	14	(Zielkiewicz, 1991)
		70	7.01	0.12	2.03	0.06	7.11	0.09	10	(Zielkiewicz, 1991)
2-butanol	propane	55	1.60	0.19	1.10	0.2	1.95	0.21	12	(Freshwater & Pike, 1967)
		75	1.23	0.15	1.01	0.17	1.82	0.18	12	(Freshwater & Pike, 1967)
		95	1.37	0.11	1.11	0.14	1.88	0.15	12	(Freshwater & Pike, 1967)

Table 3.2 Predicted VLE results for alcohol-hydrocarbon systems by the PC-SAFT-JC and PC-SAFT-GV (continued).

system		T (°C)	PC-SAFT-JC		PC-SAFT-GV		non- Polar PC-SAFT		N data pt	Ref.
			AAD P (%)	AAD y x 10 <sup>2</sup>	AAD P (%)	AAD y x 10 <sup>2</sup>	AAD P (%)	AAD y x 10 <sup>2</sup>		
	propylene	60	5.58	0.17	3.87	0.15	3.06	0.15	12	(Freshwater & Pike, 1967)
		80	5.54	0.21	3.83	0.16	3.02	0.14	12	(Freshwater & Pike, 1967)
		95	6.36	0.07	4.08	0.06	3.03	0.06	9	(Freshwater & Pike, 1967)
	hexene	60	0.80	0.05	3.73	0.07	5.56	0.10	14	(Zielkiewicz, 1993)
	toluene	60.16	0.83	0.46	3.48	0.37	5.08	0.34	15	(Zielkiewicz, 1991)
		80.29	1.09	0.43	2.87	0.33	4.30	0.30	14	(Zielkiewicz, 1991)
	benzene	25	1.77	n. a.	4.19	n. a.	5.99	n. a.	8	(Zielkiewicz, 1991)
		45	1.66	0.2	3.84	0.19	5.61	0.20	11	(Zielkiewicz, 1991)

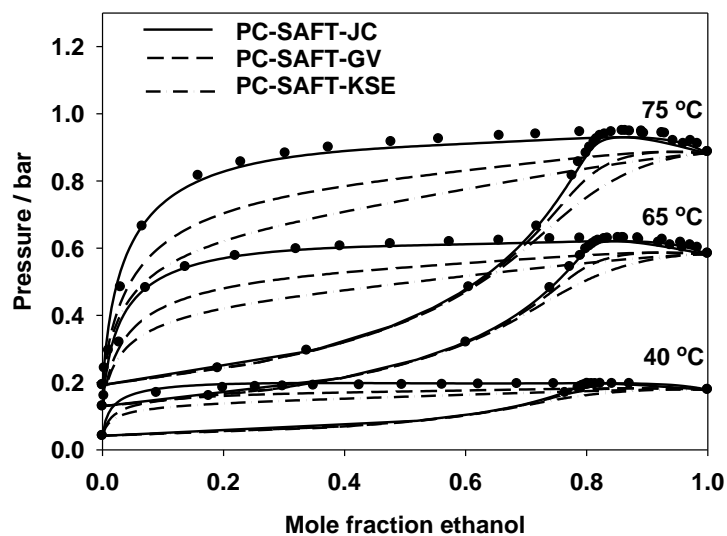


Figure 3.3 Predicted results of vapor-liquid equilibrium ( $k_{ij} = 0$ ) by the PC-SAFT-JC, PC-SAFT-GV and PC-SAFT-KSE for the ethanol (1)/octane (2) system at 40 °C, 65 °C and 75 °C.

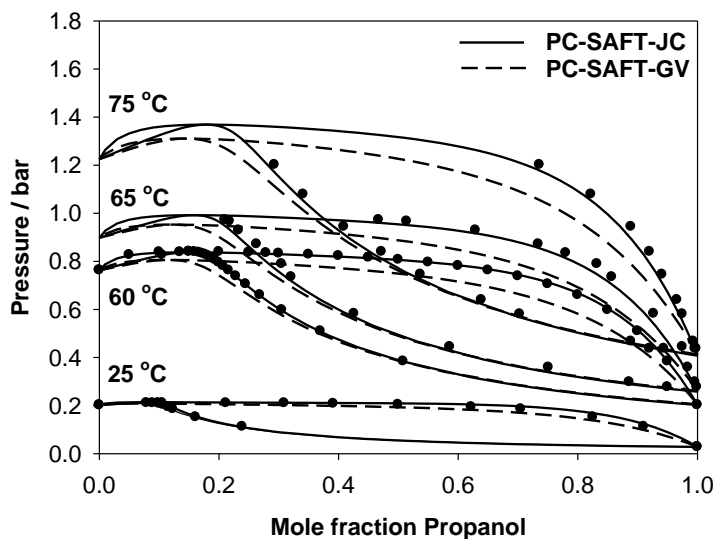


Figure 3.4 Predicted results of vapor-liquid equilibrium ( $k_{ij} = 0$ ) by the PC-SAFT-JC and PC-SAFT-GV for the 1-propanol(1)/hexane (2) system at 25 °C, 60 °C, 65 °C and 75 °C.

Interestingly, at temperatures higher than those given in Table 3.3, it was found that the PC-SAFT-JC gives very satisfactory prediction of the methanol-hydrocarbon systems without the need to introduce a binary interaction parameter. Therefore, it is important to determine the temperatures at which the PC-SAFT-JC can be used without showing liquid-liquid splitting. In order to determine the temperatures at which liquid-liquid splitting occurs, the PC-SAFT-JC is tested for methanol-butane/pentane/hexane/benzene/toluene systems at different temperatures. For all these systems, it was found that the liquid-liquid splitting occurs at temperature less than approximately 70 °C. The prediction capability of the PC-SAFT-JC is very satisfactory at 70 °C and above for methanol containing systems as shown in Table 3.2 and Figure 3.7. It should be noted that the liquid-liquid splitting for methanol containing systems was also observed with PC-SAFT-GV but at lower temperatures as shown in Table 3.3.

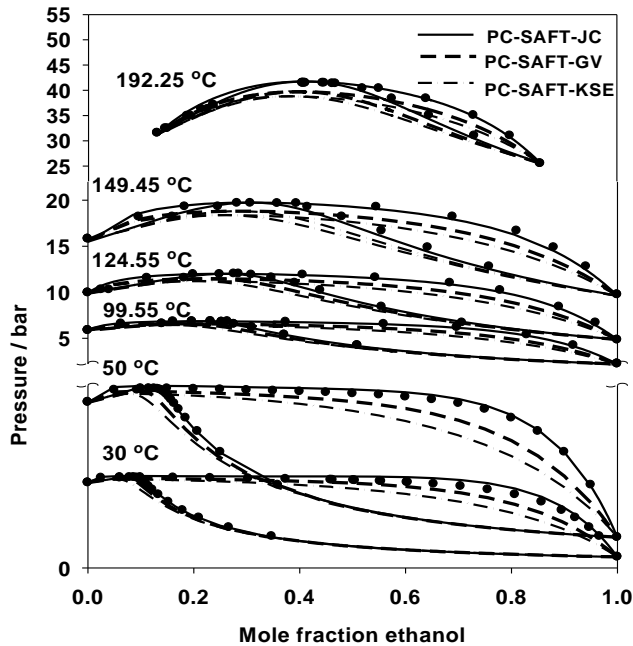


Figure 3.5 Predicted results of vapor-liquid equilibrium ( $k_{ij} = 0$ ) by the PC-SAFT-JC, PC-SAFT-GV and PC-SAFT-KSE for the ethanol (1)/pentane (2) system at 30 °C, 50 °C, 99.55 °C, 124.55 °C, 149.45 °C and 192.25 °C.

Table 3.3 Predicted VLE results for methanol containing systems by PC-SAFT-JC, PC-SAFT-GV and PC-SAFT-KSE.

system		T (°C)	PC-SAFT-JC		PC-SAFT-GV		PC-SAFT-KSE		N data pt	Ref.
			AAD P (%)	AAD y x 10 <sup>2</sup>	AAD P (%)	AAD y x 10 <sup>2</sup>	AAD P (%)	AAD y x 10 <sup>2</sup>		
methanol	butane	50	Liquid-Liquid Splitting		5.62	0.06	9.19	0.17	10	(Leu et al., 1990)
	hexane	40	Liquid-Liquid Splitting				12.6	n. a.	25	(Wolff & Hoeppe, 1968)
		60	Liquid-Liquid Splitting		5.44	n. a.	12.5	n. a.	25	(Wolff & Hoeppe, 1968)
	benzene	25	Liquid-Liquid Splitting				2.26	n. a.	15	(Zielkiewicz, 1991)
		45	Liquid-Liquid Splitting		7.18	n. a.	4.95	n. a.	33	(Zielkiewicz, 1991)
		55	Liquid-Liquid Splitting		7.57	0.10	4.56	0.06	9	(Zielkiewicz, 1991)
	toluene	50	Liquid-Liquid Splitting		7.68	n. a.	5.63	n. a.	15	(Zielkiewicz, 1991)

Interestingly, the PC-SAFT-KSE did not predict erroneous liquid-liquid splitting. This is most likely related to the magnitude of the dipolar term as was shown in Figure 3.2-d. In addition, the PC-SAFT-KSE was found to perform better than PC-SAFT-JC and PC-SAFT-GV for methanol-aromatic compounds as shown on Table 3.3. However, it gives only a qualitative representation for alcohol-hydrocarbon systems shown in Figure 3.3 to Figure 3.7. The AADs in pressure obtained from the Economou term (PC-SAFT-KSE) for the systems shown in Table 3.2 were found to range from 6.7 to 27 % with an average value of 14.3 %.

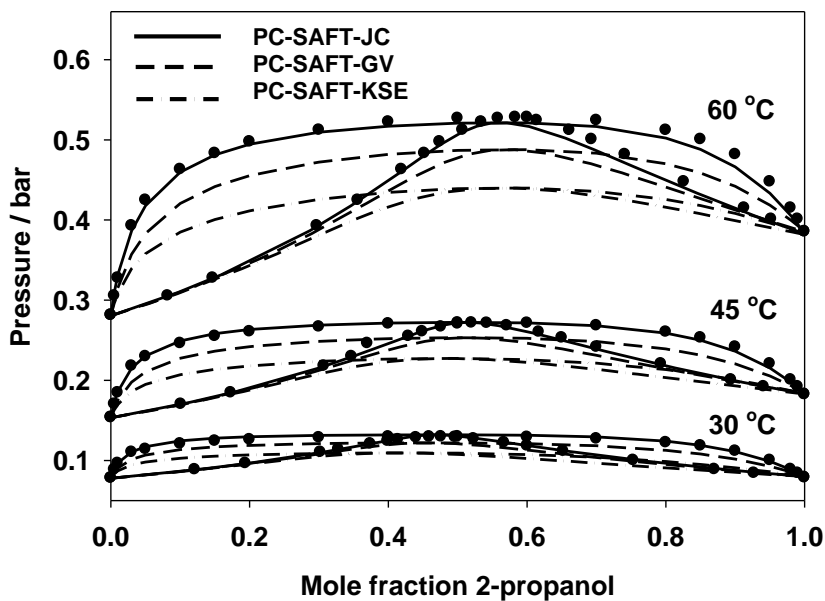


Figure 3.6 Predicted results of vapor-liquid equilibrium ( $k_{ij} = 0$ ) by the PC-SAFT-JC, PC-SAFT-GV and PC-SAFT-KSE for the 2-propanol (1)/heptane (2) system at 30 °C, 45 °C, and 60 °C.

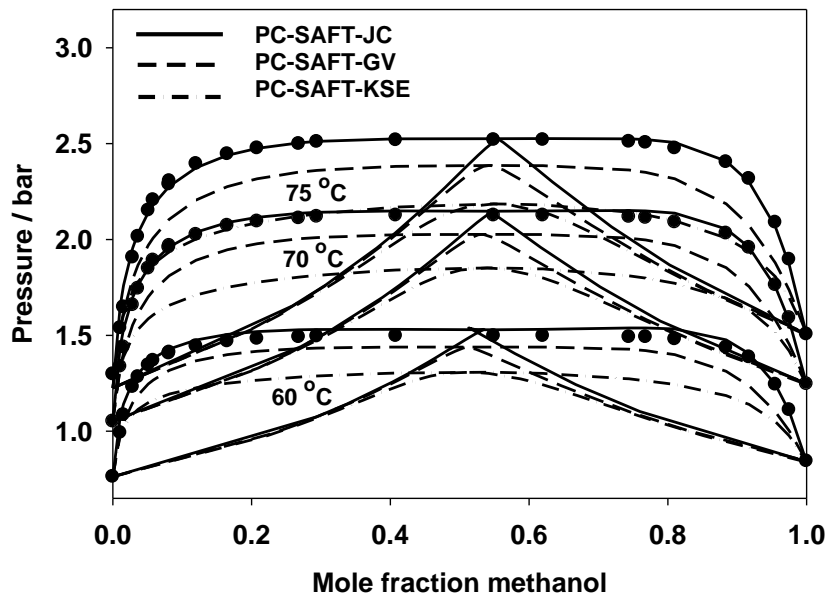


Figure 3.7 Predicted results of vapor-liquid equilibrium ( $k_{ij} = 0$ ) by the PC-SAFT-JC, PC-SAFT-GV and PC-SAFT-KSE for the methanol (1)/hexane (2) system at 60 °C, 70 °C, and 75 °C.

The PC-SAFT-GV improves the prediction of alcohol-hydrocarbon systems compared to non-polar PC-SAFT but the improvement is not as satisfactory as that obtained by the PC-SAFT-JC as seen in Figure 3.3 to Figure 3.7 and Table 3.2. However, the PC-SAFT-GV model is capable of representing some systems very well, such as the 2-butanol-propane shown in Figure 3.8. Moreover, the PC-SAFT-GV in general performs better than the PC-SAFT-JC for binaries with benzene and toluene, as well as the 2-butanol-propylene system.

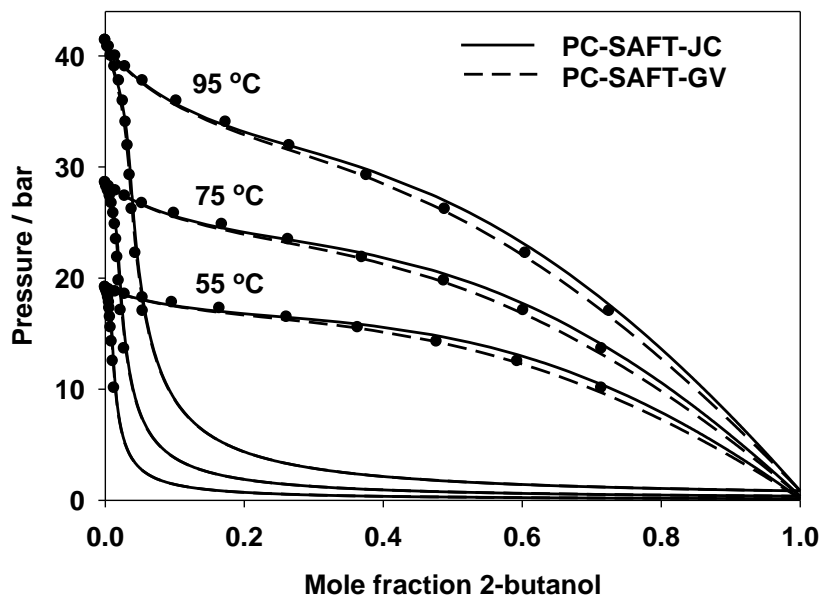


Figure 3.8 Predicted results of vapor-liquid equilibrium ( $k_{ij} = 0$ ) by the PC-SAFT-JC and PC-SAFT-GV for the 2-butanol (1)/propane (2) system at 55 °C, 75 °C, and 95 °C.

### 3.5.3.2 Alcohol-alcohol systems

The non-polar PC-SAFT is expected to perform satisfactorily for short-chain aliphatic alcohol-alcohol systems such as methanol-ethanol, methanol-2-propanol and ethanol-butanol because the degree of non-ideal behavior is not substantial in such systems due to similarity in size and interactions. Therefore, employing the dipolar PC-SAFT in these systems may not be necessary. This is shown in Table 3.4 where the AADs obtained by using the three polar SAFT models and the non-polar one are presented. As seen in the table the PC-SAFT-KSE is the most accurate for the ethanol/propanol system from 50 to 80 °C but not at 40 °C. As seen it is not necessary to include the dipolar term in order to predict the ethanol-1-propanol VLE phase behavior. However, when the size difference between the two molecules increases, the dipolar PC-SAFT performs better. For instance, ethanol-decanol and 1-propanol-decanol systems have been studied by Tamouza et al. (2005) by GC-SAFT. The absolute average deviations of pressure were found to be in the range of 10 to 14 % at different temperatures. This large deviation of pressure is significantly reduced by the PC-SAFT-JC to a maximum of 3 % as shown in Table 3.5. The PC-SAFT-JC gives quantitative representation for asymmetric alcohol-alcohol mixtures including 2-alcohols as shown in Table 3.5 for ethanol, propanol, 2-propanol with decanol binary

systems. PC-SAFT-KSE performs satisfactorily at some temperatures as shown on Table 3.5 and better than the PC-SAFT-GV except for 1-propanol-decanol system. The phase diagram of the ethanol-decanol system is shown in Figure 3.9. To explore more alcohol-alcohol systems, Figure 3.10 and Figure 3.11 show isobaric methanol-octanol system and ethanol-pentanol system at 75 °C. As seen both PC-SAFT-JC and PC-SAFT-GV predict the two systems quantitatively very well and better than the PC-SAFT-KSE. It should be noted that these two systems cannot be represented quantitatively by the non-polar PC-SAFT unless binary interaction parameters are introduced.

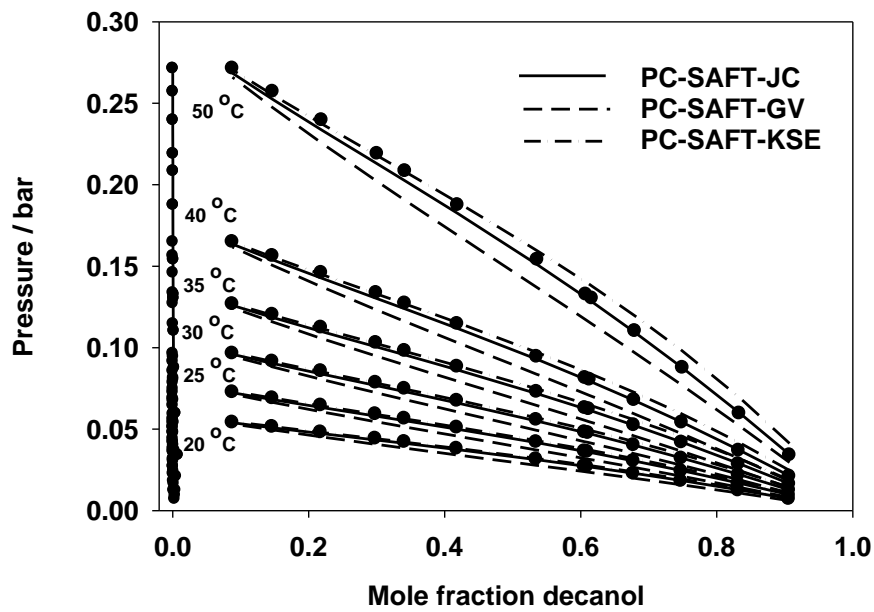


Figure 3.9 Predicted results of vapor-liquid equilibrium ( $k_{ij} = 0$ ) by the PC-SAFT-JC, PC-SAFT-GV and PC-SAFT-KSE for the 1-decanol (1)/ethanol (2) system at 20 °C, 25 °C, 30 °C, 35 °C, 40 °C and 50 °C.

Table 3.4 Predicted VLE results for short chain alcohol-alcohol system by PC-SAFT-JC, PC-SAFT-GV, PC-SAFT-KSE and non-polar SAFT.

system		T (°C)	PC-SAFT-JC		PC-SAFT-GV		PC-SAFT-KSE		non-polar PC-SAFT		N data pt	Ref.
			AAD P (%)	AAD y x 10 <sup>2</sup>	AAD P (%)	AAD y x 10 <sup>2</sup>	AAD P (%)	AAD y x 10 <sup>2</sup>	AAD P (%)	AAD y x 10 <sup>2</sup>		
methanol	ethanol	40	1.24	0.10	1.99	0.11	1.61	0.10	0.73	0.09	11	(Tamouza et al., 2005)
methanol	2-propanol	55	1.09	0.02	2.15	0.03	1.82	0.03	1.41	0.02	20	(Tai et al., 1972)
ethanol	propanol	40	0.07	0.00	0.61	0.00	2.22	0.03	1.05	0.01	11	(Singh & Benson, 1968)
		50	4.54	0.03	3.93	0.03	2.15	0.01	3.43	0.03	9	(Tamouza et al., 2005)
		60	4.71	0.03	4.03	0.04	2.12	0.01	3.54	0.03	9	(Tamouza et al., 2005)
		70	5.65	0.03	4.94	0.04	2.95	0.01	4.48	0.03	9	(Tamouza et al., 2005)
		80	4.73	0.04	3.99	0.04	1.92	0.02	3.56	0.03	9	(Tamouza et al., 2005)

Table 3.5 Predicted VLE results for alcohol-alcohol system by PC-SAFT-JC, PC-SAFT-GV and PC-SAFT-KSE.

system		T (°C)	PC-SAFT-JC		PC-SAFT-GV		PC-SAFT-KSE		N data pt	Ref.
			AAD P (%)	AAD <sub>y</sub> x 10 <sup>2</sup>	AAD P (%)	AAD <sub>y</sub> x 10 <sup>2</sup>	AAD P (%)	AAD <sub>y</sub> x 10 <sup>2</sup>		
ethanol	pentanol	75	1.40	1.28	2.44	1.23	5.36	1.72	11	(Singh et al., 1969)
methanol	decanol	20	2.83	0.00	9.37	0.00	3.99	0.00	10	(Nagashima et al., 2004)
		25	3.15	0.00	9.70	0.00	4.22	0.00	10	(Nagashima et al., 2004)
		30	3.52	0.00	9.98	0.00	4.52	0.00	10	(Nagashima et al., 2004)
		35	3.80	0.00	9.98	0.00	5.15	0.00	10	(Nagashima et al., 2004)
		40	4.53	0.00	10.4	0.00	5.29	0.00	10	(Nagashima et al., 2004)
		50	5.39	0.00	10.8	0.00	6.17	0.00	10	(Nagashima et al., 2004)
ethanol	decanol	20	1.42	0.00	9.86	0.00	3.21	0.00	13	(Nagashima et al., 2004)
		25	1.40	0.00	9.85	0.00	3.53	0.00	13	(Nagashima et al., 2004)
		30	1.39	0.00	9.79	0.00	3.92	0.00	13	(Nagashima et al., 2004)
		35	1.43	0.00	9.72	0.00	4.37	0.00	13	(Nagashima et al., 2004)
		40	1.49	0.00	9.64	0.00	4.84	0.00	13	(Nagashima et al., 2004)
		50	1.67	0.00	9.51	0.00	5.88	0.00	13	(Lancia et al., 1996)
propanol	decanol	20	3.13	0.00	9.79	0.00	13.9	0.00	12	(Lancia et al., 1996)
		25	2.97	0.00	9.45	0.00	12.4	0.00	12	(Lancia et al., 1996)
		30	2.84	0.00	9.16	0.00	11.0	0.00	12	(Lancia et al., 1996)
		35	2.69	0.00	8.86	0.00	9.65	0.00	12	(Lancia et al., 1996)
		40	2.56	0.00	8.61	0.00	8.44	0.00	12	(Lancia et al., 1996)
		50	2.45	0.00	8.30	0.00	6.49	0.00	12	(Lancia et al., 1996)
2-propanol	decanol	20	1.15	0.00	4.07	0.00	1.78	0.00	11	(Singh et al., 1969)
		25	0.76	0.00	4.25	0.00	1.97	0.00	11	(Singh et al., 1969)
		30	0.59	0.00	4.36	0.00	2.26	0.00	11	(Singh et al., 1969)
		35	0.58	0.00	4.49	0.00	2.57	0.00	11	(Singh et al., 1969)
		40	0.67	0.00	4.61	0.00	2.95	0.00	11	(Singh et al., 1969)
		50	1.20	0.00	4.99	0.00	3.90	0.00	11	(Singh et al., 1969)
ethylene glycol	1,2-propylene glycol	98	4.33	0.02	35.8	0.09	8.07	0.04	10	(Lancia et al., 1996)
		110	1.99	0.03	37.4	0.09	6.79	0.04	8	(Lancia et al., 1996)
		122	2.63	0.02	37.0	0.08	6.86	0.02	9	(Lancia et al., 1996)

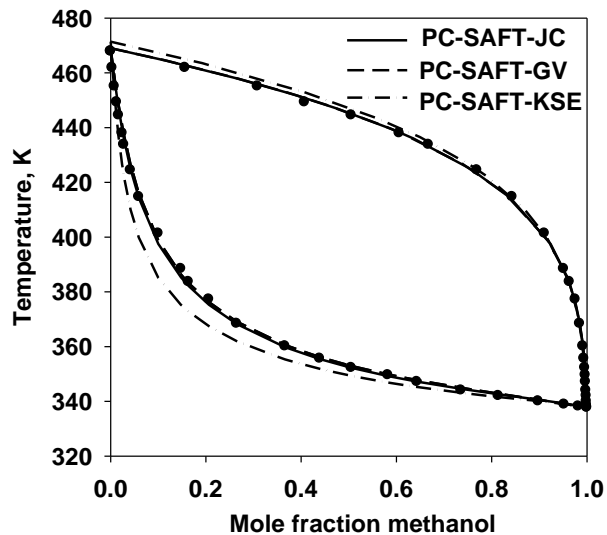


Figure 3.10 Predicted results of vapor-liquid equilibrium ( $k_{ij} = 0$ ) by the PC-SAFT-JC, PC-SAFT-GV and PC-SAFT-KSE for the methanol (1)/octanol (2) system at 1.013 bar.

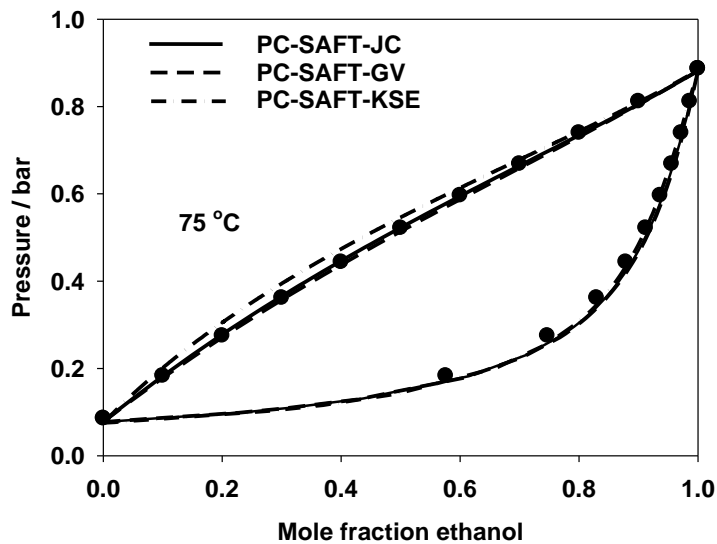


Figure 3.11 Predicted results of vapor-liquid equilibrium ( $k_{ij} = 0$ ) by the PC-SAFT-JC, PC-SAFT-GV and PC-SAFT-KSE for the ethanol (1)/pentanol(2) system at 75 °C.

Systems including glycols are very interesting because they have at least two polar functional groups. Unfortunately, VLE data for glycol-alcohol systems are scarce. However, excess enthalpy data for ethylene glycol with some monohydric alcohols systems were found (Nagashima et al., 2004). The ability of the PC-SAFT-JC model to predict these excess enthalpy data is demonstrated in Figure 3.12 for four systems with ethylene glycol at 35 °C. It is clear that the PC-SAFT-JC is capable of representing these systems satisfactorily. Surprisingly, the two other polar models did not perform as well. For example, the AAD in excess enthalpy for PC-SAFT-KSE and PC-SAFT-GV were respectively as follows (>100, 72.7%) for methanol, (85.8, 11.7%) for ethanol, (>100%, >100%) for propanol and (26.1, 97%) for 2-propanol at 35 °C. The AADs in excess enthalpy for PC-SAFT-JC for these systems were 9.9, 8.7, 4.8 and 4.7%. Apparently, a binary interaction parameter is required in order to have quantitative representation with PC-SAFT-KSE and PC-SAFT-GV.

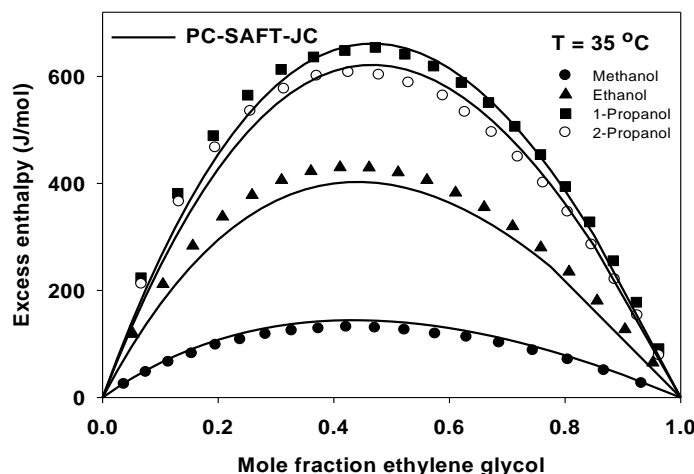


Figure 3.12 Predicted excess enthalpy ( $k_{ij} = 0$ ) by the PC-SAFT-JC for the ethylene glycol(1)/methanol (2)/ethanol(2)/propanol(2)/2-propanol(2) systems at 35 °C.

It is also important to demonstrate the influence of temperature on the predictive capability of the PC-SAFT-JC for the same systems. Figure 3.13 shows the excess enthalpy data for these systems at 25 °C. It is clear that the PC-SAFT-JC compares with the data at 25 °C equally well for 2-propanol. It does slightly better for ethanol but slightly worse for methanol and 1-propanol.

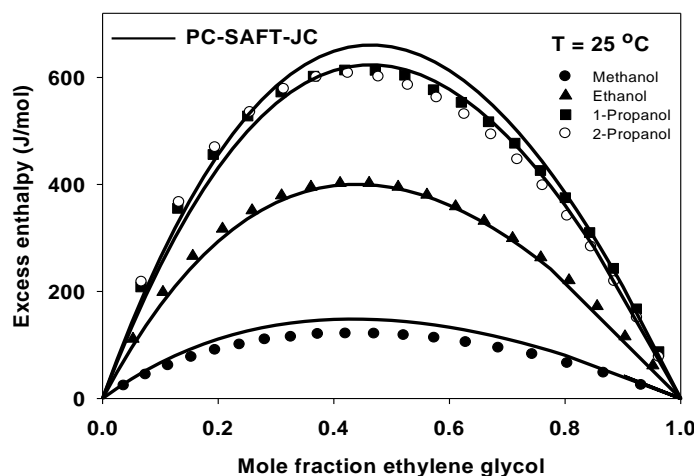


Figure 3.13 Predicted excess enthalpy ( $k_{ij} = 0$ ) by the PC-SAFT-JC for the ethylene glycol(1)/methanol(2)/ethanol(2)/propanol(2)/2-propanol systems at 25 °C.

Finally, systems where each component has two dipolar functional groups such as ethylene glycol-1,2-propylene glycol are modeled with the PC-SAFT-JC equation of state. The maximum absolute average deviation in pressure was found to be 4.3 % at 98 °C. The AAD in pressure decreases at higher temperatures as seen in Table 3.5. It is also seen in this table that the PC-SAFT-KSE performs better than PC-SAFT-GV for the ethylene glycol-1,2-propylene glycol system.

### 3.5.3.3 Water-alcohol and water-hydrocarbon systems

In this section, different alcohols having one and two dipolar functional groups are considered. Table 3.6 lists the water-alcohol systems tested and the AADs obtained by the PC-SAFT-JC model. The other two polar models (PC-SAFT-GV and PC-SAFT-KSE) were also employed and it was found that the minimum of AADs in pressure was around 9 %. As seen this is considerably higher than those obtained by the JC version. It is conceivable that the GV and KSE versions can perform better if one searches for other pure component parameter sets for water. Furthermore, because the number of suggested association sites (two, three or four) for water is not consistent in the literature, one could also take that into consideration. In this study,

two association sites are assumed. The prediction capability of the JC version for simple aliphatic alcohols is found to be very satisfactory except at low temperatures. For instance, the ethanol-water phase behavior is represented well from 79 to 350 °C. However, at 30 °C the absolute average deviation in pressure is 9 % as shown in Table 3.6. The PC-SAFT-JC also represents 2-propanol-water system without the need to introduce a binary interaction parameter from 150-300 °C as shown in Figure 3.14 and Table 3.6.

Glycol-water systems were also examined. Table 3.6 shows the AADs for ethylene glycol, 1,2-propylene glycol systems with water at three different temperatures. These two systems have also been studied by Li and Englezos (2003) using the original non-polar SAFT (Chapman et al., 1990) by adjusting the SAFT to two binary interaction parameters, namely dispersion and association interaction parameters. It was found that PC-SAFT-JC is capable of representing the phase behaviour equally well but without the need for any adjustable binary parameters. Figure 3.15 and Figure 3.16 show the prediction capability of the PC-SAFT-JC for the ethylene glycol and 1, 2-propylene glycol systems with water. As seen the predictions compare very well with the data.

Table 3.6 Predicted VLE results for water-alcohol system by PC-SAFT-JC.

system		T (°C)	PC-SAFT-JC		N data pt	Ref.
			AAD P (%)	AAD $y \times 10^2$		
water	methanol	60	5.53	0.01	18	(Kurihara et al., 1995)
water	ethanol	30	9.56	0.15	23	(Kurihara et al., 1995)
		50	4.09	0.08	24	(Kurihara et al., 1995)
		70	0.97	0.03	24	(Kurihara et al., 1995)
		90	1.56	0.01	24	(Barr-David & Dodge, 1959)
		150	2.16	0.03	17	(Barr-David & Dodge, 1959)
		200	2.22	0.05	17	(Barr-David & Dodge, 1959)
		250	1.28	0.05	18	(Barr-David & Dodge, 1959)
		275	1.32	0.06	13	(Barr-David & Dodge, 1959)
		300	0.94	0.10	9	(Barr-David & Dodge, 1959)
		325	1.16	0.10	7	(Barr-David & Dodge, 1959)
		350	1.17	0.17	4	(Barr-David & Dodge, 1959)
water	2-propanol	150	2.32	0.06	19	(Barr-David & Dodge, 1959)
		200	2.15	0.04	18	(Barr-David & Dodge, 1959)
		250	0.76	0.06	16	(Barr-David & Dodge, 1959)
		275	1.01	0.06	18	(Barr-David & Dodge, 1959)
		300	1.27	0.24	6	(Barr-David & Dodge, 1959)
water	1,2-propylene glycol	98	2.32	0.11	10	(Lancia et al., 1996)
		110	3.80	0.10	11	(Lancia et al., 1996)
		122	4.48	0.08	10	(Lancia et al., 1996)
water	ethylene glycol	98	6.29	0.34	12	(Lancia et al., 1996)
		110	4.79	0.23	14	(Lancia et al., 1996)
		122	4.02	0.14	16	(Lancia et al., 1996)

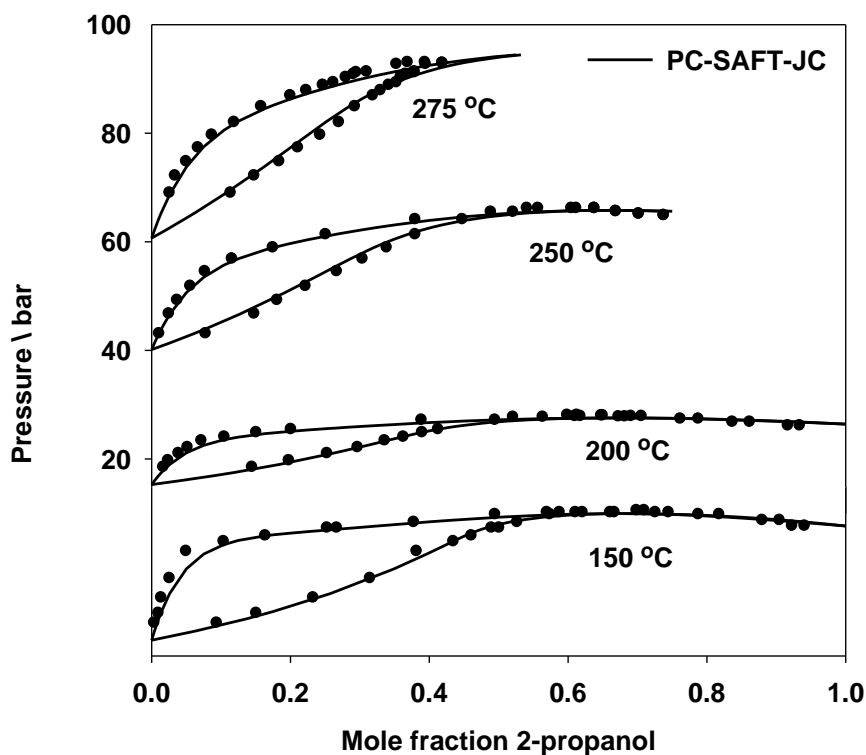


Figure 3.14 Predicted results of vapor-liquid equilibrium ( $k_{ij} = 0$ ) by the PC-SAFT-JC for 2-propanol (1)/water(2) system at 150 °C, 200 °C, 250 °C and 275 °C.

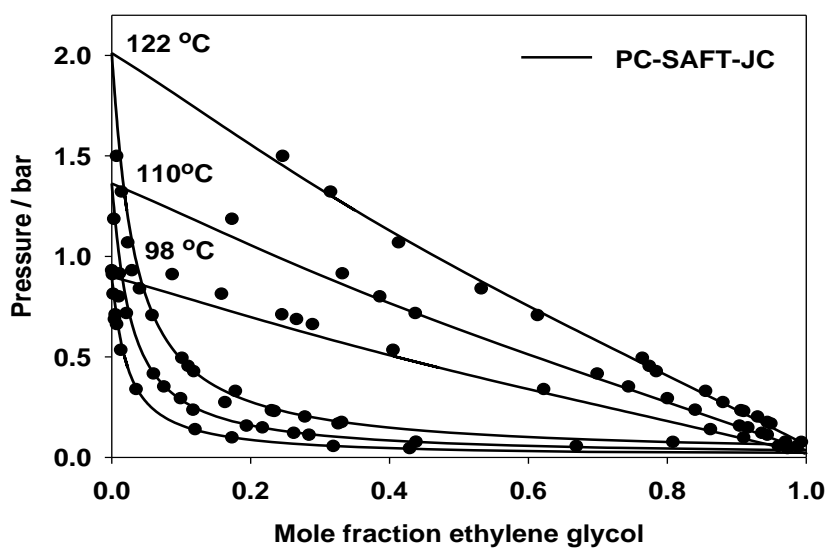


Figure 3.15 Predicted results of vapor-liquid equilibrium ( $k_{ij} = 0$ ) by the PC-SAFT-JC for ethylene glycol (1)/water(2) system at 98 °C, 110 °C and 122 °C.

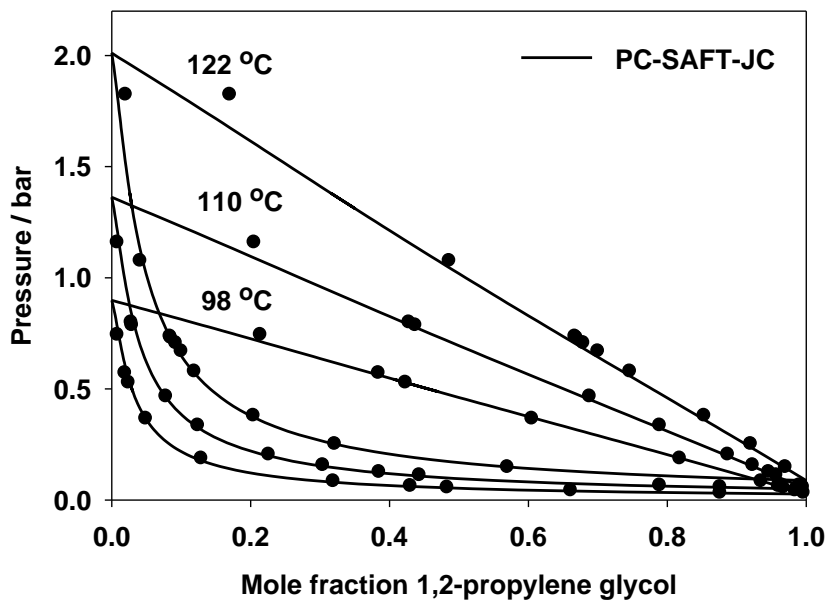


Figure 3.16 Predicted results of vapor-liquid equilibrium ( $k_{ij} = 0$ ) by the PC-SAFT-JC for propylene glycol (1)/water(2) system at 98 °C, 110 °C and 122 °C.

The three dipolar PC-SAFT versions were found to improve the prediction of the hydrocarbon-water systems. However, the results are not satisfactory at high temperatures. Figure 3.17 shows water-propane data at different temperatures along with predictions by the PC-SAFT-JC and PC-SAFT-GV models. The prediction capability is satisfactory at 65.5 and 110 °C but not at 148.9 °C.

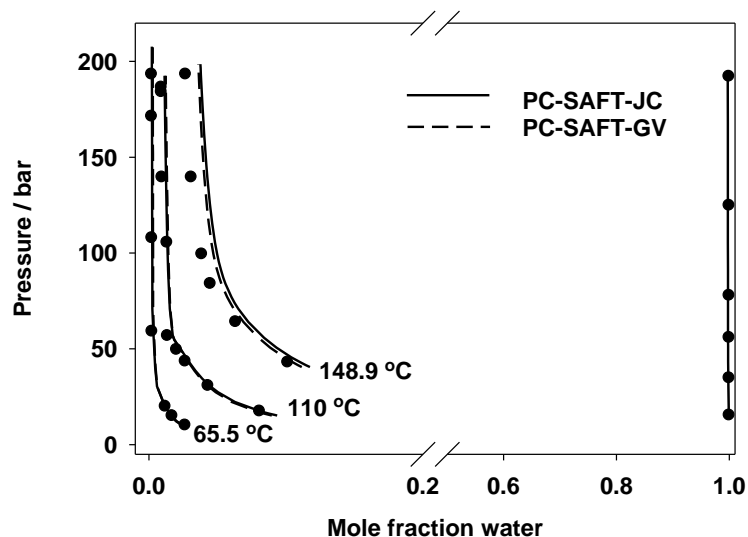


Figure 3.17 Predicted results of vapor-liquid equilibrium ( $k_{ij} = 0$ ) by the PC-SAFT-JC and PC-SAFT-GV for water (1)/propane(2) system at 65.5 °C, 110 °C and 148.9 °C.

### 3.6 Discussion

Based on the results obtained in this work it is clear that the incorporation of the dipolar term to the PC-SAFT for modeling associating compounds requires an effective optimization technique to estimate the pure component parameters values. The simplex method provides a suitable optimization technique that significantly reduces the number of parameter sets that give accurate correlation of the pure data. In many cases, it was possible to obtain the unique solution. For the PC-SAFT-JC, estimating the unique solution of one component enabled fixing the value of the product  $mx_p$  for the rest of the components within a homologous series. For alcohols with one functional group, the product was found to be equal to 0.7 while for glycols with two dipolar functional groups, it was 1.5. Therefore, this product can be fixed when one requires parameter values for specific compounds that are not available in Table 3.1 to avoid any complexities.

The performance of the dipolar terms differs depending on the chosen systems. In most of the studied systems, it was found that the performance of the PC-SAFT-JC is superior. However, for systems such as short-chain alkanol-aromatic hydrocarbon systems, the performance of the PC-SAFT-GV is better. Although both PC-SAFT-JC and PC-SAFT-GV

approaches successfully predict the VLE behaviour of alcohol-hydrocarbon systems, they predict erroneous phase behavior for certain methanol-hydrocarbon systems at temperatures  $< 40$  °C for PC-SAFT-GV and  $< 70$  °C for PC-SAFT-JC. On the other hand it is noted that the PC-SAFT-KSE (Economou term) did not predict erroneous liquid-liquid splitting.

The PC-SAFT-JC was satisfactorily capable of predicting glycol systems having two dipolar functional groups without the need to introduce a binary interaction parameter. It has been shown that the magnitude of the dipolar interactions for the PC-SAFT-JC is larger than those of the PC-SAFT-GV and PC-SAFT-KSE. That gives the PC-SAFT-JC the capability to predict highly non-ideal systems such as alcohol-hydrocarbon systems. For the water-hydrocarbon systems, the prediction capability of the dipolar PC-SAFT is less satisfactory than that for alcohol-hydrocarbon, alcohol-alcohol and water-alcohol systems.

Although quantitative representation of the phase behavior was possible in many systems the prediction capability was not the same at all temperatures. One reason is that the effect of polarizability was not taken into account. For example, the average dipole moment of water approximately equals 2.5 in the bulk liquid (Shirono & Daiguji, 2006) while it is equal to 1.85 in the gas phase (Clough et al., 1973).

### 3.7 Conclusions

In this chapter, the dipolar PC-SAFT has been employed to predict phase equilibria of binary systems of water-alcohol-hydrocarbon using three dipolar terms. Pure compound parameters were correlated using vapor pressure and liquid density for alcohols including glycols having two dipolar functional groups. It was found that the simplex technique is more appropriate than the Gauss Newton method with the Marquardt-Levenberg correction that is commonly used. The simplex method considerably decreases the number of parameter sets that produce accurate correlation of the pure data and in many cases, it provides a unique solution. The predictive capability has been investigated and compared for the three dipolar term with the PC-SAFT. Quantitative representation was possible for several cases using the dipolar PC-SAFT. In general, it was found that the Jog and Chapman term is superior to the other two dipolar terms. However, its predictive capability for some systems such as methanol and ethanol with benzene and toluene is not as good.

## CHAPTER 4

# MULTIPHASE EQUILIBRIUM AND SIMULTANEOUS TESTING OF PHASE STABILITY

### 4.1 Introduction

In the previous chapter, the predictive calculations were limited to vapour-liquid equilibrium (VLE). VLE calculations are simple compared to the computation of other classes of phase equilibrium such as liquid-liquid (LLE) and vapour-liquid-liquid (VLLE). A survey of the literature reveals that attention was almost always confined to vapour-liquid equilibrium when theory-based equations of state are utilized. Very little attention has been paid to other multiphase classes of phase equilibrium although they play an essential role in simulation and design of chemical processes such as distillation and extraction.

Most equations of state in general fail to give accurate representation of mixtures in LLE and VLLE. Thus, evaluation of any theory-based EOS with any sort of modification should not be limited to VLE mixtures; it should however be expanded to multiphase systems to show how powerful that EOS is. Unfortunately, the multiphase computations are complicated and the complexity increases when theory-based EOS is utilized. The foundation of multiphase methods, as chemical engineers use it today, has been established in early 1980s and has been attributed to the pioneering work of Baker (1981), Michelsen (1982) and Heidemann (1983). Although extensive work has been carried out since that time, the computation of multiphase systems is still not easy to conduct or even digest for the newcomers who want easy and efficient methods.

In this chapter, we present and modify an elegant method which is simpler than those developed by Baker and Michelsen. The method is based on the work of Gupta et al. (1990; 1991). Although Gupta et al.'s method presented advantages over other methods available in literature, their algorithm has some weaknesses. For instance, the algorithm fails to converge when phase fraction approaches zero (Abdel-Ghani, 1995). Furthermore, they were unable to utilize an equation that was derived for stability and phase fraction without modification (equation 4-8). The proposed algorithm in this chapter presents a solution to these weak points,

explores new features and shows how to conduct stability and multiphase equilibrium calculations using SAFT. The theory based-equation used is mainly PC-SAFT with the incorporation of various interactions such as hydrogen bonding, dipolar and quadrupolar terms. The adjustable parameter of PC-SAFT is given in Table A.1 in **Appendix A**. Other equations of state are also utilized such as simplified SAFT and CK-SAFT. For the dipolar and quadrupolar terms, the developments by Gross' group are utilized in this chapter. The mathematical description of the dipolar term was given in **Chapter 3** (section 3.3.2). The quadrupolar term is given in Chapter 5 (section 5.2.1). The suggested algorithm is tested on water-alcohol-hydrocarbon-CO<sub>2</sub> mixtures.

This chapter is organized as follows: section 4.2 summarizes the approaches that are normally followed for conducting multiphase equilibrium calculations; section 4.3 highlights the challenge in multiphase calculations. Then, section 4.4 is devoted to Gupta et al.'s method and in section 5.5, the proposed algorithm is given. The rest of this chapter is devoted to the evaluation of the proposed algorithm. Finally, conclusions are given in section 4.7.

## **4.2 Multiphase equilibrium calculations**

The most common procedure utilized for multiphase calculations is the so-called flash calculation. The problem statement is simply given as follows: for a mixture exhibiting any number of phases coexisting in equilibrium; and the feed compositions ( $z$ ), temperature ( $T$ ) and pressure ( $P$ ) are given, determine the vapour and liquid compositions of each component in mixture. The calculation is generally carried out either by the Gibbs energy minimization method or equation-solving techniques. In equation-solving techniques, finding the mole fraction of phases is also required.

### **4.2.1 The Gibbs energy minimization method**

If we consider a system of  $N$  components and  $\pi$  phases at specified temperature ( $T$ ) and pressure ( $P$ ), then the Gibbs free energy of this system is given by:

$$G = \sum_{k=1}^{\pi} \sum_{i=1}^N n_{ik} \mu_{ik} \quad 4-1$$

where  $n_{ik}$  is the number of moles of each component  $i$  in phase  $k$  whereas  $\mu_{ik}$  is the chemical potential of component  $i$  in phase  $k$ . The objective of phase equilibrium calculation is to minimize the Gibbs free energy over all possible states to determine the number of moles ( $n_{ik}$ ) of each component  $i$  in phase  $k$ . The determination of the number of moles should satisfy two constraints. The first constraint is the conservation of the total number of moles:

$$\sum_{k=1}^{\pi} n_{ik} = z_i \quad 4-2$$

where  $z_i$  represents the feed composition of component  $i$ . The second constraint is to make sure that the number of moles of a component in a phase are always positive:

$$n_{ik} \geq 0 \quad (i = 1, \dots, N; k = 1, \dots, \pi) \quad 4-3$$

Various methodologies have been developed under the abovementioned minimization approach by many researchers. Examples of those who follow this approach are Heidemann (1974), Gautam & Seider (1979), Soares et al. (1982), Castier et al. (1989), Song & Larson (1991), Pan & Firoozabadi (1998) and Lucia et al. (2000).

#### 4.2.2 Equation-solving technique

An alternative and equivalent route for the determination of phase equilibrium can be obtained by equation-solving techniques rather than minimization. The equivalency arises from the fact that the determination of the Gibbs free energy at a minimum is equivalent to the equality of component fugacities. The equation-solving techniques combine mass balances and equilibrium relations into a set of non-linear algebraic equations. Different approaches have been suggested for equation-solving techniques (Gupta et al., 1990; Gupta et al., 1991; Han & Rangaiah, 1998). There are many approaches that follow the class of equation-solving techniques in computing multiphase equilibria. The governing equations differ from method to method but they are all based on the combination of mass balances and equilibrium relations. The reader could consult Teh and Rangaiah (2002) for details of some of these approaches. The Gupta et al.

method is of equation solving technique type. Thus, the governing equations are given in section 4.4.

### **4.3 Challenge of the multiphase equilibrium calculations**

The above two approaches are commonly utilized in the literature depending upon the preferences of their users. Irrespective of which method is adopted, the essence of phase equilibrium calculations is always to ensure the determination of the global minimum Gibbs free energy of a system at fixed isothermal and isobaric conditions. The main challenge in multiphase equilibrium calculations is that the number of the available phases in a system at equilibrium is not known a priori. A common way to overcome the encountered phase difficulty is to utilize stability criteria (Baker et al., 1981; Michelsen, 1982) to determine whether an obtained solution is thermodynamically stable. This can be handled either by assuming a fixed number of phases and checking the stability of the final solution (Iglesias-Silva et al., 2003) or by following a sequential procedure by adding a phase in the computation and testing the stability (Gautam & Seider, 1979; Michelsen, 1982; Nghiem & Li, 1984; Wu & Bishnoi, 1986).

### **4.4 Gupta et al.'s method**

In this section, the Gupta et al is explored and the governing equations are given. Then, the proposed algorithm of Gupta et al. to solve the governing equation is presented.

#### **4.4.1 Governing equations of the Gupta et al. method**

The Gupta et al. method formulates the problem as a set of coupled non-linear equations that describe phase equilibrium, chemical equilibrium and the stability of the system with inequality constraints. Thus, it is an equation-solving technique type that combines mass balance and equilibrium relations as well as stability equations with inequality constraints. The advantages of the Gupta methodology are its simplicity and its ability to provide insight into the phase behaviour as it tracks the appearance or disappearance of the phases. In principle, the method presents the necessary and sufficient conditions for phase equilibrium and it offers a simple and clear stability criterion for multiphase reacting/non-reacting systems at a fixed pressure and temperature.

The appropriate set of equations which describe the stability and the isothermal-isobaric flash calculations of reacting and non-reacting systems are formulated by Gupta et al (1990; 1991). The main governing equations of non-reacting systems at constant pressure and temperature are summarized here as follows:

**Phase fraction summation**

$$\sum_{k=1}^{\pi} \alpha_k = 1 \quad 4-4$$

where  $\pi$  is the number of phases and  $\alpha_k$  is the phase fraction.

**Mole fraction summation**

$$\sum_{i=1}^N (K_{ik} e^{\theta_k} - 1) x_{ir} = 0 \quad (k = 1, \dots, \pi; k \neq r) \quad 4-5$$

$$x_{ir} = z_i / \left[ \left( \sum_{i=1}^{nc} z_i \right) \left( 1 + \sum_{\substack{j=1 \\ j \neq r}}^{\pi} (K_{ij} e^{\theta_j} - 1) \alpha_j \right) \right] \quad (i = 1, \dots, N; j = 1, \dots, \pi; j \neq r) \quad 4-6$$

**Phase equilibrium and stability relations**

$$x_{ik} = K_{ik} x_{ir} e^{\theta_k} \quad (i = 1, \dots, N; k = 1, \dots, \pi; k \neq r) \quad 4-7$$

$$\alpha_k \theta_k = 0 \quad (k = 1, \dots, \pi; k \neq r) \quad 4-8$$

Subject to

$$\alpha_k \geq 0 \quad \text{and} \quad \theta_k \geq 0 \quad 4-9$$

where

$$K_{ik} = \varphi_{ir} / \varphi_{ik} \quad 4-10$$

In the above equations,  $\mathbf{z}$  is feed composition,  $\mathbf{x}$  is mole fraction,  $\theta_k$  is the stability variable,  $N$  is the number of components and  $\varphi_{ik}$  is the fugacity coefficient of component  $i$  in phase  $k$ . Furthermore, subscript  $r$  denotes a reference phase. The number of equations required to describe the phase equilibrium and stability of a specific system at a fixed temperature and pressure is equal to  $[\pi(N+2) - 1]$  for  $[\pi(N+2) - 1]$  unknowns, namely  $(\pi) \alpha_k$ ,  $(\pi-1) \theta_k$  and  $(N.\pi)x_{ik}$ . It should be emphasized that equations 4-8 and 4-9 imply that either the phase fraction ( $\alpha_k$ ) or the stability variable ( $\theta_k$ ) or both must be zero. In case the phase fraction becomes zero, this indicates that the stability variable must be either a positive for an unstable phase or zero for an incipient phase. In a similar manner, if the stability variable becomes zero, then the phase fraction must be positive for a stable phase or zero for an incipient phase. These possible cases for phase ( $k$ ) are summarized in Table 4.1. It should be noted that equations 4-8 and 4-9 give the relationship between stability variables and phase fraction at the global minimum of Gibbs energy. Finally, as demonstrated by Gupta et al., at the point of minimum Gibbs free energy, the stability variables must satisfy the following relation which is written in terms of fugacity ( $f_{ik}$ ):

$$\theta_k = \ln \left( \frac{f_{ik}}{f_{ir}} \right) \quad (i = 1, \dots, N; k = 1, \dots, \pi; k \neq r) \quad 4-11$$

Table 4.1 State of Phase  $k$  in equations 4-8 and 4-9.

	Stability variable ( $\theta_k$ )	Phase fraction ( $\alpha_k$ )	State of Phase $k$
Case I	zero	positive	stable
Case II	positive	zero	unstable
Case III	zero	zero	incipient

#### 4.4.2 Gupta et al. algorithm

As discussed in the previous section, the proposed methodology of Gupta et al. (1991) for simultaneous stability and multiphase flash calculation provided a unified set of simultaneous non-linear equations with inequality constraints. Gupta et al. have proposed to partition the system of equations into two groups to be solved in two nested loops. The first group consisted of

equations 4-4, 4-5 and 4-6. These equations were solved for phase fractions ( $\alpha_k$ ) and stability variables ( $\theta_k$ ) by the Newton-Raphson method in the inner loop. The second group consisted of equations 4-6 and 4-7 in the outer loop to calculate mole fractions. The mole fractions were updated in the outer loop and accelerated by the use of the General Dominant Eigenvalue Method (GDEM) (Crowe & Nishio, 1975). The K-values, which were initiated with Michelsen stability analysis (Michelsen, 1982), were re-calculated from equation 4-10 by the use of a chosen model in the outer loop. As previously indicated, modifications were included in their work to avoid singular and ill-conditioned Jacobian. The stability equation (equation 4-8) was replaced by the following equation:

$$\frac{\alpha_k \theta_k}{(\alpha_k + \theta_k)} = 0 \quad 4-12$$

The equation describes the equivalent behaviour of equation 4-8 in the appearance and disappearance of a phase. It improves the conditioning of Jacobian significantly. The singularities of the Jacobian, when both phase fraction and its corresponding stability variable become zero, were also avoided in the way that both would never become equal to zero during computation. Furthermore, during computations, the phase fractions become negative which of course violates inequality 4-9. In that case Gupta et al. forced the phase fraction to be zero. The corresponding stability variable was then re-calculated from equation 4-5.

Moreover, during computations, some of the appearing phases may have the same compositions and compressibility (i.e. trivial solution). If that occurs, Gupta et al. suggested adding the phases together to decrease the number of phases and the next computations were performed only for the distinct phases.

## 4.5 The proposed algorithm

In this section, the proposed algorithm is given and its advantages over Gupta's methodology are discussed. Similar to Gupta et al. approach, equations 4-4, 4-5 and 4-6 are solved in the inner loop but without modifying equation 4-8 and with the inclusion of the inequality constraint (equation 4-9). This requires an iterative method other than Newton-Raphson method which cannot handle inequality constraints. A recent iterative method which could solve systems of nonlinear equalities and inequalities has been proposed by Macconi et al. (2009). The method will be referred as trust-region Gauss-Newton method. It is implemented

efficiently using MATLAB in a solver called TRESNEI (Morini & Porcelli, 2010). Unlike the Newton-Raphson method, the trust-region Gauss-Newton method is capable of handling inequality constraints and has global convergence properties. The use of TRESNEI will avoid some of the tedious Gupta et al work of controlling phase fraction and re-calculated stability variable. TRESNEI would help to obtain phase fraction and stability variables from solving directly equations 4-4, 4-5, 4-8 and 4-9.

Similar to Gupta et al., the mole fraction vector is selected as the iterative variable in the flash computations. However, our updating procedure differs from that of Gupta et al. The updating procedure of Kinoshita and Takamatsu (1986) is utilized in our approach. We found that the Kinoshita and Takamatsu updating procedure is relatively insensitive to the initial estimates of mole fraction. The combination of trust-region Gauss-Newton method and Kinoshita and Takamatsu makes it possible to avoid Gupta's initialization strategies, particularly for water-hydrocarbon containing systems.

The initial estimates of mole fraction are based on specifying a value of 0.99 to any potential component that may form liquid and to the lightest component in the vapour phase. This initialization is found to be effective for water-hydrocarbon containing systems. For example, the water-pentane system might form a maximum of three phases (Vapour-Liquid-Liquid). It is adequate in our approach to start with a mole fraction value of 0.99 for pentane in the pentane rich liquid-phase, a value of 0.99 for water in the water-rich liquid phase and a value of 0.99 for the lightest component in the vapour phase.

Unlike Gupta et al. algorithm, the current algorithm doesn't encounter a problem when the phase fraction approaches zero. Furthermore, an important feature of the current algorithm is its ability to handle more than one absent phase (more than one unstable phase) at the same time. The feature would assist in figuring out which absent phases would appear first when one changes P-T conditions. This feature will be illustrated further in section 4.6.1.1.

As previously indicated, SAFT is utilized in this work. SAFT is not cubic and the method of finding density (or volume) roots differs from that of cubic equations of state. To determine density roots, it is necessary to use a reliable iterative method for solving the equation of state for density. It is also important to use a small termination tolerance on the function value ( $\epsilon=10^{-14}$ ). TRESNEI works effectively in finding density roots. Besides TRESNEI, we tested trust-region

dogleg method, which is a variant of the Powell dogleg method (Rabinowitz, 1970). This method is also successful in finding the density roots of all the cases that have been studied. There are other reported reliable methods that could be used to find density roots of SAFT such as the extended dogleg method (Aslam & Sunol, 2006), homotopy continuation (Lucia & Luo, 2001), and interval analysis (Xu et al., 2002).

## **4.6 Evaluation of the proposed algorithm**

In this section, several examples are considered for evaluating the proposed scheme of several systems. In all studied systems, the binary interaction parameter is set to zero. Of course, the PC-SAFT may not be able to predict accurately the behaviour of many systems if binary interaction parameters are not employed. However, it is interesting to assess SAFT as a predictive tool as will be demonstrated in next chapter.

### **4.6.1 Water/octane/hexane/pentane/butane/propane mixture**

The first considered mixture is a synthetic system of water and paraffins. The system has been studied before by Heidemann (1974), Peng and Robinson (1976) and Erbar (1973). The overall mole composition is made up of 0.1667 propane, 0.1667 n-butane, 0.2 n-pentane, 0.0667 hexane, 0.1333 n-octane and 0.2667 water. The PC-SAFT with the proposed methodology is applied to study this mixture at fixed pressure ( $P = 24.1$  bar) and a temperature range of 390 to 460 K. Both association and dipolar terms are included to take account of hydrogen bonding and dipole-dipole interactions of water molecules, respectively. The condensation curves are obtained and shown in Figure 4.1. The general characteristic of the curves are similar to those obtained before (Heidemann, 1974; Erbar, 1973; Peng & Robinson, 1976) although different equations of state were utilized. As seen in Figure 4.2, when the mixture is cooled from its vapour state, the formation of a hydrocarbon-rich liquid phase appears first.

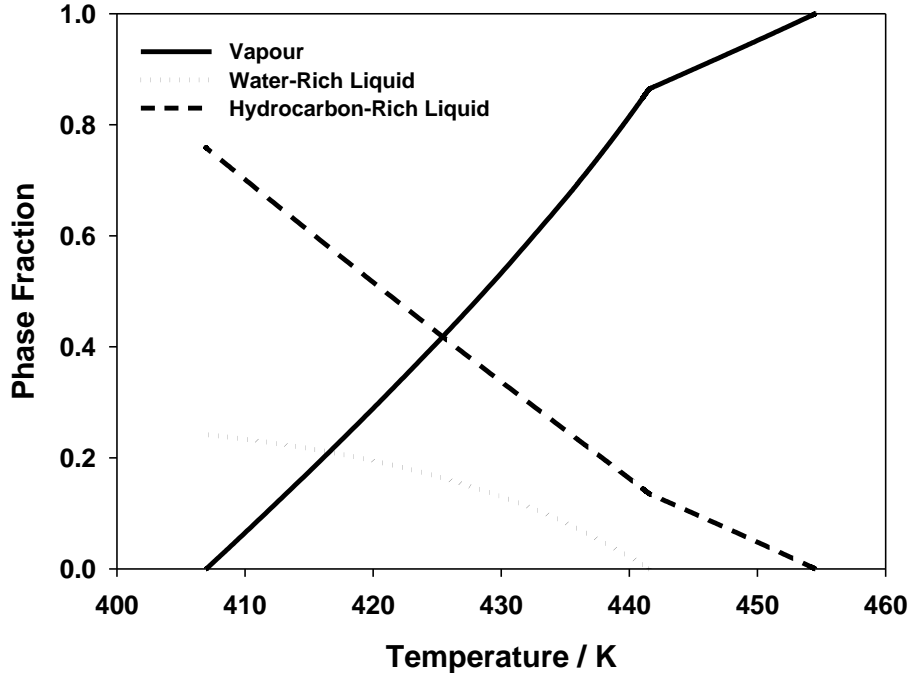


Figure 4.1 Phase composition of water-paraffin mixture at 24.1 bar predicted by dipolar PC-SAFT.

To demonstrate the proposed scheme, it is advantageous to show the computational details in this example. It should be noted that the system may have up to three phases in the selected temperature range (Vapour only, Vapour-Liquid, Liquid-Liquid and Vapour-Liquid-Liquid). An isobaric (24.1 bar) temperature path is followed by starting from 460 K (vapour only) to 390 K (Liquid-Liquid). We assume that the system consists of a maximum of three phases and the vapour is the reference phase. The reference phase could be switched to one of the liquid phases when the system doesn't show vapour phase as demonstrated below. Table 4.2 shows values for the phase fractions and stability variables for this mixture for seven temperatures from 390 to 460 K at 24.1 bar. The initial values of phase fractions and stability variables are arbitrary and set to zero in this example. In the following, computation details of Table 4.2 are demonstrated for each region.

#### 4.6.1.1 One phase region (vapour only)

At a temperature equal to 460 K, the vapour phase fraction is equal to 1 and the other two phase fractions of liquid phases are zero. This indicates that the two liquid phases are absent and

we only have a vapour phase. Although one could delete a phase from the three phases during computation when the system shows only one phase (here vapour phase), the computation is conducted without deleting any phase. The stability variables of the two liquid phases at this temperature are positive (0.4816 for water-rich liquid phase and 0.05660 for hydrocarbon-rich liquid phase). The stability variable value of the hydrocarbon-rich liquid phase is much less than that of the water-rich liquid phase. This indicates that decreasing the temperature makes the hydrocarbon-rich liquid phase appear first. This feature has been explored from using our proposed algorithm that, unlike Gupta et al.'s algorithm, could handle more than one absent phase.

The change of phases and stability variables vs. iteration number are depicted in Figure 4.2. The figure illustrates the effectiveness of the proposed scheme with the trust-region Gauss-Newton method in providing fast convergence. Computation is started with zero values for stability variables and phase fractions. As iteration proceeds, the phase fraction of the vapour ( $\alpha_V$ ) and hydrocarbon-rich liquid ( $\alpha_{L_{HC}}$ ) appear first while the water-rich liquid phase ( $\alpha_{L_W}$ ) remains zero and its stability variable ( $\theta_{L_W}$ ) becomes positive. At the third iteration, the hydrocarbon-rich liquid phase disappears and its stability variable ( $\theta_{L_{HC}}$ ) attains a positive value. Both liquid stability variables converge to positive values while their phase fractions become zero indicating that they are unstable phases. The smaller magnitude of the stability variable of hydrocarbon-rich liquid phase confirms the behaviour observed before in Figure 4.1 in which hydrocarbon-rich liquid phase would appear first if temperature is decreased.

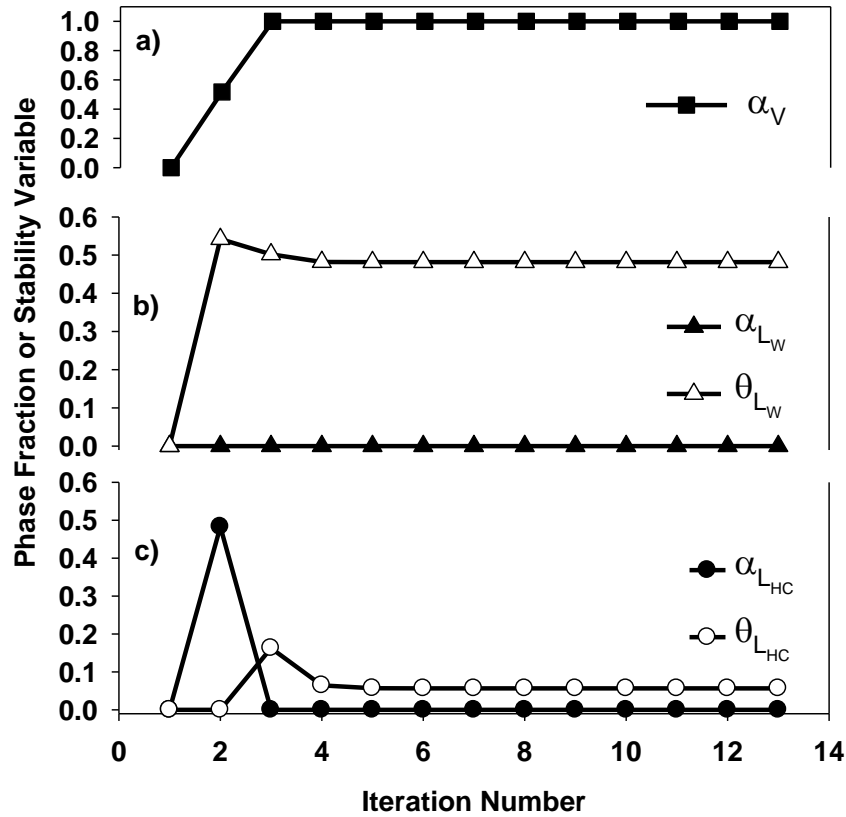


Figure 4.2 Phase fraction ( $\alpha$ ) and stability variable ( $\theta$ ) vs. iteration number for water-paraffin mixture at 24.1 bar and 460 K for: a) Vapour (stable); b) Water-rich liquid phase (unstable); c) Hydrocarbon-rich liquid phase (unstable).

#### 4.6.1.2 Incipient hydrocarbon-rich liquid and vapour-liquid phase region

As the temperature is decreased, the hydrocarbon-rich liquid phase is about to appear at 454.513 K where both its phase fraction and stability variable are zero as shown in Table 4.2. This demonstrates that at this condition (24.1 bar and 454.513 K) the hydrocarbon-rich liquid phase is incipient and a slight decrease in temperature brings the system to the two phase region; namely vapour and hydrocarbon-rich liquid phases. An example of the vapour and hydrocarbon-rich liquid phase is at a temperature of 450 K. The phase fraction of the water-rich liquid phase is still zero at this temperature indicating that it is absent and its stability variable is still positive (0.2382). Therefore, the water-rich liquid phase is still unstable at this condition but its stability value gets smaller.

Table 4.2 Phase fractions and stability variables of Water-Paraffin mixture at 24.1 bar.

T(K)	water-rich liquid phase (L <sub>W</sub> )		Hydrocarbon-rich liquid phase (L <sub>H<sub>C</sub></sub> )		Vapour phase (V)		Mixture State	Iter #	CPU <sup>c</sup> time (sec.)
	$\alpha_{L_W}$	$\theta_{L_W}$	$\alpha_{L_{HC}}$	$\theta_{L_{HC}}$	$\alpha_V$	$\theta_V$			
460.000 <sup>a</sup>	0.0000	0.4816	0.0000	0.0566	1.0000	—	Vapour only	13	10
454.513 <sup>a</sup>	0.0000	0.3629	0.0000	0.0000	1.0000	—	L <sub>H<sub>C</sub></sub> incipient	13	11
450.000 <sup>a</sup>	0.0000	0.2382	0.0483	0.0000	0.9517	—	Vapour-L <sub>H<sub>C</sub></sub>	13	10
441.531 <sup>a</sup>	0.0000	0.0000	0.1356	0.0000	0.8644	—	L <sub>W</sub> incipient	13	10
420.000 <sup>a</sup>	0.1948	0.0000	0.5163	0.0000	0.2889	—	V-L <sub>W</sub> -L <sub>H<sub>C</sub></sub>	13	9
406.981 <sup>a</sup>	0.2418	0.0000	0.7582	0.0000	0.0000	—	L <sub>W</sub> -L <sub>H<sub>C</sub></sub>	12	17
390.000 <sup>b</sup>	0.2517	—	0.7483	0.0000	0.0000	0.1849	L <sub>W</sub> -L <sub>H<sub>C</sub></sub>	12	7

<sup>a</sup> vapour is the reference phase

<sup>b</sup> water-rich liquid phase is the reference phase

<sup>c</sup> Intel Pentium Dual E2200 2.2 GHz.

More insight into the behaviour of the phase fraction and stability variables during the iteration is shown in Figure 4.3 and Figure 4.4 at 454.513 and 450 K; respectively. The iteration represents the number of times the composition vectors are updated. As shown in Figure 4.3, the phase fraction and stability variable converge to zero for hydrocarbon-rich liquid phase at the 5th iteration. In Figure 4.4, the phase fraction of hydrocarbon-rich liquid phase starts developing after the 2nd iteration where its stability variable approaches zero and then the phase becomes present at the third iteration. The appearance of the hydrocarbon liquid phase is accompanied by a decrease in the vapour phase fraction which converges to 0.9517.

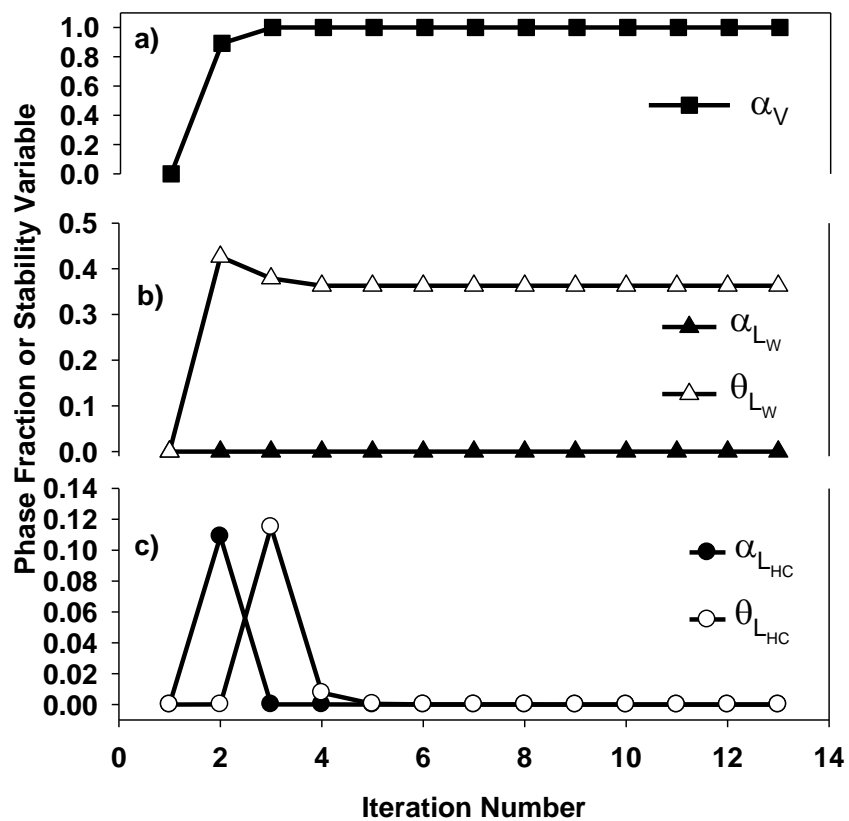


Figure 4.3 Phase fraction ( $\alpha$ ) and stability variable ( $\theta$ ) vs. iteration number for water-paraffin mixture at 24.1 bar and 454.513 K for: a) Vapour (stable); b) Water-rich liquid phase (unstable); c) Hydrocarbon-rich liquid phase (incipient).

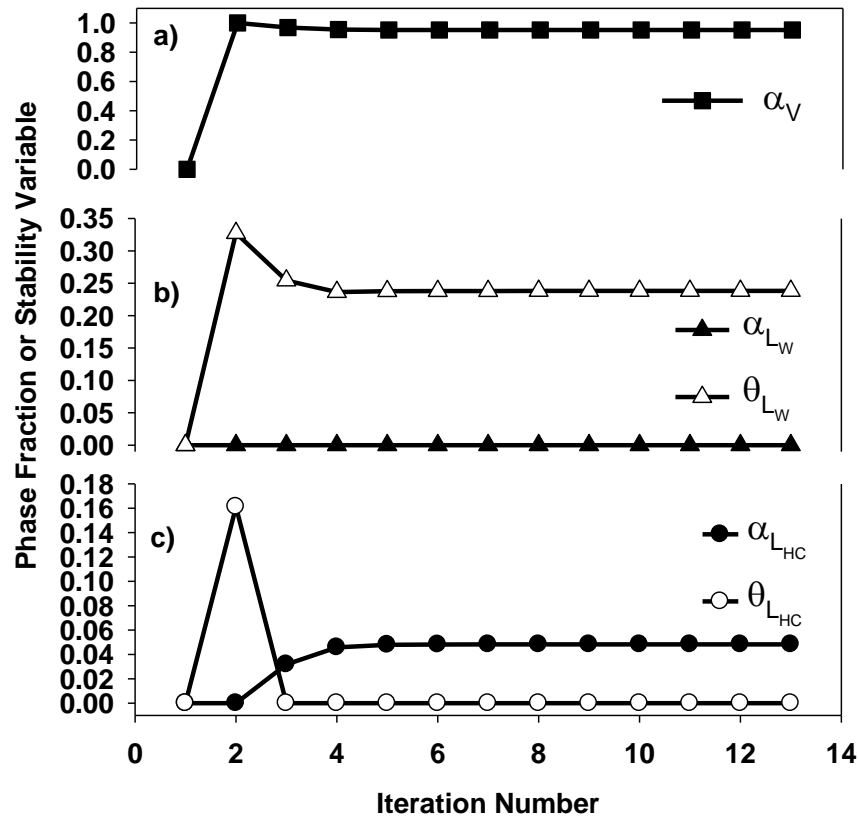


Figure 4.4 Phase fraction ( $\alpha$ ) and stability variable ( $\theta$ ) vs. iteration number for water-paraffin mixture at 24.1 bar and 450 K for: a) Vapour (stable); b) Water-rich liquid phase (unstable); c) Hydrocarbon-rich liquid phase (stable).

#### 4.6.1.3 Incipient water-rich liquid and vapour-liquid-liquid phase region

The water-rich liquid phase is incipient at temperature equals to 441.531 K as shown in Table 4.2 where both stability variable and phase fraction have zero values. Both phase fraction and stability variable are zero (i.e. incipient) after the 3rd iteration as shown in Figure 4.5. If the temperature is slightly decreased, the mixture coexists in the Vapour-Liquid-Liquid region. An illustration of the characteristics of the vapour-liquid-liquid region is given in Table 4.2 and Figure 4.6 at 420 K. As seen in Table 4.2, the liquid phase fractions are positive and their corresponding stability variables are zero indicating that they are present. In Figure 4.6, the change of the stability variable and phase fraction with iteration is depicted. Both stability

variables of the two liquid phases are zero while their phase fractions are positive showing that they are stable.

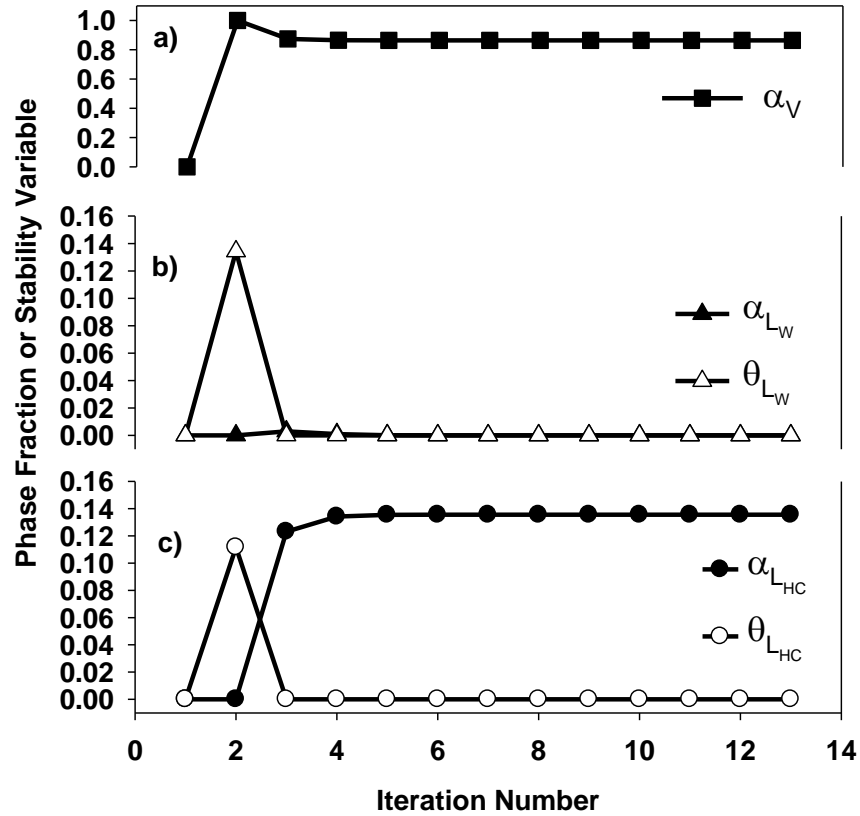


Figure 4.5 Phase fraction ( $\alpha$ ) and stability variable ( $\theta$ ) vs. iteration number for water-paraffin mixture at 24.1 bar and 441.53 K for: a) Vapour (stable); b) Water-rich liquid phase (incipient); c) Hydrocarbon-rich liquid phase (stable).

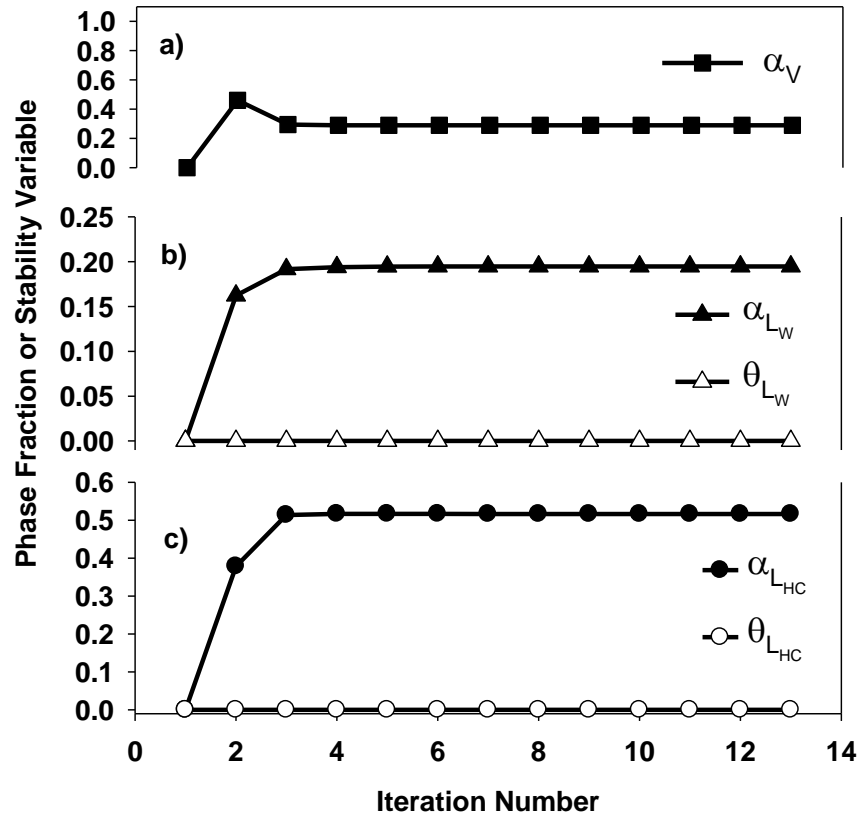


Figure 4.6 Phase fraction ( $\alpha$ ) and stability variable ( $\theta$ ) vs. iteration number for water-paraffin mixture at 24.1 bar and 420 K for: a) Vapour (stable); b) Water-rich liquid phase (stable); c) Hydrocarbon-rich liquid phase (stable).

#### 4.6.1.4 Liquid-liquid phase

If we continue cooling the mixture, the vapour phase, which is the reference phase, disappears at 406.981 K indicating that the mixture exhibits two liquid phases; namely, water-rich and hydrocarbon-rich liquid phases. At this point, both the two liquid phase fractions are positive and their corresponding stability variables are zero whereas the vapour phase fraction is zero. A fast convergence of phase fraction and the stability variables is achieved as shown in Figure 4.7. It should be emphasized here, as previously indicated, that the proposed scheme doesn't encounter any computation difficulty when the phase fraction approaches zero even if that phase is the reference phase. The disappearance of the vapour phase at temperature equal or less than 406.981 K and 24.1 bar makes it necessary to switch the reference phase to one of the liquid phases

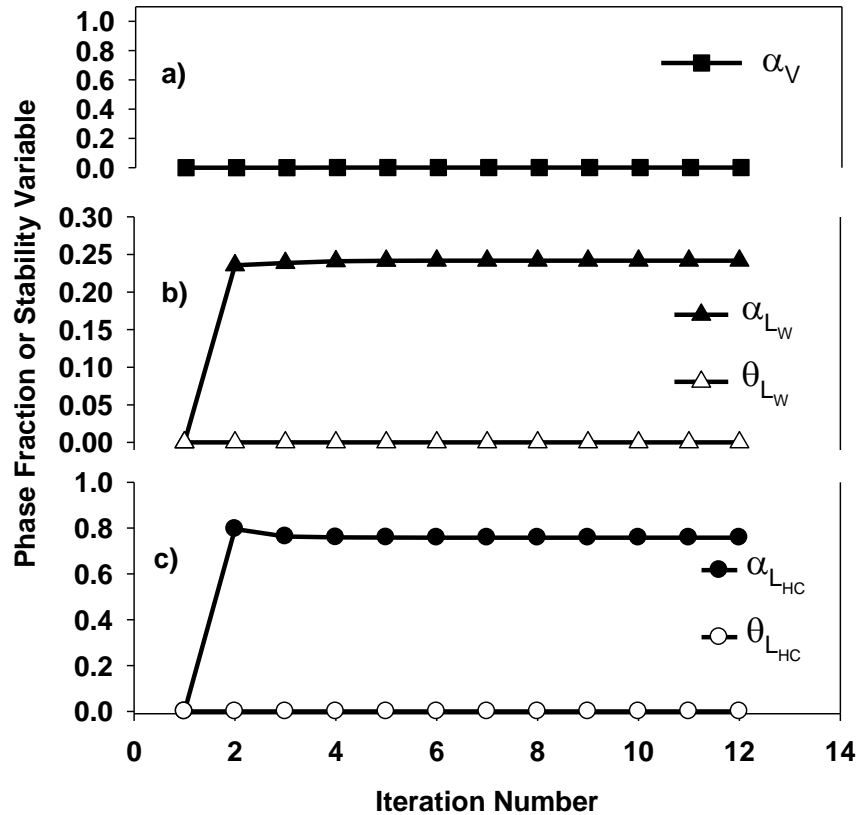


Figure 4.7 Phase fraction ( $\alpha$ ) and stability variable ( $\theta$ ) vs. iteration number for water-paraffin mixture at 24.1 bar and 406.981 K for: a) Vapour (incipient); b) Water-rich liquid phase (stable); c) Hydrocarbon-rich liquid phase (stable).

if computation is required for temperatures less than 406.981 K. If the reference phase is maintained to be the vapour phase, a decrease in temperature would cause the vapour phase fraction to be negative. A negative value is of course not a physical value. However, it is an indication of improper selection of the reference phase.

The reference phase is switched to the water-rich liquid phase for the flash calculation at a temperature less than 406.981 K where the system exhibits liquid-liquid equilibrium. For example, at 390 K, the vapour phase is absent and its stability variable is positive (0.1849) as shown in Table 4.2. The characteristics of the phase fractions and stability variables with iterations are shown on Figure 4.8. It is clear that the phase fraction of vapour is zero and its corresponding stability variable (see Figure 4.8) becomes positive at the 2nd iteration. Finally, it should be noted that equation 4-11 is verified in all the studied conditions.

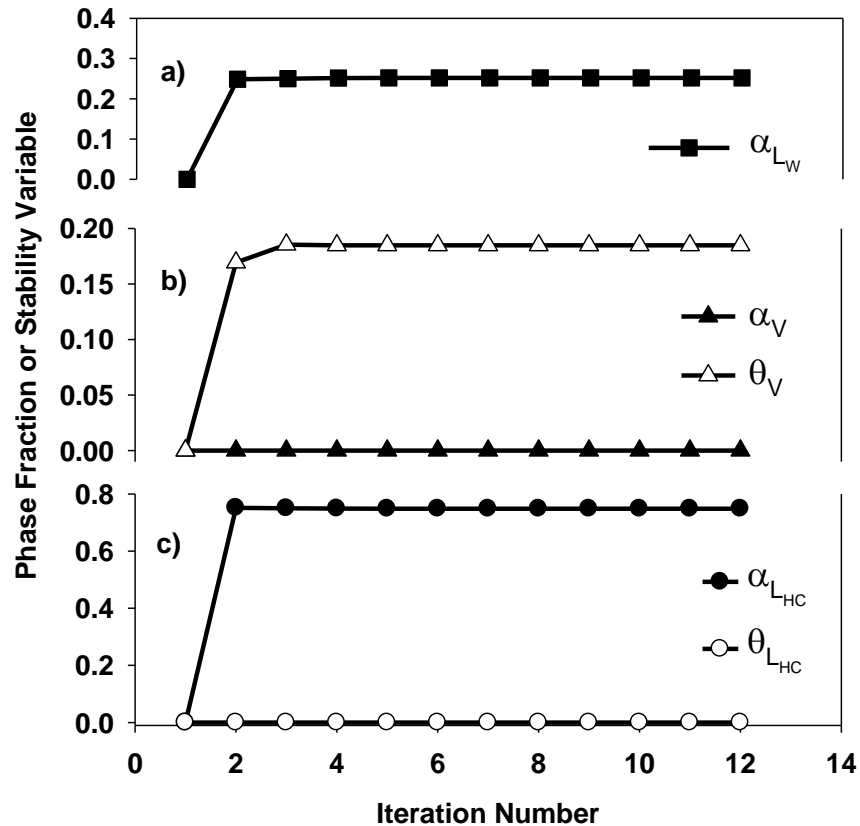


Figure 4.8 Phase fraction ( $\alpha$ ) and stability variable ( $\theta$ ) vs. iteration number for water-paraffin mixture at 24.1 bar and 390 K for: a) Vapour (unstable); b) Water-rich liquid phase (stable); c) Hydrocarbon-rich liquid phase (stable).

#### 4.6.2 Ethylene glycol/water/propane/methane

The second mixture that was examined is the ethylene glycol-water-propane-methane quaternary. Dipole-dipole interactions are considered for both ethylene glycol and water. The dipole-dipole interactions are represented with two polar functional groups of the ethylene glycol. Hydrogen bonding interactions are also taken into account for water and ethylene glycol. Experimental data was reported for this mixture by Ng et al. (1986) at two different P-T values. The system shows vapour-liquid-liquid behaviour according to the reported experimental P-T values. A comparison of the experimental and the calculated mole fraction of this system with the

proposed scheme is shown in Table 4.3. As seen in the table, dipolar PC-SAFT predicts the mole fractions of this system well.

Table 4.3 Equilibrium phase composition (mole fraction) of methane-propane-water-ethylene glycol system.

	T = 273.15 K			P = 70.4 bar			
	Feed	V	V (exp.)	L <sub>HC</sub>	L <sub>HC</sub> (exp.)	L <sub>W</sub>	L <sub>W</sub> (exp.)
MEG	0.092	3.620E-07	.....	2.204E-06	3.400E-06	0.2236	0.2243
water	0.317	1.207E-04	.....	1.277E-04	4.000E-05	0.7702	0.7736
propane	0.284	0.1566	0.1542	0.5394	0.5660	2.562E-03	2.770E-04
methane	0.307	0.8433	0.8458	0.4605	0.4340	3.719E-03	1.790E-03
	T = 283.15 K			P = 69.0 bar			
	Feed	V	V (exp.)	L <sub>HC</sub>	L <sub>HC</sub> (exp.)	L <sub>W</sub>	L <sub>W</sub> (exp.)
MEG	0.090	8.746E-07	....	4.497E-06	3.000E-06	0.2235	0.2244
water	0.311	2.266E-04	.....	2.211E-04	7.200E-05	0.7700	0.7736
propane	0.288	0.1961	0.1984	0.5834	0.6018	2.928E-03	3.760E-04
methane	0.311	0.8037	0.8016	0.4163	0.3982	3.583E-03	1.580E-03

The proposed scheme is also applied for this mixture at a range of pressures at a fixed temperature (283.15 K) to show the change of phase fractions of the three phases. The phase fraction vs. pressure is depicted in Figure 4.9. As seen in the figure, as the pressure increases the mole phase fraction of vapour decreases while the phase fraction of hydrocarbon-rich liquid phase increases. However, the phase fraction of the water-rich liquid phase remains constant as the pressure increases. There is no experimental data to verify this behaviour but prediction of similar systems (will be given in next chapter) which have been studied and compared to experimental at different pressures supports this behaviour.

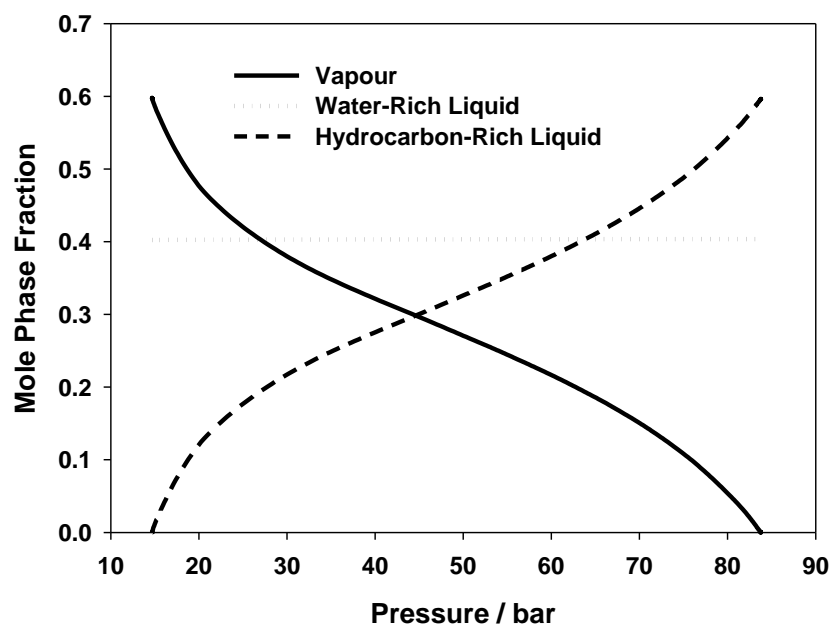


Figure 4.9 Mole phase fraction vs. Pressure of methane-propane-water-ethylene glycol at 283.15 K predicted by dipolar PC-SAFT.

The proposed scheme performs the calculation of this system without any difficulty although the mole phase fraction was approaching zero for hydrocarbon-rich liquid phase around 15 bar and for Vapour phase around 84 bar. In this example, the computations were performed for the vapour-liquid-liquid region but can be extended to other phase regions as done with water-paraffins system. The vapour phase was selected as the reference phase in this example. Furthermore, the number of iterations didn't exceed 18 for each selected P-T values while the total CPU time is about 60 seconds.

#### 4.6.3 Ethylene glycol/ water/hexane/propane/CO<sub>2</sub>/methane

The experimental data of this six-component mixture were reported by Ng et al. (1986) at two different temperatures (263.15 and 283.15 K) and a fixed pressure of 68 bar. The reported data show that this system exhibits Vapour-liquid-liquid equilibrium at these conditions. To examine this system with the proposed scheme, the PC-SAFT is utilized with the inclusion of dipolar and hydrogen bonding interactions of ethylene glycol and water as well as quadrupole interactions for carbon dioxide. Figure 4.10 represents the phase fraction and its corresponding stability variables vs. iteration. The stability variables are arbitrary initiated with non-zero values. Nonetheless, a fast convergence is achieved and equations 4-8 and 4-9 are verified. At the 2nd

iteration, the stability variables go to zero where the phase fractions of both liquids appear and proceed to converge at 10 iterations. The total CPU time is around 43 seconds. Table 4.4 illustrates the comparison between experimental and calculated mole fractions.

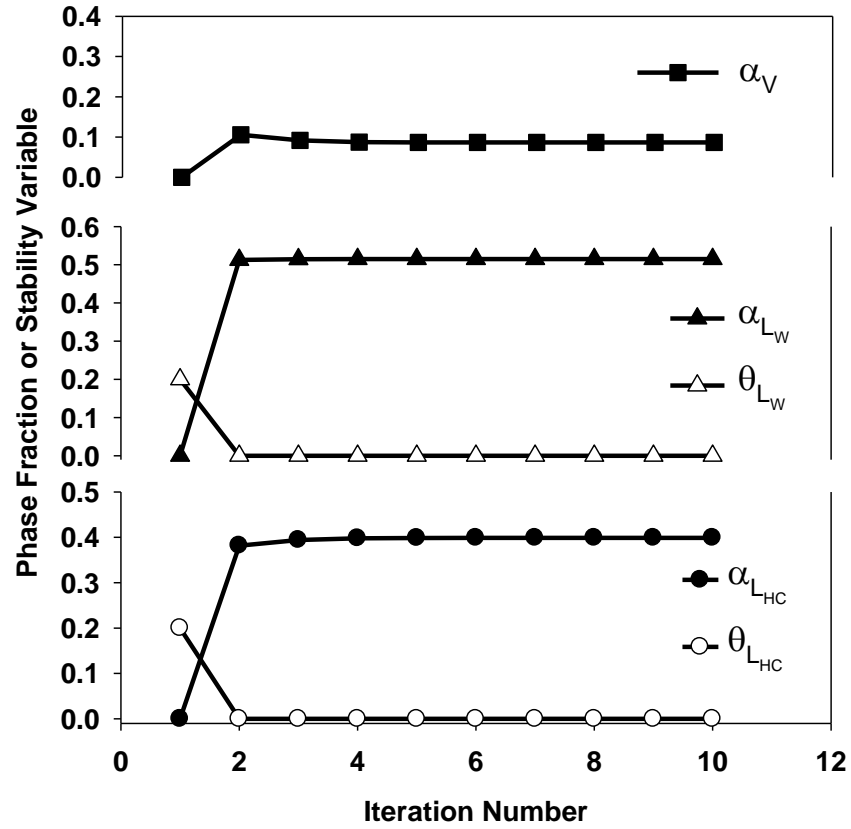


Figure 4.10 Phase fraction ( $\alpha$ ) and stability variable ( $\theta$ ) vs. iteration number for ethylene glycol-water-hexane-carbon dioxide-methane mixture at 68 bar and 283.15 K for: a) Vapour (stable); b) Water-rich liquid phase (stable); c) Hydrocarbon-rich liquid phase (stable).

Table 4.4 Equilibrium phase composition (mole fraction) for ethylene glycol-water-hexane-propane-carbon dioxide-methane.

	T = 263.15 K			P = 68 bar			
	Feed	V	V (exp.)	L <sub>HC</sub>	L <sub>HC</sub> (exp.)	L <sub>W</sub>	L <sub>W</sub> (exp.)
EG	0.114	1.120E-07	...	2.175E-06	5.400E-06	0.2241	0.2235
H2O	0.392	6.232E-05	....	9.172E-05	4.400E-05	0.7704	0.7705
C6H14	0.198	0.0034	0.0041	0.4183	0.4500	2.974E-04	2.00E-05
C3H8	0.049	0.0180	0.0217	0.1025	0.1100	3.982E-04	3.00E-05
CO2	0.049	0.0832	0.1199	0.0992	0.0948	0.00114	0.00448
CH4	0.198	0.8953	0.8543	0.3800	0.3452	0.00373	0.00148
	T = 283.15 K			P = 68 bar			
	Feed	V	V (exp.)	L <sub>HC</sub>	L <sub>HC</sub> (exp.)	L <sub>W</sub>	L <sub>W</sub> (exp.)
EG	0.115	6.899E-07	...	8.737E-06	1.200E-05	0.2233	0.2234
H2O	0.397	2.270E-04	....	2.725E-04	9.600E-05	0.7708	0.7704
C6H14	0.195	0.0066	0.0071	0.4640	0.4800	4.019E-04	2.600E-06
C3H8	0.049	0.0275	0.0297	0.1120	0.1154	5.022E-04	4.800E-05
CO2	0.049	0.1044	0.1306	0.0989	0.0870	1.28E-03	4.45E-03
CH4	0.195	0.8613	0.8326	0.3248	0.3176	3.68E-03	1.67E-03

#### 4.6.4 Water-hydrocarbon and other systems

The proposed algorithm was successfully tested for several water-hydrocarbon and other systems which will be given in the next chapter. These systems exhibit various phase behaviours including vapour-liquid, Liquid-liquid and vapour-liquid-liquid equilibrium. For these systems, two SAFT versions (Huang & Radosz, 1991; Fu & Sandler, 1995) have been utilized with the addition of hydrogen bonding and dipolar interactions; namely, simplified SAFT and PC-SAFT.

Finally, although we have employed PC-SAFT with the addition of association, dipolar and quadrupole, the total CPU time was not expensive even for cross-association components (eg. water-ethylene glycol systems). As far as our knowledge goes, the only available study for computing phase stability and equilibrium using SAFT for cross association systems is the one that conducted by Xu et al (2002). They described a reliable computing phase stability and equilibrium using interval analysis. Their work was limited to mainly VLE and binary systems. The study showed expensive computing time for conducting stability and equilibrium calculations for cross-association systems. For example, the total CPU time of 1-butanol-ethanol system was 1816.1 seconds at T=343 K, P=0.35 bar and  $z_{\text{butanol}}=0.65$  (feed composition) using the CK-SAFT (Huang & Radosz, 1991) with a binary interaction parameter equals to 0.011. For the

sake of comparison, we studied this system at the same conditions and the same SAFT version (CK-SAFT). The total CPU time is about 30 seconds which is significantly faster than that of Xu et al (2002). The phase fraction of vapour, which is the reference phase, is 0.97082 while the liquid phase fraction is 0.029177 and its corresponding stability variable is  $1.5955e-22$  indicating that it is stable. Our algorithm shows a third: an absent phase with a stability variable equals 2.4917.

## 4.7 Conclusions

The procedure suggested originally by Gupta (1990) to perform multiphase equilibrium and stability calculations was modified. The new scheme combines the trust-region Gauss-Newton method (Macconi et al., 2009) and the updating procedure of Kinoshita and Takamatsu (1986). Unlike the classical iterative method, the trust-region Gauss-Newton method is capable of solving non-linear equations with inequality constraints and it has global convergence properties. The computational scheme utilizes a simple initialization procedure. The current algorithm doesn't encounter problems when the phase fraction approaches zero. Furthermore, it could handle more than one absent phase easily. The proposed computation scheme was evaluated for water-ethylene glycol-hydrocarbon systems with/without carbon dioxide. Hydrogen bonding and polar (dipolar and quadrupole) interactions were included and computations were performed without the use of binary interaction parameters. The scheme is proved to be efficient for multiphase calculations for water-hydrocarbon containing systems.

## CHAPTER 5

# EVALUATING THE PREDICTIVE CAPABILITY OF POLAR AND POLARIZABLE SAFT TO MULTIPHASE SYSTEMS

### 5.1 Introduction

In **Chapter 3**, the dipolar PC-SAFT was evaluated by predicting the VLE of water-alcohol-hydrocarbon mixtures. The achieved success raised two issues. The first issue is related to the performance of dipolar SAFT in multiphase systems where the success of any equation of state is generally limited. The dipolar SAFT is therefore required to be further explored to show if the limitation of equations of state in multiphase systems can be resolved or at least improved. The second issue is about the role of other electrostatic interactions such as quadrupole-quadrupole, dipole-quadrupole and polarization. These interactions were ignored in the study of the VLE. Despite the fact that these other interactions were not considered, the dipolar PC-SAFT-JC showed excellent prediction for the VLE. This raises a question concerning Chapman's dipolar term: Is the magnitude of the Chapman term realistic? In other words, are the dipole-quadrupole, quadrupole-quadrupole and polarization interactions negligible for the studied systems in Chapter 3?. On the other hand, the PC-SAFT-GV and PC-SAFT-KSE were unable to give good results for many studied mixtures in Chapter 3. This raises another question: What if these electrostatic interactions were incorporated in the Gross and Economou terms; would it then be possible to obtain quantitative prediction?

In this chapter, the issues raised above are explored. The prediction of the dipolar PC-SAFT is evaluated for water-alcohol-hydrocarbon mixtures for liquid-liquid equilibrium (LLE) and vapour-liquid-liquid equilibrium (VLLE) using the PC-SAFT-JC and PC-SAFT-GV. Then, other electrostatic interactions are incorporated into the PC-SAFT-GV to demonstrate its influence on the prediction of multiphase systems. Further, the dipole-dipole interactions are incorporated into another version of the SAFT; namely the simplified SAFT. The simplified SAFT is evaluated to predict some mixtures to show the effect of using different SAFT versions. The induced dipole-dipole interaction is considered by the renormalized perturbation theory

(RPT) of Wertheim (1973a; 1973b; 1977a; 1977b). Extending the RPT to other induced interactions is not straightforward. In chapter 7, an alternative approach is developed to account for any sort of polarization interactions. For the quadrupole-quadrupole interaction, the term developed by Gross (2005) is utilized. The present chapter starts with the presentation of the polar and polarizable terms (section 5.2). In section 5.3, model parameter estimation values are given. Then, in section 5.4, the role of induced dipole-dipole and quadrupole-quadrupole interactions is studied. The last two sections 5.7 and 5.6 are devoted to the description of liquid-liquid and vapour-liquid-liquid systems for water-alcohol-hydrocarbon mixtures.

## 5.2 Polar and polarizable terms

The dipolar terms of Chapman and Gross were given in **Chapter 3**. In the previous chapter, the quadrupole-quadrupole term was utilized in the multiphase calculation of CO<sub>2</sub> system without giving details. Here, we give a detailed description of the quadrupole-quadrupole term that was developed by Gross (2005). Then, a detailed description of the RPT is given.

### 5.2.1 Quadrupole-quadrupole term

The quadrupole-quadrupole term of Gross (2005) is suitable for our purpose since it has taken the molecular shape into account. The term was essentially developed by the use of a third order perturbation theory. The Padé approximant was utilized:

$$\frac{A^{QQ}}{NkT} = \frac{A_2/NkT}{1 - A_3/A_2} \quad 5-1$$

where  $A_2$  and  $A_3$  represent the second and third order perturbation terms.  $A_2$  and  $A_3$  are respectively given by:

$$\frac{A_2}{NkT} = -\pi \left(\frac{3}{4}\right)^2 \rho \sum_i \sum_j x_i x_j \frac{\varepsilon_{ii}}{kT} \frac{\varepsilon_{jj}}{kT} \frac{\sigma_{ii}^5 \sigma_{jj}^5}{\sigma_{ij}^7} n_{Q,i} n_{Q,j} Q_i^{*2} Q_j^{*2} J_{2,ij} \quad 5-2$$

and

$$\begin{aligned}
\frac{A_3}{NkT} &= \frac{\pi}{3} \left(\frac{3}{4}\right)^3 \rho \sum_i \sum_j x_i x_j \left(\frac{\epsilon_{ii}}{kT}\right)^{\frac{3}{2}} \left(\frac{\epsilon_{jj}}{kT}\right)^{\frac{3}{2}} \frac{\sigma_{ii}^{\frac{15}{2}} \sigma_{jj}^{\frac{15}{2}}}{\sigma_{ij}^{12}} \\
&\quad \times n_{Q,i} n_{Q,j} Q_i^{*3} Q_j^{*3} J_{3,ij} + \frac{4\pi^2}{3} \left(\frac{3}{4}\right)^3 \rho^2 \\
&\quad \times \sum_i \sum_j \sum_k x_i x_j x_k \frac{\epsilon_{ii}}{kT} \frac{\epsilon_{jj}}{kT} \frac{\epsilon_{kk}}{kT} \frac{\sigma_{ii}^5 \sigma_{jj}^5 \sigma_{kk}^5}{\sigma_{ij}^3 \sigma_{ik}^3 \sigma_{jk}^3} n_{Q,i} n_{Q,j} n_{Q,k} Q_i^{*2} Q_j^{*2} Q_k^{*2} J_{3,ijk}
\end{aligned} \tag{5-3}$$

where  $J_2$  and  $J_3$  are functions adjusted to molecular simulation data for vapor-liquid equilibria of the two-center Lennard-Jones (2CLJ) plus point quadrupole. In the above equations,  $n_Q$  is the number of quadrupole moments per molecule and  $Q^{*2}$  is the dimensionless squared quadrupole moment. Other nomenclatures were already defined in section 3.3.

## 5.2.2 The renormalized perturbation theory

The RPT was originally developed by Wertheim (1973a; 1973b; 1977a; 1977b) for dipolar polarizable particles. The theory replaces the many body interactions with an effective dipolar pair potential. The RPT was extended to mixtures by Venkatasubramanian et al. (1984), Joslin et al. (1985) and Gray et al (1985). Recently, Kleiner and Gross (2006) applied the RPT to non-spherical molecules. They considered only induced dipole-dipole interactions. Because the application of the RPT requires a permanent dipole-dipole term, they used Gross's dipolar term. The effective dipolar polarizable term was given by:

$$\frac{A^{DD,eff}}{NkT} = \frac{A'^{DD}}{NkT} + \frac{1}{2} \sum_i x_i \alpha_i^* T_i^* \left( \frac{1}{x_i} \frac{\partial}{\partial \mu_i^{*eff}} \left( \frac{A'^{DD}}{NkT} \right) \right)_{\rho,T}^2 \tag{5-4}$$

where  $\alpha_i^*$  represents the dimensionless molecular polarizability and  $\mu_i^{*eff}$  is the dimensionless effective dipole moment of a molecule. The  $A'^{DD}$  is given in the Padé approximant form:

$$\frac{A'^{DD}}{NkT} = \frac{A_2'^{DD}/NkT}{1 - A_3'^{DD}/A_2'^{DD}} \tag{5-5}$$

where

$$\frac{A_2'^{DD}}{NkT} = -\pi\rho \sum_i \sum_j x_i x_j \frac{\epsilon_i}{kT} \frac{\epsilon_j}{kT} (Z_i^A Z_j^A - Z_i^B Z_j^B) \frac{\sigma_i^3 \sigma_j^3}{\sigma_{ij}^3} J_{2,ij}^{DD} \tag{5-6}$$

$$\frac{A_3'^{DD}}{NkT} = -\frac{4}{3}\pi^2\rho^2 \sum_i \sum_j \sum_k x_i x_j x_k \frac{\varepsilon_i}{kT} \frac{\varepsilon_j}{kT} \frac{\varepsilon_k T}{k} (Z_i^A Z_j^A Z_k^A - Z_i^B Z_j^B Z_k^B) \frac{\sigma_i^3 \sigma_j^3 \sigma_k^3}{\sigma_{ij} \sigma_{ik} \sigma_{jk}} J_{3,ijk}^{DD} \quad 5-7$$

$$Z_i^A = (\mu_i^{*eff})^2 + 3T_i^* \alpha_i^* \quad 5-8$$

and

$$Z_i^B = 3T_i^* \alpha_i^* \quad 5-9$$

In the above equations,  $\mu_i^{*eff}$  is the dimensionless effective dipole moment of molecule i and  $\alpha_i^*$  is the dimensionless molecular polarizability of molecule i.

### 5.3 Model parameter estimation

The estimated parameter values of PC-SAFT-JC and PC-SAFT-GV were given in Table 3.2. Table 5.1 lists pure parameter values of the induced PC-SAFT-GV (PC-SAFT-GV-I) and induced PC-SAFT-GV plus quadrupolar term (PC-SAFT-GV-I-QQ). The pure parameter values are obtained by minimizing the vapour pressure and liquid density of pure data. The quadrupole moments are adjusted as an additional parameter due to the unavailability of the experimental values.

Table 5.1 Pure parameter values

Compound	EOS	m	$\sigma$ (Å)	$\varepsilon/k$ (K)	$\kappa^{AB}$	$\varepsilon^{AB}/k$ (K)	$x_p$	$\mu$ (D)	Q (DÅ)	$\alpha$ (Å <sup>3</sup> )	%AAD		T (K)	Data Ref.
											P <sup>sat</sup>	$\rho$		
Methanol	SSAFT	1.7566	16.97	92.477	0.079593	2694.3	0.22381	1.7			2.7096	3.123	212-497	(Daubert et al., 1989)
ethanol	SSAFT	2.7433	15.481	88.8	0.066932	2618	0.19776				0.91808	1.8382	195-510	(Yaws, 2003)
ethanol	PCSAFT-GV+I	2.4888	3.129	189.57	0.04065	2519.7		1.7			0.45342	0.38402	195-510	(Yaws, 2003)
ethanol	PCSAFT-GV+Q+I	2.2968	3.2285	185.88	0.041893	2532.7		1.7	3.6039	5.13	0.49208	0.51917	195-510	(Yaws, 2003)
1-propanol	PCSAFT-GV+I	3.132	3.171	209.96	0.031837	2328.1		1.7			1.0771	0.24831	210-500	(Yaws, 2003)
1-propanol	PCSAFT-GV+Q+I	2.8207	3.3037	210.55	0.030588	2379.8		1.7	4.2894	6.96	1.0897	0.24364	210-500	(Yaws, 2003)
water	PC-SAFT-JC	1.1923	2.918	180.02	0.085953	1680.2	0.74316	2.1549			0.8	3.1	273.15-634	(Wanger & Prub, 2002)

## 5.4 The role of induced dipole-dipole and quadrupole-quadrupole interactions in VLE

As shown in **Chapter 3**, the PC-SAFT-JC predicted the VLE of alcohol-hydrocarbon systems well. However, the prediction of PC-SAFT-GV was not as good. Here, the role of other electrostatic interactions is explored by incorporating them into PC-SAFT-GV. The VLE prediction of the PC-SAFT-GV, PC-SAFT-GV-I and PC-SAFT-GV-I-QQ are compared for ethanol-pentane system as shown in Figure 5.1. Although PC-SAFT-GV-I gives better prediction than the PC-SAFT-GV, it is still not in good agreement with the experimental data. However, the PC-SAFT-GV-I-QQ prediction is in good agreement with the experimental data. To show if the good agreement of PC-SAFT-GV-I-QQ is not a coincidental case, other systems are studied. Figure 5.2 displays the VLE of 1-propanol-heptane mixture. As seen in the figure, the PC-SAFT-GV-I-QQ compares well with the experimental data.

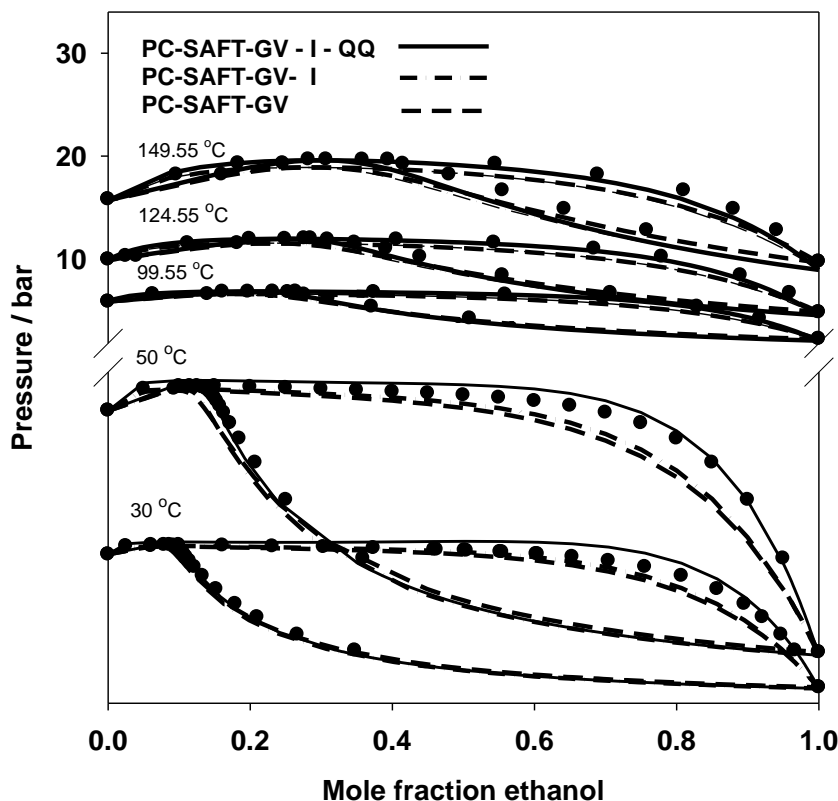


Figure 5.1 Predicted results of vapor-liquid equilibrium ( $k_{ij} = 0$ ) by the PC-SAFT-GV, PC-SAFT-GV-I and PC-SAFT-GV-I-QQ for the ethanol (1)/pentane (2) system at 30 °C, 50 °C, 99.55 °C, 124.55 °C, and 149.55 °C.

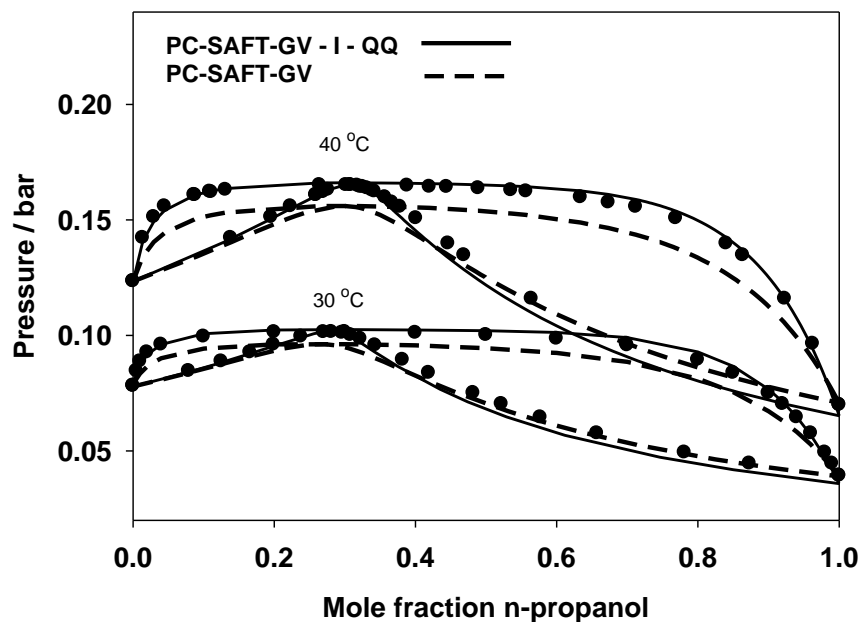


Figure 5.2 Predicted results of vapor-liquid equilibrium ( $k_{ij} = 0$ ) by the PC-SAFT-GV and PC-SAFT-GV-I-QQ for the n-propanol (1)/heptane (2) system at 30 °C and 40 °C.

The above studied systems were predicted well by the PC-SAFT-JC in **Chapter 3**. This suggests that the PC-SAFT-GV-I-QQ is equivalent to the PC-SAFT-JC. This is a result of the magnitude of the Chapman term which is much higher than that of the Gross's term. The large magnitude of Chapman's term could be explained by the simulation study conducted by Vega et al. (2005). Vega et al. showed that the vertical alignment of the dipole moment (as in the Chapman's term) gives higher dipolar contribution than that of axial alignment (as in the Gross's term).

## 5.5 Liquid-liquid equilibrium systems

In this section, the dipolar PC-SAFT and simplified SAFT are utilized to predict multiphase systems including liquid-liquid and vapour-liquid-liquid of water-alcohol-hydrocarbon systems.

### 5.5.1 Alcohol-hydrocarbon mixtures

In the literature, the reported LLE experimental data is abundant for methanol/ethanol-hydrocarbon mixtures; particularly for methanol mixtures. For example, Hölscher et al. (1986), Deiters

and Schneider (1986), Hradetzky and Lempe (1991), Orge et al. (1997) and Matsuda and Ochi (2004) reported experimental data for methanol-hydrocarbons. Experimental data for ethanol-long chain hydrocarbons was reported by Matsuda and Ochi (2004). The SAFT has been used before to obtain the LLE of methanol-hydrocarbon mixtures (Yarrison and Chapman; 2004). However, that study was based on adjusting the mixture experimental data to obtain accurate results. Here, the objective is to avoid the mixture experimental data and evaluate the prediction capability by incorporating various intermolecular forces in the SAFT model. In chapter 3, it was indicated that methanol and ethanol systems showed some complexity at low temperatures; particularly methanol systems as was shown in Chapter 3. Hence, the prediction of the LLE is not expected to be in good agreement with the experimental data. However, it is advantageous to evaluate the LLE of methanol and ethanol systems to gain more insight into the dipolar PC-SAFT.

In order to evaluate the dipolar SAFT prediction for LLE of methanol-hydrocarbon mixtures, two systems are first chosen; namely methanol-hexane and methanol-decane. For methanol-decane, Figure 5.3 displays the LLE behaviour for both PC-SAFT-GV and PC-SAFT-JC. It is apparent that the PC-SAFT-JC overestimates the upper critical solution temperature (UCST) while the PC-SFAT-GV underestimates the UCST.

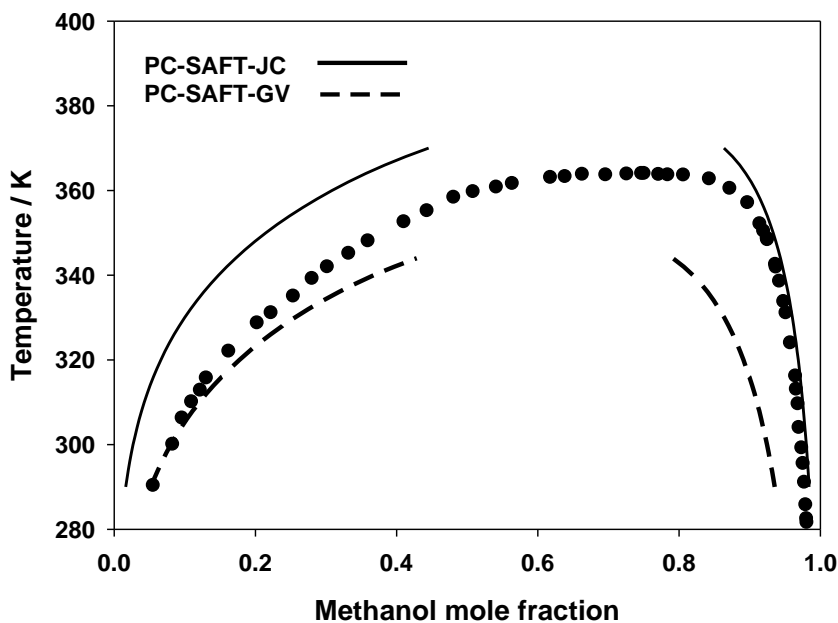


Figure 5.3 Predicted results of liquid-liquid equilibrium ( $k_{ij} = 0$ ) by the PC-SAFT-JC and PC-SAFT-GV for the methanol (1)/n-decane (2) system. Experimental data were taken from Matsuda and Ochi (2004).

For the methanol-hexane system, as shown in Figure 5.4, both PC-SAFT-GV and PC-SAFT-JC overestimate the UCST. The PC-SAFT-JC is much worse than PC-SAFT-GV. This is again related to the higher magnitude of Chapman's term compared to Gross's term. This behaviour is expected since the prediction of VLE was not possible at low temperatures as shown in **Chapter 3**. Because the PC-SAFT-GV overestimates the UCST of methanol-hexane and underestimates the UCST of methanol-decane, it is expected to work better with hydrocarbons shorter than decane and longer than hexane such as the methanol-octane system. Figure 5.5 displays the PC-SAFT-GV prediction of this mixture. As seen, the prediction of methanol-octane is better than methanol-hexane/decane systems but it is still not satisfactory. Since the addition of dipole-dipole interactions led to overestimation of the UCST as shown in Figure 5.4, the incorporation of other electrostatic interactions such as quadrupole-quadrupole and polarization interactions is expected to render the prediction of the UCST worse.

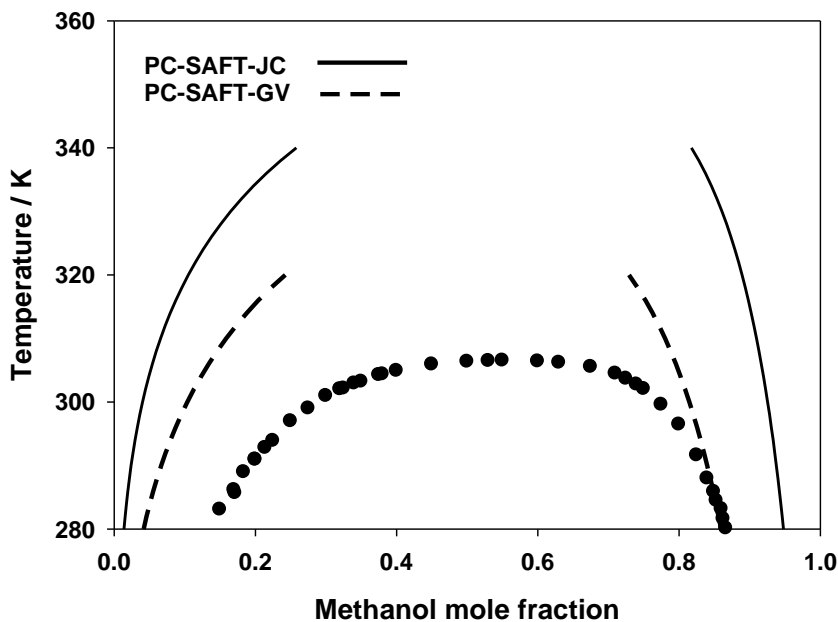


Figure 5.4 Predicted results of liquid-liquid equilibrium ( $k_{ij} = 0$ ) by the PC-SAFT-JC and PC-SAFT-GV for the methanol (1)/hexane (2) system. Experimental data were taken from Hradetzky and Lempe (1991).

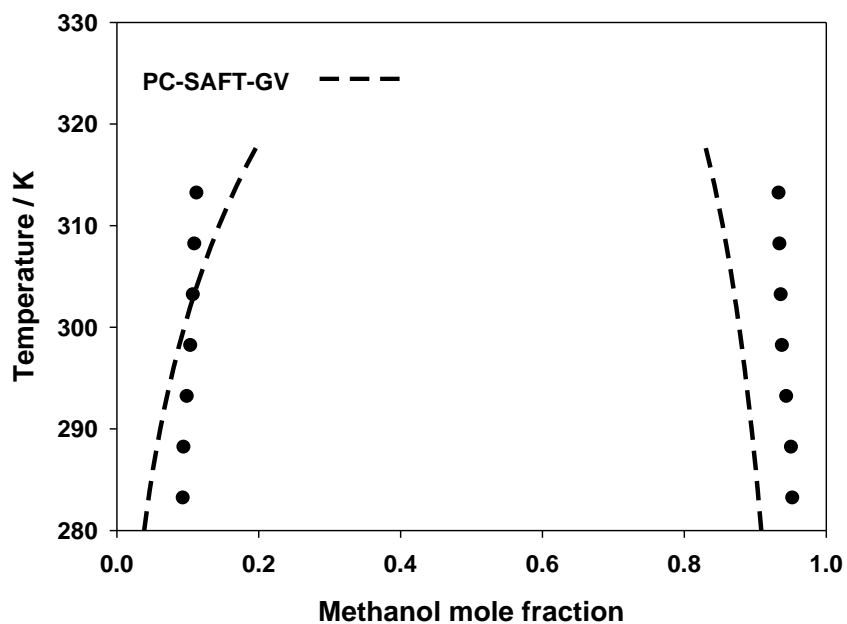


Figure 5.5 Predicted results of liquid-liquid equilibrium ( $k_{ij} = 0$ ) by the PC-SAFT-GV for the methanol (1)/octane (2) system. Experimental data were taken from Orge et al. (1997).

To show the influence of using different pure parameter sets, methanol-octane is again studied using both PC-SAFT-GV with another different parameter set (Kleiner and Gross, 2006) and PC-SAFT-JC with a new pure parameter set. The new pure parameter values of PC-SAFT-GV and PC-SAFT-JC are listed in Table 5.1. Figure 5.5 shows the results of these models. As seen, the PC-SAFT-GV prediction with set 1 is much better than that of set 2. On the other hand, the prediction of PC-SAFT-JC with set 2 is better than that of the previous set of PC-SAFT-JC parameters that were used in Figures 5.3 and 5.4; particularly for the methanol-rich phase.

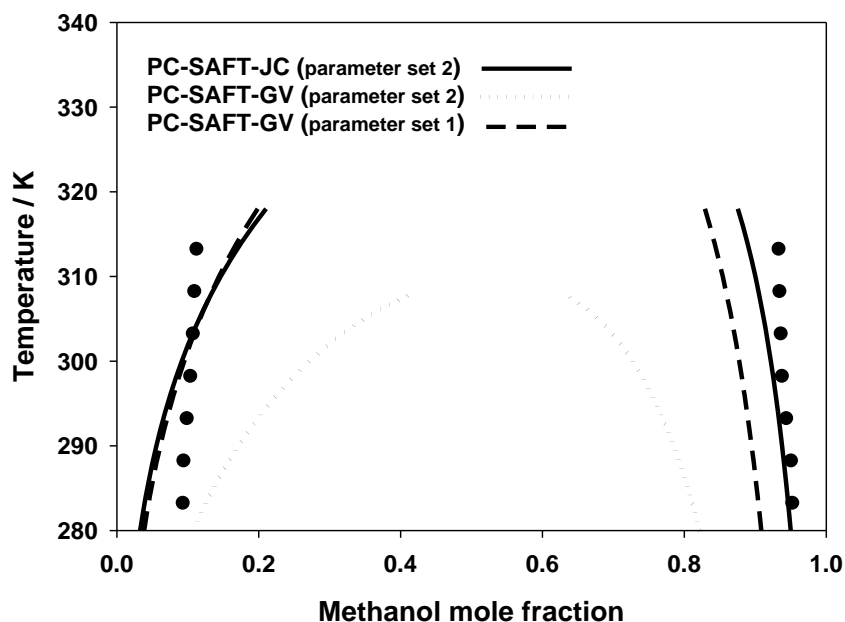


Figure 5.6 Predicted results of liquid-liquid equilibrium ( $k_{ij} = 0$ ) by the PC-SAFT-GV and PC-SAFT-JC for the methanol (1)/octane (2) system. Experimental data were taken from Orge et al. (1997).

For ethanol-hydrocarbon systems, the reported LLE experimental data by Hiroyuki and Ochi (2004) for ethanol + tetradecane/ hexadecane systems are used. Figure 5.6 and Figure 5.7 show the comparison of the prediction of PC-SAFT-GV and PC-SAFT-JC with the reported experimental data. It is clear that both models are not in good agreement with the data. The PC-SAFT-JC significantly overestimates the UCST while the PC-SAFT-GV substantially underestimates the UCST. The use of different pure parameter sets with PC-SAFT-JC for ethanol is also explored. The prediction of PC-SAFT-JC is significantly improved for ethanol- hexadecane mixture but it is still unable to give a satisfactory quantitative prediction, as shown in Figure 5.9.

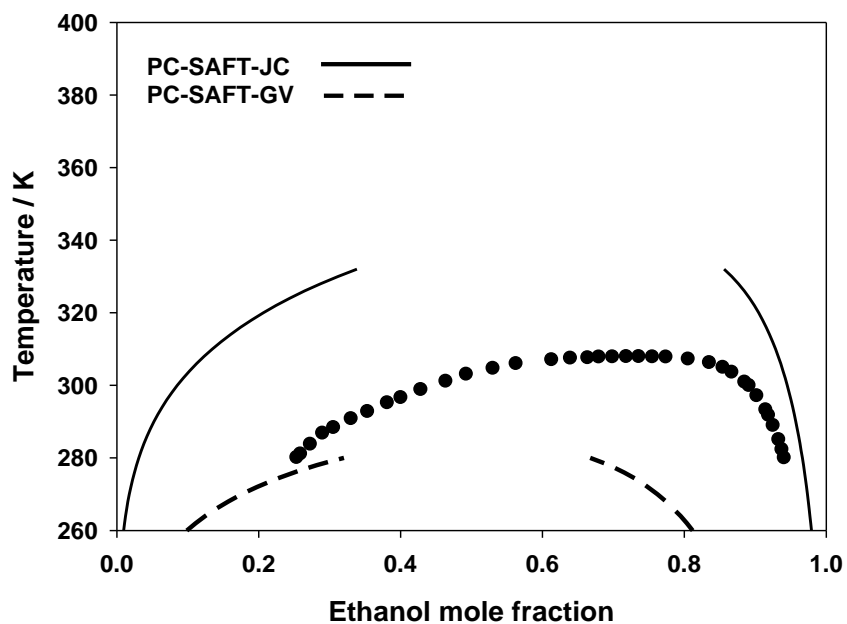


Figure 5.7 Predicted results of liquid-liquid equilibrium ( $k_{ij} = 0$ ) by the PC-SAFT-GV and PC-SAFT-JC for the ethanol (1)/tetradecane (2) system. Experimental data were taken from Matsuda and Ochi (2004).

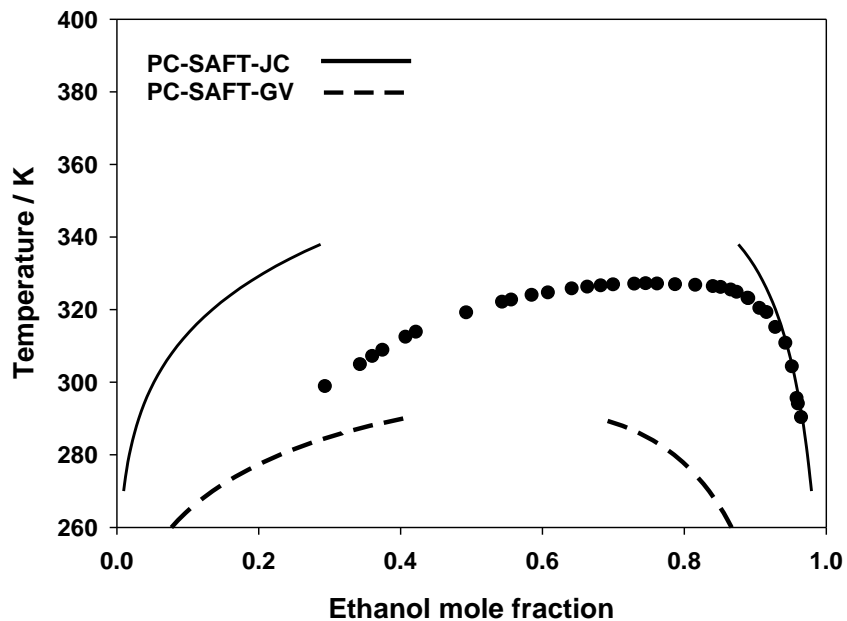


Figure 5.8 Predicted results of liquid-liquid equilibrium ( $k_{ij} = 0$ ) by the PC-SAFT-GV and PC-SAFT-JC for the ethanol (1)/hexadecane (2) system. Experimental data were taken from Matsuda and Ochi (2004).

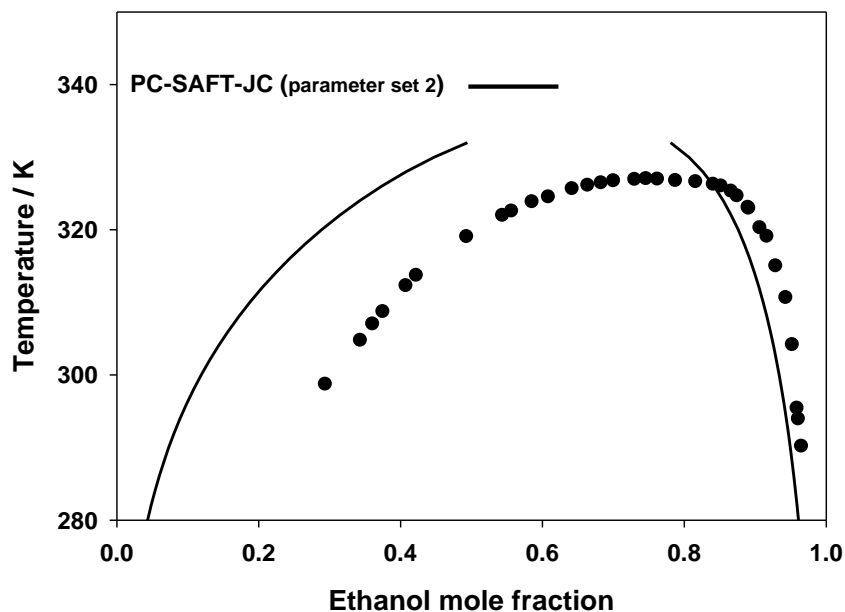


Figure 5.9 Predicted results of liquid-liquid equilibrium ( $k_{ij} = 0$ ) by the PC-SAFT-JC for the ethanol (1)/hexadecane (2) system. Experimental data were taken from Matsuda and Ochi (2004).

### 5.5.1.1 Prediction of dipolar simplified SAFT

The use of one version of SAFT might not reflect the performance of SAFT theory in LLE. Here, the prediction capability of the simplified SAFT is explored. The simplified SAFT is first extended by incorporating the dipolar interactions. The pure parameter values of simplified SAFT with incorporation of Chapman's term (SSAFT-JC) are given in Table 5.1 for methanol and ethanol. The SSAFT-JC is used to predict the LLE of methanol-hydrocarbon systems. Figure 5.8 to 5.13 display the comparison of the prediction of the SSAFT-JC with experimental data for methanol-pentane/hexane/heptane/octane/decane; respectively. Although the prediction of SSAFT-JC is satisfactory for the methanol-hexane system at the methanol-rich phase, the SSAFT-JC again overestimates the UCST. The prediction of SSAFT-JC gets worse for a longer or shorter hydrocarbon chain than hexane as seen in the figures.

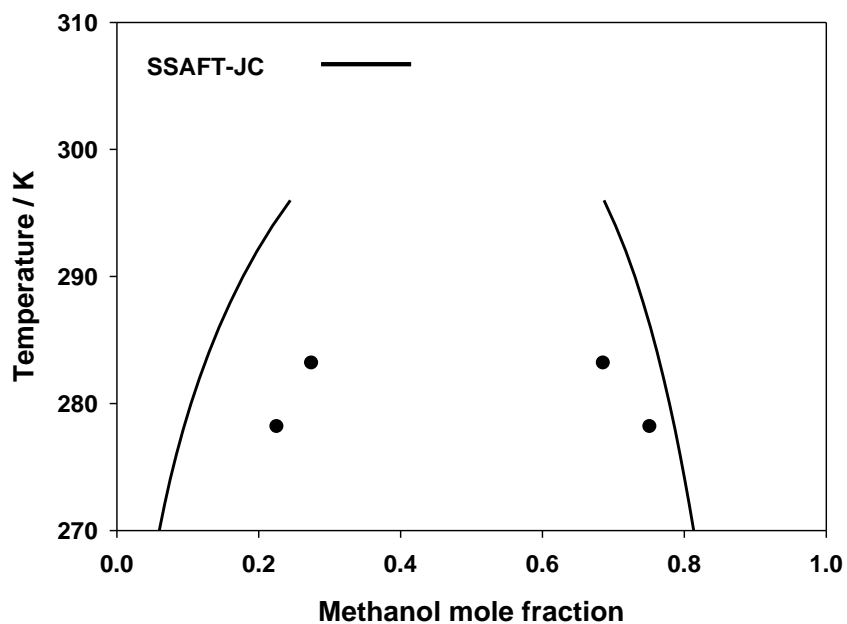


Figure 5.10 Predicted results of liquid-liquid equilibrium ( $k_{ij} = 0$ ) by the SSAFT-JC for the methanol (1)/pentane (2) system. Experimental data were taken from Orge et al. (1997).

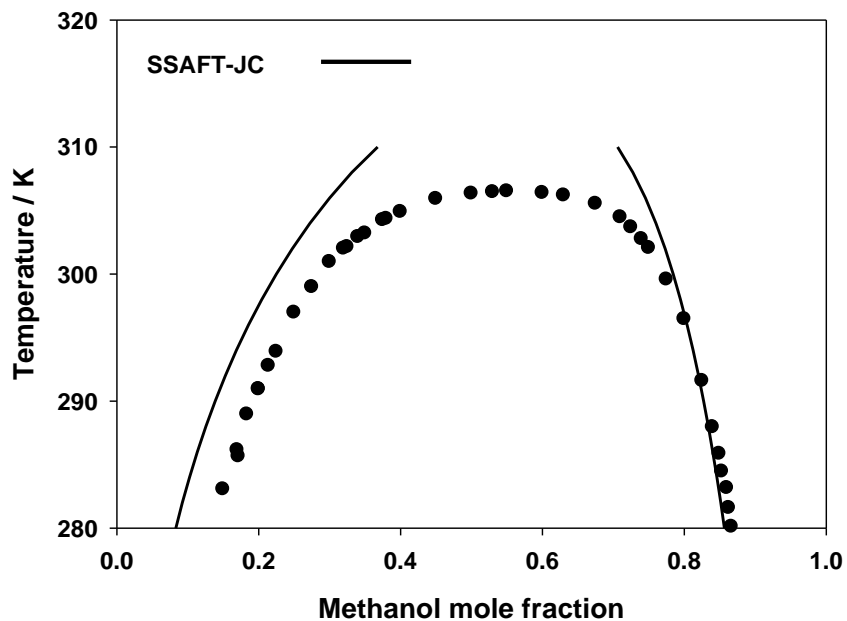


Figure 5.11 Predicted results of liquid-liquid equilibrium ( $k_{ij} = 0$ ) by the SSAFT-JC for the methanol (1)/hexane (2) system. Experimental data were taken from Hradetzky and Lempe (1991).

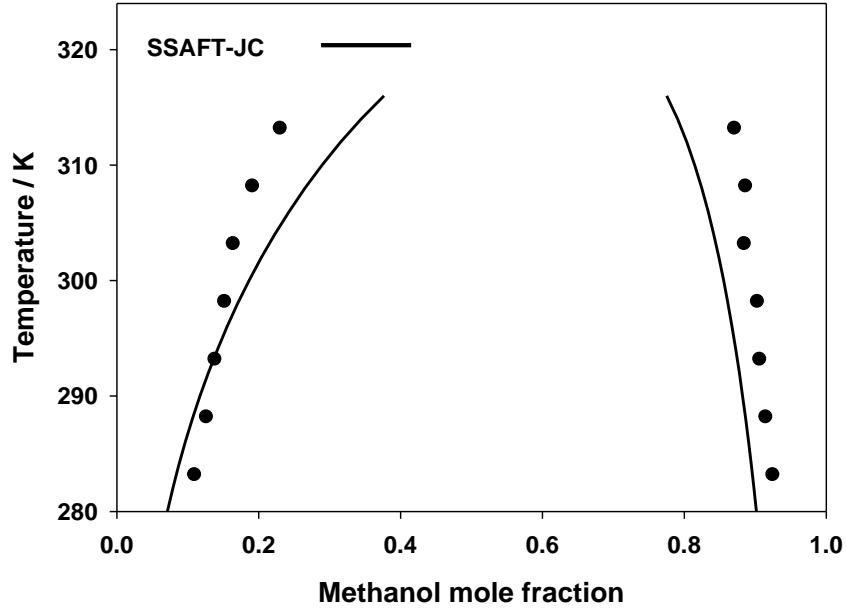


Figure 5.12 Predicted results of liquid-liquid equilibrium ( $k_{ij} = 0$ ) by the SSAFT-JC for the methanol (1)/heptane (2) system. Experimental data were taken from Orge et al. (1997).

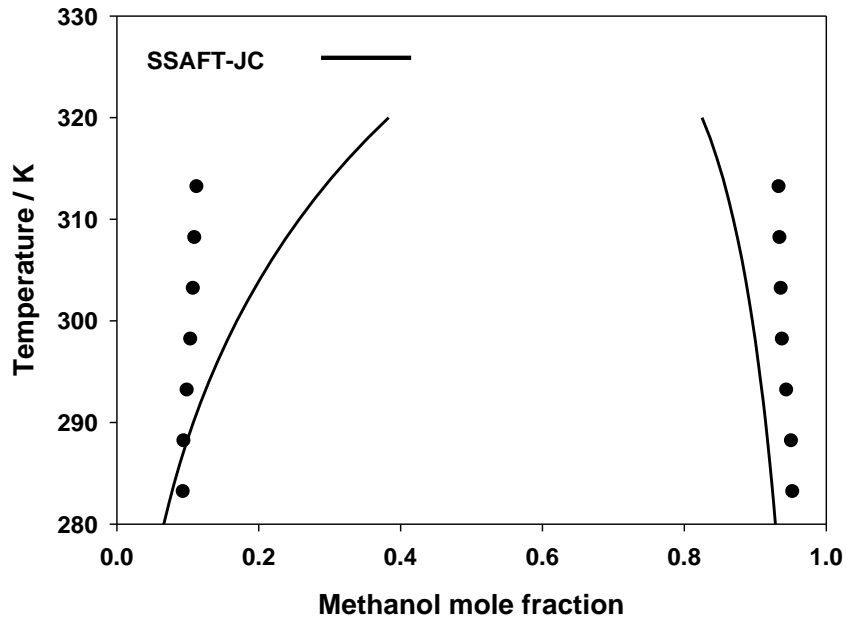


Figure 5.13 Predicted results of liquid-liquid equilibrium ( $k_{ij} = 0$ ) by the SSAFT-JC for the methanol (1)/octane (2) system. Experimental data were taken from Orge et al. (1997).

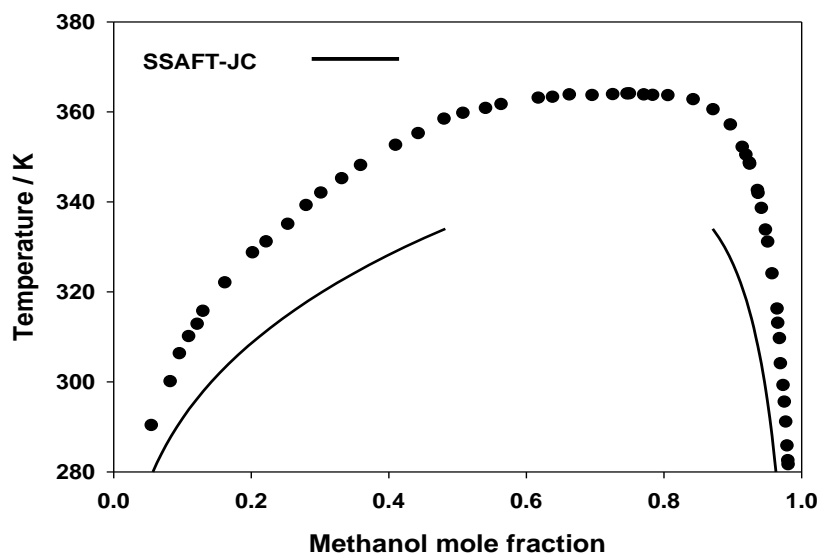


Figure 5.14 Predicted results of liquid-liquid equilibrium ( $k_{ij} = 0$ ) by the SSAFT-JC for the methanol (1)/decane (2) system. Experimental data were taken from Matsuda and Ochi (2004).

For ethanol mixtures, the LLE of ethanol-tetradecane is predicted by the SSAFT-JC. The system is depicted in Figure 5.15. The prediction capability of the SSAFT-JC significantly overestimates the UCST. This result is similar to the result obtained with PC-SFAT-JC. Therefore, both simplified SAFT and PC-SAFT give similar results for the ethanol systems examined.

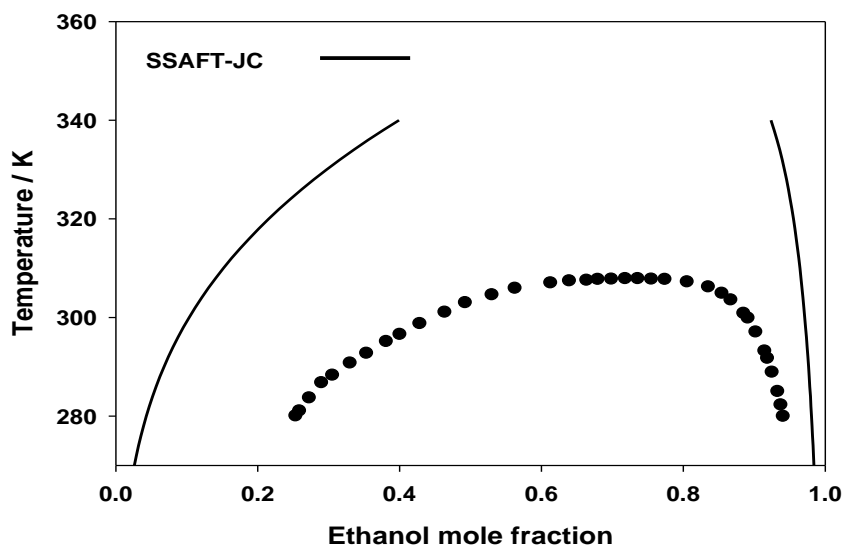


Figure 5.15 Predicted results of liquid-liquid equilibrium ( $k_{ij} = 0$ ) by the SSAFT-JC for the ethanol (1)/tetradecane (2) system. Experimental data were taken from Matsuda and Ochi (2004).

## 5.5.2 Water-hydrocarbon mixtures

It is known that modeling water-hydrocarbon mixtures is a very challenging problem. Many attempts have been made to model them using the SAFT EOS. For instance, Voutsas et al (2000) studied several water-hydrocarbon mixtures using the SAFT and cubic plus association (CPA) equations of state. Their study revealed that the SAFT doesn't offer any improvement over the CPA. A more accurate study was carried out by Vega et al. (2009) using the soft-SAFT. The calculated mole fractions were in good agreement with the experimental data. In both studies, adjustable mixture parameters were used by fitting the mixture experimental data to the SAFT. Moreover, Vega et al. (2009) adjusted the soft-SAFT pure parameters to a limited temperature range (300-450 K) in order to obtain accurate results.

In this section, multiphase water-hydrocarbon systems are first examined using both PC-SAFT-JC and PC-SAFT-GV and compared to experimental data. It should be noted that experimental data have been taken from the data reported by Maczynski et al (2004). In **Chapter 3**, it was indicated that the accuracy of the PC-SAFT-GV and PC-SAFT-JC in VLE was not similar to those of other systems. To show how the PC-SAFT-GV and PC-SAFT-JC perform in LLE, the water-hexane mixture is first examined. As seen, in Figure 5.16, both models predict the water mole fraction in the hydrocarbon-rich phase very well. However, they fail to give satisfactory results for the mole fraction of hexane in the water-rich phase. The same conclusion is drawn from the study of other water-hydrocarbon systems as shown in Figure 5.16 and Figure 5.17 for heptane and n-octane; respectively.

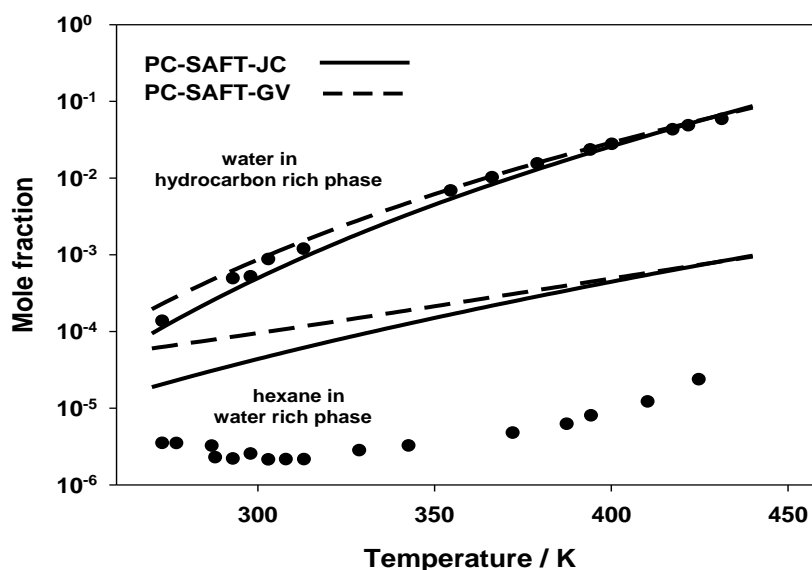


Figure 5.16 Predicted mole fractions of liquid-liquid equilibrium ( $k_{ij} = 0$ ) by the SSAFT-JC and PC-SAFT-GV for the water (1)/hexane (2) system.

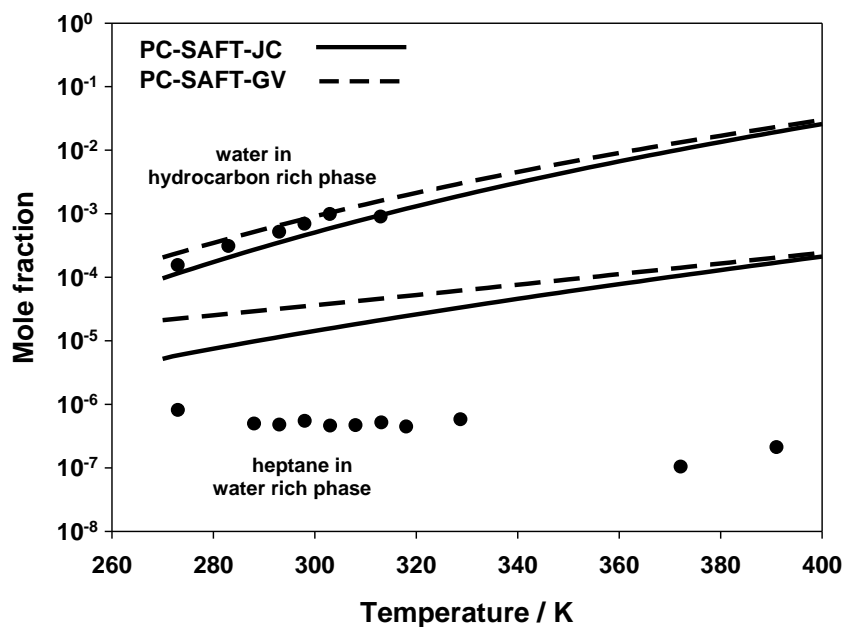


Figure 5.17 Predicted mole fractions of liquid-liquid equilibrium ( $k_{ij} = 0$ ) by the PC-SAFT-JC and PC-SAFT-GV for the water (1)/heptane (2) system.

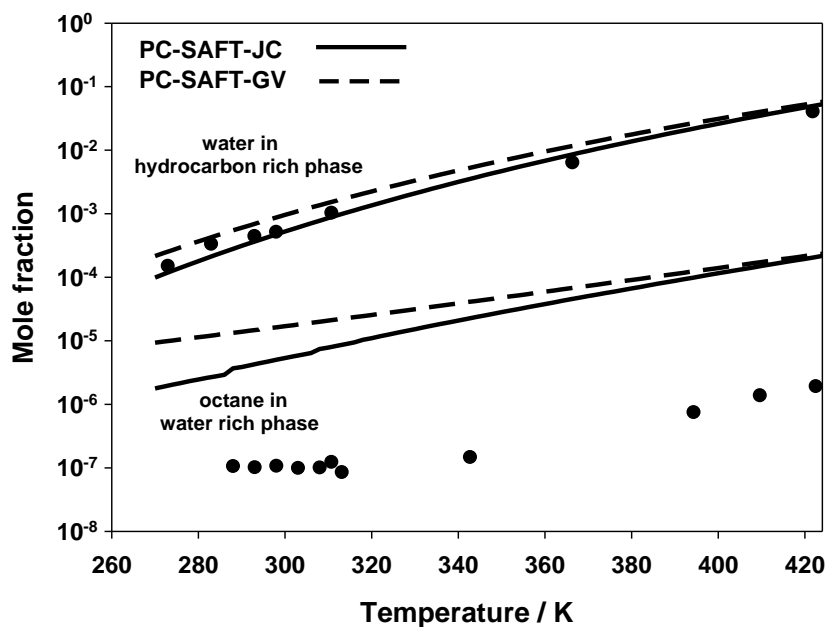


Figure 5.18 Predicted mole fractions of liquid-liquid equilibrium ( $k_{ij} = 0$ ) by the PC-SAFT-JC and PC-SAFT-GV for the water (1)/octane (2) system.

The previous mentioned studies showed that satisfactory results are only possible by giving special consideration to the process of determining the pure parameter values. For example, Vega et al. (2009) indicated that if one needs to describe the phase behaviour of water-hydrocarbon mixtures in near-ambient conditions, it is important to fit pure data around these conditions. Furthermore, the previous studies followed the common practice that is normally utilized to describe the phase behaviour in such mixtures by correlating mixture data using binary interaction parameter. Of course, if binary interaction parameter was avoided in those studies, quantitative prediction is not possible. This approach is not purely predictive. In this work, an attempt is made to obtain satisfactory results from the PC-SAFT-JC by both avoiding the selection of a narrow temperature range of pure data in adjusting the pure parameters and avoiding the correlation of mixture experimental data. The temperature of the pure data ranges from 273.15 to 634 K. The dipole moment of water was not fixed to the gas phase value which is 1.85 D. Instead, the dipole moment is considered as an adjustable parameter. The pure parameter values are given in Table 5.1.

To study water-hydrocarbon mixtures using the new set of the pure parameter values, the water-hexane system is again considered. The LLE prediction of the PC-SAFT-JC is shown in Figure 5.18. It is clear that the PC-SAFT-JC is able to predict the mutual solubilities in good agreement with the experiment data. Unlike other studies, the accuracy obtained here is based on pure prediction. The PC-SAFT-JC was not adjusted to mixture experimental data. The PC-SAFT-JC prediction gives similar results for other water-n-alkane mixtures such as water-pentane, water-heptane, water-octane and water-decane. The water-octane mixture is shown in Figure 5.19. The prediction of water-cyclohexane is given in Figure 5.20. It is apparent from these figures that the PC-SAFT-JC is able to describe quantitatively the phase behaviour of the LLE. It should be emphasized that all the previous studies in the literature that describe the phase behaviour of water-hydrocarbons were correlation studies. But here, the phase behaviour is captured through a process based solely on prediction without correlating mixture experimental data. The experimental data is utilized in this work just for the sake of comparison.

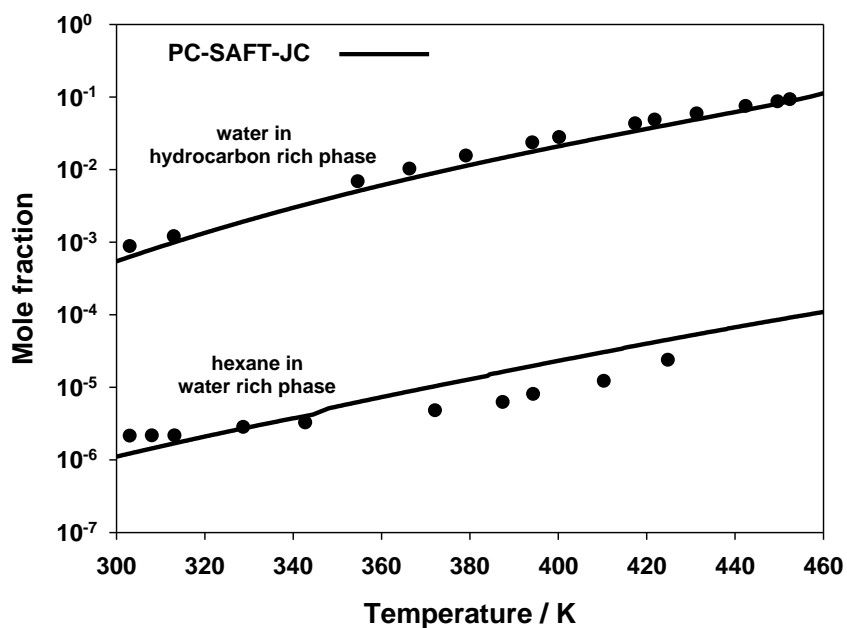


Figure 5.19 Predicted mole fractions of liquid-liquid equilibrium ( $k_{ij} = 0$ ) by the PC-SAFT-JC for the water (1)/hexane (2) system.

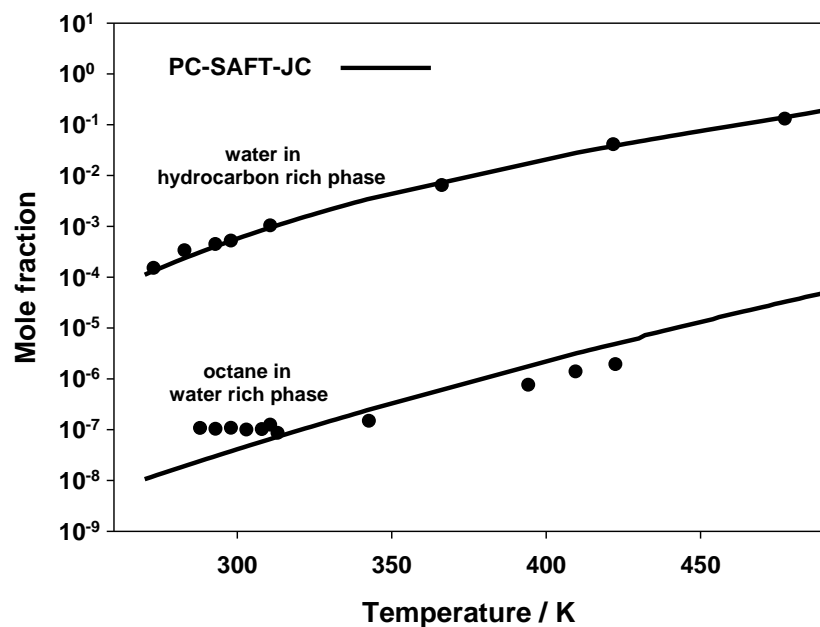


Figure 5.20 Predicted mole fractions of liquid-liquid equilibrium ( $k_{ij} = 0$ ) by the PC-SAFT-JC for the water (1)/octane (2) system.

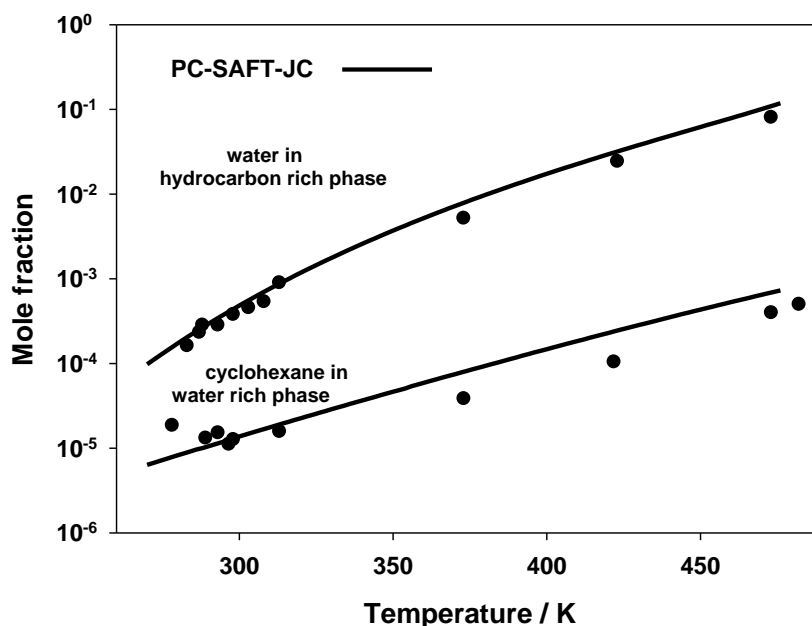


Figure 5.21 Predicted mole fractions of liquid-liquid equilibrium ( $k_{ij} = 0$ ) by the PC-SAFT-JC for the water (1)/cyclohexane (2) system.

## 5.6 Vapour-liquid-liquid equilibrium systems

### 5.6.1 Water-ethylene glycol-hydrocarbon mixtures

In this section, the study is extended to examine multicomponent mixtures. Table 5.2 lists several water-ethylene glycol-hydrocarbons mixtures. These mixtures exhibit VLLE behaviour. To demonstrate the predictive capability of the PC-SAFT-JC and PC-SAFT-GV, the methane-water-ethylene glycol-methylcyclohexane is examined first. The experimental data for this mixture was reported by Chen et al. (1988) and Ashcroft et al. (1995).

Table 5.2 Water-ethylene glycol-hydrocarbon mixtures

Mixtures	Type of Equilibrium
methane-water-ethylene glycol-propane	VLLE
methane-water-ethylene glycol-methylcyclohexane	VLLE
methane-water-ethylene glycol-hexane	VLLE
methane-water-ethylene glycol-octane	VLLE

The phase behaviour of this mixture was also correlated by using Peng-Robinson equation of state (PR EOS) (Ashcroft et al., 1995). The results from the prediction of the PC-SAFT-JC with pure parameter set

2 (PC-SAFT-JC2), PC-SAFT-JC with pure parameter set 1 (PC-SAFT-JC1), PC-SAFT-GV and the correlated PR are given in Table 5.3. A careful inspection of the predicted results of the dipolar SAFT models reveals that they are almost identical. The prediction of the mole fractions for the three phases by the dipolar SAFT models is in very satisfactory agreement with the experimental data. However, the PC-SAFT-JC2 is better than other dipolar SAFT versions in the concentration of methylcyclohexane in the water rich phase ( $L_W$ ). As seen, the mole fraction of methylcyclohexane predicted by the PC-SAFT-JC2 is equal to 7.474E-06 which compares well to the experimental value (6.00E-06). The values predicted by the PC-SAFT-JC1 and PC-SAFT-GV are 0.0002 and 0.001; respectively. It should be also noted that the prediction of the dipolar SAFT is almost equivalent for the correlated PR EOS. For the other mixtures in Table 5.2, similar conclusions are drawn for the ethylene glycol-water-methylcyclohexane-methane mixture.

Table 5.3 Predicted mole fractions of ethylene glycol-water-methylcyclohexane-methane by PC-SAFT-JC2, PC-SAFT-JC1, PC-SAFT-GV and PR.

		T = 276 K				P = 70 bar			
		Feed	V	V (exp.)	$L_{HC}$	$L_{HC}$ (exp.)	$L_W$	$L_W$ (exp.)	
PC-SAFT-JC2	MEG	0.045	2.31E-07	< 1e-6	4.588E-07	7.100E-05	0.1350	0.1330	
	water	0.291	0.000128	0.00014	1.318E-04	1.400E-04	0.8642	0.8650	
	MCH	0.193	0.0020889	0.0013	0.6539	0.7380	7.474E-06	6.00E-06	
	methane	0.471	0.9977828	0.9986	0.3460	0.2620	0.0008	0.0023	
		Feed	V	V (exp.)	$L_{HC}$	$L_{HC}$ (exp.)	$L_W$	$L_W$ (exp.)	
PC-SAFT-JC1	MEG	0.045	8.779E-08	< 1e-6	1.95E-07	7.100E-05	0.1346	0.1330	
	water	0.291	1.347E-04	0.00014	0.0001183	1.400E-04	0.8620	0.8650	
	MCH	0.193	0.0021	0.0013	0.6539132	0.7380	0.0002	6.00E-06	
	methane	0.471	0.9978	0.9986	0.3459685	0.2620	0.0032	0.0023	
		Feed	V	V (exp.)	$L_{HC}$	$L_{HC}$ (exp.)	$L_W$	$L_W$ (exp.)	
PC-SAFT-GV	MEG	0.045	3.029E-07	< 1e-6	8.28E-06	7.100E-05	0.1345	0.1330	
	water	0.291	1.481E-04	0.00014	0.0002449	1.400E-04	0.8613	0.8650	
	MCH	0.193	0.0021	0.0013	0.6538065	0.7380	0.0011	6.00E-06	
	methane	0.471	0.9978	0.9986	0.3459405	0.2620	0.0030	0.0023	
		Feed	V	V (exp.)	$L_{HC}$	$L_{HC}$ (exp.)	$L_W$	$L_W$ (exp.)	
PR	MEG	0.045	.....	< 1e-6	8.20E-04	7.100E-05	0.1360	0.1330	
	water	0.291	2.300E-04	0.00014	9.50E-03	1.400E-04	0.8640	0.8650	
	MCH	0.193	0.0024	0.0013	0.67	0.7380	.....	6.00E-06	
	methane	0.471	0.9974	0.9986	0.32	0.2620	0.0013	0.0023	

## 5.7 Conclusions

In this chapter, the predictive capability of the dipolar SAFT in multiphase systems was evaluated. Both the Chapman and Gross terms were considered. Because the Gross term didn't give a satisfactory quantitative prediction of VLE, as we saw in Chapter 3, the polarization and quadrupole-quadrupole interactions were now incorporated. It was found that the addition of these interactions enabled quantitative prediction of VLE almost similar to what was found for Chapman's term in Chapter 3. However, the Chapman term still performs slightly better. The incorporation of only induced dipole-dipole interactions was not enough, with Gross's term, to give a satisfactory quantitative prediction.

In the study of the VLLE and LLE, the same pure parameter values that were used in Chapter 3 were first utilized with both PC-SAFT-JC and PC-SAFT-GV. For alcohol-hydrocarbons; particularly methanol/ethanol-hydrocarbon mixtures, it was found that the PC-SAFT-JC model significantly overestimates the UCST. The incorporation of other electrostatic interactions for the study of LLE was not considered since these interactions would contribute to further overestimation of the UCST. For short-hydrocarbon-chain, the PC-SAFT-GV also overestimates the UCST, while for long-hydrocarbon-chains the PC-SAFT-GV underestimates the UCST. This is expected due to the complexity of the phase behaviour of the methanol/ethanol systems at low temperatures. To study methanol/ethanol-hydrocarbon systems, the simplified SAFT was used to test how other versions perform. It was found that the simplified SAFT gives fairly good results for the methanol-hexane system. However, it performs similarly to the PC-SAFT-JC and PC-SAFT-GV for other systems. For water-hydrocarbon systems, it was found that both PC-SAFT-GV and PC-SAFT-JC were in good agreement with the experimental data in the hydrocarbon-rich phase. However, both gave poor prediction in the water-rich phase.

To assess the influence of different pure parameter values with the PC-SAFT-JC, new parameter values for water were obtained and utilized to predict the behaviour of water-hydrocarbon mixtures. It was found that the PC-SAFT-JC gave quantitative prediction of the mole fraction in both hydrocarbon-rich and water-rich phases without having to adjust any parameters by using experimental data. Other multicomponent mixtures were also studied and it was found that the prediction is satisfactory particularly with the new pure parameter values.

## CHAPTER 6

# ACCURATE PHASE EQUILIBRIUM CALCULATION WITHOUT ANALYTICAL DERIVATIVES

### 6.1 Introduction

In the last three decades, thermodynamic modeling of real fluids and mixtures has been increasingly directed towards models inspired from statistical mechanics theories or models constructed from molecular simulation data. The interest in these models has been motivated by the shortcomings of classical thermodynamic models. Although more accurate description of real fluid and mixtures has been achieved by these models, the developments are accompanied by an increase in the mathematical complexity. For instance, Mecke et al. (1997) developed a Helmholtz free energy term for attractive dispersion force containing 34 terms with 204 adjustable parameters. There are similar complicated Helmholtz free energy terms which are impractical to use due to their complexity, even though they have shown good accuracy. Table 6.1 lists examples of common complex terms that describe the contribution of various types of molecular interactions.

In the previous chapters, it was shown that various terms were incorporated into the SAFT model when mixtures were studied. For instance, when dipolar and quadrupole terms were incorporated into the PC-SAFT along with the chain, hard sphere, dispersion and association terms, the final EOS is very complicated. It is not only the complexity of the terms that makes the use of these models difficult, but also the determination of their derivatives. For instance, the computation of phase equilibrium and thermodynamic properties using theory-based equations is obtained by determining the higher partial derivatives of these complicated terms with respect to mole fraction, density, temperature etc. The difficulty of obtaining the partial derivatives analytically would limit the use, evaluation and comparison of these models since more complicated equations would arise from differentiation.

Table 6.1 Examples of molecular models

<b>Models</b>	<b>Source</b>	<b>NP*</b>
Repulsion and dispersion	Nicolas et al. (1979)	33
Repulsion and dispersion	Johnson et al. (1993)	33
Dispersion	Mecke et al. (1997)	204
Dispersion	Fischer et al.	24
dipole-dipole	Muller et al. (1995)	140
dipole-dipole	Gross and Vrabec (2006)	45
dipole-quadrupole	Vrabec and Gross (2009)	33
quadrupole	Gross (2005)	45
quadrupole	Muller et al. (1995)	85

\*NP: number of adjustable parameters

However, if the analytical derivative approach is avoided, the alternative route, which is numerical differentiation, cannot be accepted unless it is very easy to implement, very accurate, robust and stable. Most of these characteristics are not available in the most commonly known methods such as finite differencing. The finite difference method is easy to implement; however, it unfortunately encounters problems in accuracy, computational efficiency and subtractive cancellation errors. Another known method that is accurate and commonly used in order to avoid analytical derivatives is automatic differentiation. It is based on systematic application of the chain rule of differentiation to computer programs to compute a function value. It computes derivatives accurately; however, it is impractical because it needs extensive computational effort for its implementation (Boudjemaa et al., 2003).

In this chapter, we present an uncommon method that demonstrates characteristics that lead to efficient computation of numerical derivatives. The method is called complex-step derivative approximation. It is robust, very easy to implement and very accurate. This method is utilized to compute the required derivatives to perform phase equilibrium calculations. The method is applied to several models with varying complexity such as simplified SAFT, CK-SAFT and PC-SAFT. Dispersion, association, dipolar and quadrupole interactions are

incorporated into one equation to show the power of the complex-step derivative approximation to give accurate calculations. The chapter starts with an introduction to the complex-step derivative approximation (section 6.2). In section 6.3, the complex-step derivative approximation is utilized to approximate the required first derivatives in phase equilibrium calculations. The final results from phase equilibrium calculations (such as mole fractions) are then compared to those obtained by the analytical first derivatives.

## 6.2 Complex-step derivative approximation

The complex-step derivative approximation was initially introduced by Lyness and Moler (1967) and Lyness (1967). The work of Lyness and Moler showed, for the first time, how to use complex variables to estimate  $n$ th derivatives of an analytical function. Their work was used by Squire and Trapp (1998) to determine the first derivative by the use of complex variables. The derivatives could easily be determined via various approaches (Squire and Trapp, 1998, Martins et al., 2003). The first derivative of complex-step approximation is very simple and given by:

$$\frac{\partial f}{\partial x} \approx \frac{Im[f(x + ih)]}{h} \quad 6-1$$

where  $Im$  represents the imaginary part of the function  $f(x + ih)$ ,  $h$  is the step-size and  $i$  is the imaginary unit. The output of the function  $Im[f(x + ih)]$  is real although it contains a complex argument. The first derivative is free from round-off error due to subtractive cancellation. Thus, the estimate of the first derivative by the complex-step derivative approximation is almost identical to the one obtained by the analytical differentiation if a very small step size is selected, as will be shown. This advantage will save tremendous effort when first derivatives are necessary to perform any kind of calculations. In this chapter, the advantage of equation 6-1 would assist in performing phase equilibrium calculations by obtaining the first derivatives of the Helmholtz free energy with respect to mole fractions and density.

The second derivatives of the Helmholtz free energy are required when thermodynamic properties like heat capacity are computed. Although, the thermodynamic properties are not conducted in this chapter, the derivatives of complex-step approximation are given. Unlike the first derivative approximation, the second derivative approximation is subject to round-off error due to the existence of function difference:

$$\frac{\partial^2 f}{\partial x^2} \approx \frac{2\{f(x) - \text{Im}[f(x + ih)]\}}{h^2} \quad 6-2$$

However, the approximation is modified by Lai and Crassidis (2007) to make it less sensitive to round-off error by:

$$\frac{\partial^2 f}{\partial x^2} \approx \frac{\text{Im}\left\{f\left(x + i\frac{1}{2}h\right) + f\left(x + i\frac{5}{2}h\right)\right\}}{h^2} \quad 6-3$$

It should be noted that the second derivative approximation is not as accurate as the first one. However, if a similar accuracy of second and higher derivatives is required, the reader could refer to the work of Lantoin et al. (2010) who presented very accurate derivatives for any arbitrary order of partial derivatives using multicomplex approximation.

### 6.3 Evaluation of simplex-step derivatives in phase equilibrium calculations

In this section, the validity of complex-step approximation is tested in phase equilibrium calculations. To do this, one needs to obtain the fugacity coefficient by differentiating the Helmholtz free energy with respect to density and mole fraction. The procedure of phase equilibrium computation is summarized in **Appendix B**. Most phase equilibrium calculations conducted in this thesis are re-conducted by employing complex-step approximation. Here, two examples are given to demonstrate its accuracy.

#### 6.3.1 Binary system

The first example shows VLE of a binary system of ethanol-pentane at different isothermal conditions using the PC-SAFT equation of state that has hard sphere, chain, dispersion, association, dipolar and quadrupole terms. The required adjustable pure parameters were given in Table 5.2. The PC-SAFT terms were summarized in **Chapter 2**. The hard sphere and chain terms are relatively simple in their mathematical formulation. The dispersion term has a total of 42 constants. The Gross dipolar term given in **Chapter 3** is based on adjusting molecular simulation data for vapor–liquid equilibria of the two-center Lennard–Jones (2CLJ)

plus pointdipole with 45 adjustable parameters. The quadrupolar term given in **Chapter 5** is also developed based on molecular simulation data for vapor–liquid equilibria of the two-center Lennard–Jones (2CLJ) but with pointquadrupole fluid with 45 adjustable parameters. Therefore, from dispersion, dipolar, and quadrupolar terms, we have a total of 132 adjustable parameters. The nontrivial association term is also incorporated to take account of hydrogen bonding interactions in ethanol.

The bubble point pressure calculations are conducted at 30, 50, 96, 125, 149 and 192 °C. The calculations are conducted twice for each isotherm; one with the aid of the complex-step derivative to approximate the required Helmholtz free energy derivatives and one with analytical derivatives. For each isotherm, the final VLE results (i.e. P-y) are compared. Then, the relative errors of calculated vapor mole fraction and pressure are calculated. The relative error is defined to be the difference between the analytical value and the numerical approximation divided by the analytical value. Table 6.2 reports only the maximum relative error of pressure and vapour mole fraction at each isotherm. The calculations are carried out by choosing the step size to be the square root of the machine accuracy ( $\epsilon=2.2\times 10^{-16}$ ). As seen in Table 6.2, the difference between the results obtained via analytical and numerical approaches is very small.

Table 6.2 Maximum relative error of pressure and vapour mole fractions.

T ( °C)	Relative error *, P(%)	Relative error *, y <sub>1</sub> (%)	N data
30	3.53E-09	2.36E-09	26
50	1.21E-09	1.09E-08	21
100	8.76E-10	1.61E-09	10
125	2.72E-10	9.50E-10	12
149	1.38E-10	6.63E-10	11
192	8.01E-11	1.81E-09	15

$$\text{Relative error} = \frac{f^{\text{analytical}} - f^{\text{numerical}}}{f^{\text{analytical}}} \times 100$$

$f^{\text{analytical}}$  = calculation is performed by the use of the analytical derivatives of Helmholtz free energy.

$f^{\text{numerical}}$  = calculation is performed by the use of the numerical derivatives of Helmholtz free energy.

Greater accuracy in results could be obtained without any stability problem if a smaller step size is chosen. Table 6.3 shows the results of bubble point pressure at T=149.45 °C and  $x_{\text{ethanol}}=0.69$  at various step sizes. This state condition is chosen for demonstration. Any other state condition could be utilized without change in the accuracy. It is clear that the accuracy of

the calculated pressure improves as the step size declines. At step size equal to  $10^{-30}$ , the pressure from the numerical approach matches the pressure of the analytical approach up to 15 significant digits. This is strong evidence that the complex-step approximation is a powerful computational method of the first derivative. The reason for this accuracy is the fact that the first derivative of the complex-step approximation is free from round-off error.

Table 6.3 Calculated Pressure at 149.45 °C and  $x_{\text{ethanol}}=0.69$  with the change of step size.

Step size	P numerical* (atm)	P analytical** (atm)
1.00E-03	16.7006473885255	16.5931592546885
1.00E-05	16.5931694690686	
1.49E-08	16.5931592547112	
1.00E-10	16.5931592546886	
1.00E-20	16.5931592546884	
1.00E-30	16.5931592546885	
1.00E-40	16.5931592546885	

\*P numerical= pressure is calculated by computing the derivatives from Helmholtz energy by the complex-step approximation.  
 \*\*P analytical= pressure is calculated by computing the derivatives from Helmholtz energy analytically.

### 6.3.2 Hydrocarbon mixture

In the second example, three different SAFT versions are considered; namely, simplified-SAFT, CK-SAFT and PC-SAFT. The three SAFT versions are used to perform flash calculations for a mixture of six hydrocarbon components at 93.33 °C and 206.4 atm. It is noted that a zero value for the binary interaction parameter ( $k_{ij}=0$ ) is used. The hydrocarbon mixture is composed of methane, ethane, n-propane, n-pentane, n-heptane and n-decane. The considered SAFT terms of the three versions are hard sphere, dispersion and chain terms. As previously indicated, the phase equilibrium calculations are performed with differentiation of the Helmholtz free energy with respect to mole fraction and density. The calculations are conducted numerically with complex-step approximation and compared to those obtained analytically. Table 6.4 compares the calculated mole fractions of the numerical and analytical approaches. The results agree at least up to 9 significant digits in the three SAFT versions and in most of the cases up to 11 significant digits.

Table 6.4 A comparison between the calculated mole fractions obtained by numerical and analytical derivatives.

	PCSAFT			
	vapor mole fraction		liquid mole fraction	
	analytical	numerical	analytical	numerical
methane	0.81161277047863	0.81161277047884	0.61427729513314	0.61427729513480
ethane	0.05657312906536	0.05657312906535	0.05934533237987	0.05934533237992
propane	0.03051915702780	0.03051915702779	0.03885951282392	0.03885951282390
n-pentane	0.04530989309500	0.04530989309495	0.08555619153739	0.08555619153716
n-heptane	0.03244806965194	0.03244806965188	0.08938926505859	0.08938926505811
n-decane	0.02353699789589	0.02353699789579	0.11257064429658	0.11257064429545
	SSAFT			
	vapor mole fraction		liquid mole fraction	
	analytical	numerical	analytical	numerical
methane	0.84975779612332	0.84975779643833	0.75230747033417	0.75230747092984
ethane	0.05546903869914	0.05546903867928	0.05822037696259	0.05822037696148
propane	0.02792421616959	0.02792421613937	0.03443371073120	0.03443371070456
n-pentane	0.03506685406258	0.03506685397213	0.06093456611981	0.06093456597148
n-heptane	0.02084666410044	0.02084666401776	0.05041260774824	0.05041260754904
n-decane	0.01093622931318	0.01093622924980	0.04369012410413	0.04369012384305
	CKSAFT			
	vapor mole fraction		liquid mole fraction	
	analytical	numerical	analytical	numerical
methane	0.84682610633350	0.84682610633350	0.69659838161840	0.69659838161840
ethane	0.05579293177746	0.05579293177746	0.05905866672077	0.05905866672077
propane	0.02844822540357	0.02844822540357	0.03715520369042	0.03715520369042
n-pentane	0.03637131680085	0.03637131680085	0.07411906333283	0.07411906333283
n-heptane	0.02159881297634	0.02159881297634	0.06773277515999	0.06773277515999
n-decane	0.01096292681524	0.01096292681524	0.06533493429815	0.06533493429815

The derivatives of complex-step derivatives are not influenced by the complexity of the dispersion term. To see if this accuracy holds for different conditions, the mixture is studied at different P-T conditions and the same conclusion is revealed. For instance, the pressure-temperature phase envelope is calculated using the PC-SAFT EOS by a series of flash calculations where the pressure is fixed and temperature is changed until a single phase is obtained. In the worst case, the comparisons between the obtained mole fractions from analytical and numerical approaches match up to 10 significant digits. Figure 6.1 depicts the P-T phase

envelope of the mixture. As seen in the figure, only one curve appears since the two curves are indistinguishable from each other.

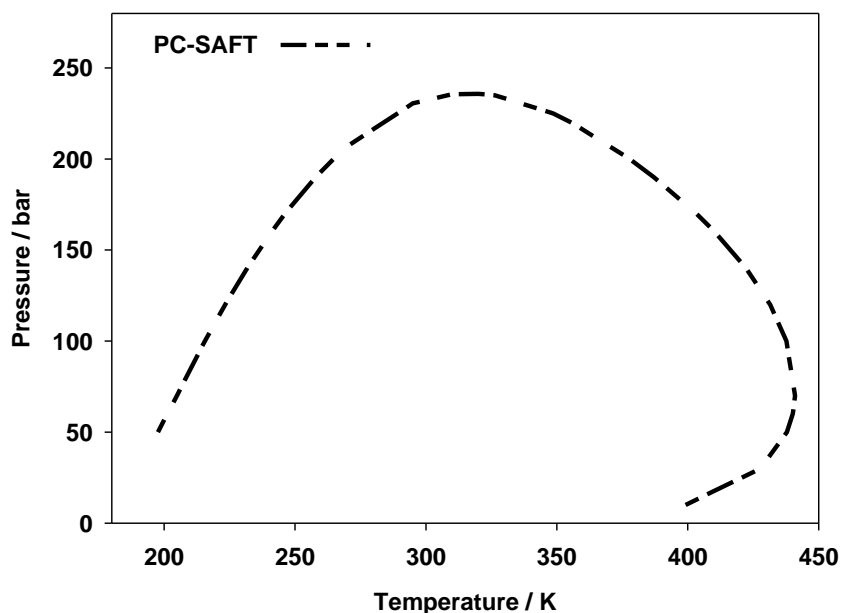


Figure 6.1 P-T envelop of methane, ethane, n-propane, n-pentane, n-heptane and n-decane mixture predicted by PC-SAFT.

## 6.4 Conclusions

In this chapter, complex-step approximation was introduced and utilized in phase equilibrium calculations. Complex-step approximation was used to obtain numerically the required derivatives from the Helmholtz free energy with respect to density and mole fraction. The accuracy of these derivatives is almost identical to the one obtained analytically. The use of complex-step approximation will save tremendous computational effort when performing phase equilibrium calculations which are based on first derivatives. It will also save substantial effort since the analytical derivatives could be avoided. The accuracy is attributed to the absence of subtractive cancellation error in the first derivative approximation. The advantage offered by the complex-step approximation could be exploited in any other application which requires the determination of the first derivatives.

## CHAPTER 7

# A GENERAL TREATMENT OF POLAR-POLARIZABLE SYSTEMS FOR AN EQUATION OF STATE

### 7.1 Introduction

Significant progress has been made in developing theories for polar molecules characterized by permanent multipole moments. The developments have mainly been attributed to statistical mechanical perturbation theories. Various models are now available for dipolar, quadrupolar and octupolar molecules with fairly good accuracy (Tsu & Gubbins, 1978b). These non-polarizable models are derived based on pairwise additive approximation. The real polar molecules, however, exhibit many-body induced polarization interactions and their energies are impossible to express as a sum of pairs. The effect of polarization interactions is not by any means negligible. For example, the average dipole moment of water increases up to 40% as a result of the large polarization (Gregory et al., 1997). The non-additivity of induced interactions undoubtedly complicates the theoretical treatment of the induction effect since knowledge of fourth and higher order correlation functions is required (Joslin et al., 1985). Unfortunately, taking into account the many-body interactions is crucial if accurate results are desired. Thus, it is not surprising that the theoretical techniques of McDonald (1974), Larsen et al. (1977) and Winkelmann (1981) for the treatment of induction effect were inaccurate since the many-body interactions were ignored. Therefore, inclusion of the many-body interactions is inevitable in any theoretical route to the treatment of the polarizability effect.

A convenient approach to the problem of the many-body interactions is to replace these interactions with an effective potential that incorporates the average many-body interaction into the interaction between pairs. The approach has been adopted by Wertheim (1973a, 1973b, 1977a, 1977b), Høye and Stell (1980) and Carnie and Patey (1982) as a basis for theoretical treatment of the polarizability effect. The studies just mentioned were successful in faithfully reproducing the microscopic structure and thermodynamic properties of polarizable particles. Unlike other approaches, the Wertheim approach, which is called the renormalization perturbation theory (RPT), has been utilized with theory-based equations of state. The RPT was formulated based on a cumbersome graphical theory for dipolar-

dipolar polarizable particles. Extension to mixtures and dipolar-quadrupolar polarizable particles were given by Venkatasubramanian et al. (1984) and Gray et al. (1985). The RPT has recently been incorporated into the SAFT EOS to take into account the polarizable dipolar-dipolar systems (Kraska & Gubbins, 1996; Kleiner & Gross, 2006). Although the RPT showed good results, it is not an easy task to make it applicable to higher polarizable multipolar molecules. Even the extension to polarizable dipolar-quadrupolar molecules that has been carried out by Gray et al. (1985) was not trivial; it was derived with different approach from that of the original complex graphical theory approach used by Wertheim.

An alternative theory to the renormalized perturbation theory is the self-consistent mean field theory proposed by Carnie and Patey (1982). The SCMF is equivalent to the RPT in terms of accuracy (Carnie and Patey, 1982). It is however based upon physical arguments rather than a mathematical approach. Further, the SCMF can be extended to take account of any polarizable multipolar interaction in a straightforward manner. The theory has been tested for various types of molecules using integral equation theories (Caillol et al., 1987). Because the SCMF was originally derived to be used with integral equation theories and molecular simulation, only the energy term was derived. In this thesis which is related to theory based equations of state, the free energy term is derived. A comparison with simulation data is also given. Moreover, the SCMF is extended to mixtures and applied to SAFT to study real mixtures. Finally, a general term is given for dipolar, quadrupole, octupole and ionic contribution of polarizable systems that is convenient for any theoretical equation of state.

This chapter is summarized as follows. First, the SCMF theory is explained and the original mathematical formulations are given (section 7.2). Section 7.3 shows the derivation of the free energy term. Extension of SCMF to mixtures is given in section 7.4. Then, the SCMF is compared to available simulation data (section 7.5). In section 7.6, the extended SCMF is employed in theory-based equation of state to study real mixtures. Some concluding remarks are provided at the end in section 7.7.

## 7.2 Self-consistent mean field theory

As previously indicated, the SCMF theory approximates the many body polarization interactions with an effective pairwise-additive interaction. In particular, the theory replaces all the instantaneous dipole moments with an effective permanent dipole moment ( $\mu_e$ ) by ignoring the fluctuations in the local electric field. The polarizable medium is characterized by the average total molecular dipole moment ( $\bar{\mu}$ ) and renormalized polarizability ( $\bar{\alpha}$ ) in the same way that permanent dipole moment ( $\mu$ ) and polarizability ( $\alpha$ ) characterize a non-polarizable system. The values describing the effective system ( $\mu_e$ ,  $\bar{\alpha}$  and  $\bar{\mu}$ ) are

determined to be self-consistent with a given dipole moment and polarizability by solving the following system of equations (Carnie and Patey, 1982; Caillol et al., 1985):

$$\bar{\mu} = \mu + C(\bar{\mu})\mu \cdot \bar{\alpha} \quad 7-1$$

$$\bar{\alpha} = \alpha + C(\bar{\mu})\alpha \cdot \bar{\alpha} \quad 7-2$$

$$\mu_e^2 = \bar{\mu}^2 + 3\bar{\alpha}kT \quad 7-3$$

where  $k$ ,  $N$  and  $T$  are Boltzmann constant, number of particles and temperature.  $C(\bar{\mu})$  is a scalar dependent function related to the energy of the effective system:

$$C(\bar{\mu}) = -\frac{2\langle U^{DD} \rangle_e}{\mu_e^2 N} - \frac{\langle U^{DQ} \rangle_e}{\mu_e \bar{\mu} N} - \frac{\langle U^{DO} \rangle_e}{\mu_e \bar{\mu} N} - \frac{\langle U^{ID} \rangle_e}{\mu_e \bar{\mu} N} \quad 7-4$$

where the energy superscripts D, Q, O and I denote the dipolar, quadrupolar, octopolar and ionic contributions, respectively.

The total average energy of the polarizable system is given by (Carnie and Patey, 1982):

$$\begin{aligned} \langle U \rangle = & \langle U^{LJ} \rangle_e + \langle U^{QQ} \rangle_e + \frac{\mu \bar{\mu}}{\mu_e^2} \langle U^{DD} \rangle_e + \frac{(\mu + \bar{\mu})}{2\mu_e} \langle U^{DQ} \rangle_e + \frac{(\mu + \bar{\mu})}{2\mu_e} \langle U^{DO} \rangle_e \\ & + \frac{(\mu + \bar{\mu})}{2\mu_e} \langle U^{ID} \rangle_e \end{aligned} \quad 7-5$$

Hence, the total average energy of a polarizable system is determined by obtaining  $\mu_e$ ,  $\bar{\mu}$  and the effective energies by solving simultaneously equations 7-1 to 7-5. The solution procedure requires a replacement of the permanent dipole moment in the non-polarizable multipole model by the obtained effective dipole moment without any modification in the non-polarizable model. It should be noted that each term of the 3<sup>rd</sup>-6<sup>th</sup> terms on the right hand side of equation 7-5 consists of two energy contributions; namely, the effective energy and the self-consistent energy.

### 7.3 The free energy of the SCMF

To facilitate the application of the SCMF theory to theory-based equation of state, it is essential to derive a general Helmholtz free energy term for the polarizable system in the NVT ensemble. Consider a polarizable system where the particles could have dipole, quadrupole, octupole and/or ions. The free Helmholtz energy of the polarizable system ( $A^{polz}$ ) could be decomposed into an effective Helmholtz free energy term ( $A^e$ ) and a self-consistent free Helmholtz energy term ( $A^{self}$ ) as follows:

$$\frac{A^{polz}}{NkT} = \frac{A^e}{NkT} + \frac{A^{self}}{NkT} \quad 7-6$$

The effective Helmholtz free energy is simply obtained from the non-polarizable model but with the replacement of the permanent dipole moment by the effective one.

To derive the self-consistent Helmholtz free energy, on the other hand, equation 7-5 is exploited to determine the energetic contribution from the self-consistent Helmholtz free energy. As indicated previously, the energy of the polarizable system in equation 7-5 contains both the effective and the self-consistent contributions. Therefore, it is possible to obtain the self-consistent energy by deducting the effective term from equation 7-5. For instance, the self-consistent energy of the dipolar contribution is given by:

$$\langle U^{DD} \rangle^{self} = \frac{\mu\bar{\mu}}{\mu_e^2} \langle U^{DD} \rangle - \langle U^{DD} \rangle^e \quad 7-7$$

It should be noted that the first term on the right hand side is a contribution of both the self-consistent and effective energies of the polarizable dipole-dipole term which is the third term on the right hand side of equation 7.5 The effective energy is available from the non-polarizable model but, as mentioned above, the permanent dipole moment should be replaced with the effective one.

Since the fluctuations in the local electric field were ignored, this suggests the square root of the induced dipole moment  $p^2$  is a non-fluctuating constant. This is consistent with the mean field approach. Thus, there are no other degrees of freedom in the model that might contribute to entropy. Therefore, the entropic contribution of the self-consistent free energy is zero. The self-consistent free energy is therefore given by:

$$\frac{A^{self}}{NkT} = \frac{U^{self}}{NkT} \quad 7-8$$

This leads us to write the total average Helmholtz free energy of the polarizable system as:

$$\frac{A^{polz}}{NkT} = \frac{(A^{DD})^e}{NkT} + \frac{(A^{DQ})^e}{NkT} + \frac{(A^{DO})^e}{NkT} + \frac{(A^{ID})^e}{NkT} + \frac{(A^{DD})^{self}}{NkT} + \frac{(A^{DQ})^{self}}{NkT} + \frac{(A^{DO})^{self}}{NkT} + \frac{(A^{ID})^{self}}{NkT} \quad 7-9$$

where the subscripts e and self denote the effective and self-consistent terms, respectively.

## 7.4 Extension of SCMF to mixtures

To extend the SCMF to mixtures for any number of components, it is simpler to begin with interacting polarizable particles of a binary mixture of A and B. The local electric field experienced on the site of the  $i$ th particle of A is a result of the local electric field arising from the other nearby A particles as well as the local electric field arising from nearby B particles. Similarly, the  $j$ th particle of B experiences local electric fields from other nearby A and B particles. Hence, the total instantaneous dipole moments of the  $i$ th and  $j$ th particles are respectively given by:

$$m_i^A = \mu_i^A + \alpha^A \cdot (E_{iA})_i \quad 7-10$$

and

$$m_j^B = \mu_j^B + \alpha^B \cdot (E_{jB})_j \quad 7-11$$

The average total molecular dipole moments of identical particles of A and B as measured in the molecular coordinate system are given by:

$$\bar{\mu}^A = \mu^A + \alpha^A \cdot \langle E_{iA} \rangle \quad 7-12$$

$$\bar{\mu}^B = \mu^B + \alpha^B \cdot \langle E_{jB} \rangle \quad 7-13$$

where  $\langle E_{iA} \rangle$  is the average local electric field felt on a particular A particle due to B and other A particles. It can be written as:

$$\langle E_{iA} \rangle = \langle E_{iA} \rangle^A + \langle E_{iA} \rangle^B \quad 7-14$$

In a similar manner,  $\langle E_{jB} \rangle$ , which is the average local electric field acting on a particular B particle due to A and B particles, is given by:

$$\langle E_{lB} \rangle = \langle E_{lB} \rangle^A + \langle E_{lB} \rangle^B \quad 7-15$$

In the forthcoming discussion, the description is illustrated in detail only for polarizable A particles, which are influenced by the surrounding A and B molecules, because the same methodology could be followed for polarizable B particles. Only the final result of the derivation of polarizable B particles is given after obtaining the results of polarizable A particles.

As demonstrated by Carnie and Patey (1982), for isotropic  $C_{2V}$  and higher symmetry molecules, the total average local electric field acting on a molecule and the average total molecular dipole moment are both in the same direction and they are related by:

$$\langle E_l \rangle = C(\bar{\mu})\bar{\mu} \quad 7-16$$

Therefore, the average local electric fields acting on A due to A and B fields are respectively given by

$$\langle E_{lA}^A \rangle = C^{AA}(\bar{\mu}^A)\bar{\mu}^A \quad 7-17$$

and

$$\langle E_{lA}^B \rangle = C^{BA}(\bar{\mu}^B)\bar{\mu}^A \quad 7-18$$

The scalar  $C^{BA}(\bar{\mu}^B)$  is related to the molecule B fields acting on molecule A. By combining equations 7-14, 7-17 and 7-18, one can write the average local electric field acting on A due to A and B molecules as:

$$\langle E_{lA} \rangle = (C^{AA}(\bar{\mu}^A) + C^{BA}(\bar{\mu}^B))\bar{\mu}^A \quad 7-19$$

Inserting the above equation into equation 7.12 to obtain:

$$\bar{\mu}^A = \mu^A + \alpha^A \cdot (C^{AA}(\bar{\mu}^A) + C^{BA}(\bar{\mu}^B))\bar{\mu}^A \quad 7-20$$

The above equation is the first required equation in extending the SCMF theory for the binary system of A and B. Equation 7-1 could be recovered from this equation by setting  $\bar{\mu}^B$  equal to zero. If the same methodology is followed for component B, it would be easy to show:

$$\bar{\mu}^B = \mu^B + \alpha^B \cdot (C^{BB}(\bar{\mu}^B) + C^{AB}(\bar{\mu}^A))\bar{\mu}^B \quad 7-21$$

Equations 7-20 and 7-21 are the extended version of equation 7-1 to a binary system.

To complete extending the SCMF equations to mixtures, we now turn our attention to the derivation of the extended version of equations 7-2 and 7-3. By iterating equations 7-12, 7-14 and 7-17, it is not difficult to show that the second equation of the SCMF formulations is given by:

$$\bar{\alpha}^A = \alpha^A + (C_D^{AA}(\bar{\mu}^A) + C_D^{BA}(\bar{\mu}^B))\alpha^A \cdot \bar{\alpha}^A \quad 7-22$$

For component B, it is given by:

$$\bar{\alpha}^B = \alpha^B + (C_D^{BB}(\bar{\mu}^B) + C_D^{AB}(\bar{\mu}^A))\alpha^B \cdot \bar{\alpha}^B \quad 7-23$$

Equations 7-22 and 7-23 are the extended version of equation 7-2 to the binary system A & B of the SCMF formulation. In a similar form to equation 7-3, the effective dipole moments of A and B are given by:

$$(\mu_e^A)^2 = (\bar{\mu}^A)^2 + 3\bar{\alpha}^A kT \quad 7-24$$

$$(\mu_e^B)^2 = (\bar{\mu}^B)^2 + 3\bar{\alpha}^B kT \quad 7-25$$

In a summary, the polarizable binary system of A and B is characterized by  $\bar{\mu}^A$ ,  $\bar{\mu}^B$ ,  $\bar{\alpha}^A$ ,  $\bar{\alpha}^B$ ,  $\mu_e^A$  and  $\mu_e^B$ . These six unknowns are determined by solving iteratively equations 7-20 to 7-25. In general, to apply the SCMF to mixtures, the number of equations required to describe a mixture is given by  $3n_c$  where  $n_c$  is the number of components.

The SCMF equations of a mixture are obviously extended into three sets. The first set of SCMF equations follow the following general form:

$$\bar{\mu}^{Ai} = \mu^{Ai} + \alpha^{Ai} \cdot C^{AiAi}(\bar{\mu}^{Ai})\bar{\mu}^{Ai} + \alpha^{Ai} \cdot \bar{\mu}^{Ai} \sum_{Aj} C^{AjAi}(\bar{\mu}^{Aj}) \quad i, j = 1, 2 \dots n_c; \quad i \neq j \quad 7-26$$

where the mixture consists of  $n_c$  components. Hence, the number of equations in the first set is equal to the number of components. The second set is described by the following  $n_c$  equations:

$$\bar{\alpha}^{Ai} = \alpha^{Ai} + \alpha^{Ai} \cdot \bar{\alpha}^{Ai} C^{AiAi} (\bar{\mu}^{Ai}) + \alpha^{Ai} \cdot \bar{\alpha}^{Ai} \sum_{Aj} C^{AjAi} (\bar{\mu}^{Aj}) \quad i, j = 1, 2 \dots nc; \quad i \neq j \quad 7-27$$

The third set consists of the following equations

$$(\mu_e^{Ai})^2 = (\bar{\mu}^{Ai})^2 + 3\bar{\alpha}^i kT \quad i = 1, 2, \dots, nc \quad 7-28$$

Equations 7-26 to 7-28 compose the required equation to apply the SCMF theory to any number of components. It should be noted that these equations contain various types of scalar dependent functions which are themselves functions of the energies of the effective system. The extension forms of the scalar dependent functions are described in the next section.

## 7.5 Extension of the scalar dependent functions

Each scalar dependent function that appeared in the previous equations is a result of two similar ( $C^{AiAi}$ ) or different particles ( $C^{AjAi}$ ). Therefore, these functions depend on the effective energy of two similar or different particles. To relate the scalar dependent functions to the effective energies, it is first necessary to relate these effective energies to the local electric fields. For the binary system of A and B, the average effective energy is related to the average local electric field felt on a particular A particle due to A and B as follows:

$$(U_{DD}^e)^{AA} = -\frac{1}{2} N x_A \mu_e^A \langle E_{iDA}^A \rangle^e \quad 7-29$$

$$(U_{DD}^e)^{BA} = -\frac{1}{2} N x_A \mu_e^A \langle E_{iDA}^B \rangle^e \quad 7-30$$

Using the local electric fields  $\langle E_{iDA}^A \rangle$  &  $\langle E_{iDA}^B \rangle$  from equations 7-17 and 7-18, the above two equations are re-arranged and written as:

$$C^{AA} = \frac{-2(U_{DD}^e)^{AA}}{N x_A \mu_e^A \mu_e^A} \quad 7-31$$

$$C^{BA} = \frac{-2(U_{DD}^e)^{BA}}{N x_A \mu_e^A \mu_e^A} \quad 7-32$$

Similarly, for the polarizable B particles,  $C^{AB}$  and  $C^{BB}$  are given by:

$$C^{AB} = \frac{-2(U_{DD}^e)^{AB}}{N x_B \mu_e^B \mu_e^B} \quad 7-33$$

$$C^{BB} = \frac{-2(U_{DD}^e)^{BB}}{N x_B \mu_e^B \mu_e^B} \quad 7-34$$

Therefore, the general form of the scalar dependent function is given by:

$$C^{AiAj} = \frac{-2(U_{DD}^e)^{AiAj}}{N x_A \mu_e^{Aj} \mu_e^{Aj}} \quad i, j = 1, 2, \dots, nc \quad 7-35$$

## 7.6 Comparison with molecular simulation data

The SCMF has been incorporated into integral equation theories and molecular dynamic simulations. The applications for different pure molecules have shown that the calculated energy, pressure, dielectric constant or radial distribution function was in good agreement with the experimental data (Caillol et al., 1987). In this section, the SCMF theory is incorporated into perturbation theories and then compared to available simulation data from the literature. The available simulation data include coexistence of vapour and liquid phases as well as pure liquid phase. They are, however, mainly limited to polarizable dipole-dipole systems.

### 7.6.1 Comparison with phase coexistence simulation data

The use of the SCMF requires the availability of a non-polarizable dipole-dipole model. Because there are many available dipole-dipole models with varying accuracy, it is expected that the results may differ depending on the dipole-dipole model used. The dipolar term developed by Twu and Gubbins, (1978a, 1978b) is considered in this section. The coefficients of the pair and triple correlation functions are taken from Lukas et al (1984). The dipolar term is then incorporated with the Wertheim perturbation theory with Lennard-Jones reference fluid. The modified Lennard-Jones equation of state developed by Johnson et al. (1993) is used. Before consideration of the SCMF, the non-polarizable model has to be compared to simulation data. Kiyohara et al. (1997) reported simulation data of phase coexistence

properties for non-polarizable and polarizable Stockmayer fluids of reduced dipole moments ( $\mu^*$ ) equal to 1 and 2 and reduced polarizabilities ( $\alpha^*$ ) equal to 0.00, 0.03, and 0.06.

Figure 7.1 and Figure 7.2 show a comparison of the non-polarizable model ( $\alpha^*=0$ ) with simulation data for temperature vs. coexistence densities at  $\mu^*=1$  & 2. As seen, the non-polarizable model is in excellent agreement with simulation data for  $\mu^*=1$ . At  $\mu^*=1$ , the agreement with simulation data is good but it is not as good as in Figure 7.1. Now, the SCMF is employed into the model to take account of the polarizability effect. Figure 7.3 depicts the coexistence densities for the polarizable Stockmayer fluids with reduced dipole moment and reduced polarizability equal to 1 and 0.03; respectively. As seen the polarizable model is in excellent agreement with simulation data. The polarizable model also compares very well with the experimental data at  $\mu^*=1$  and  $\alpha^*=0.06$  as shown in Figure 7.4.

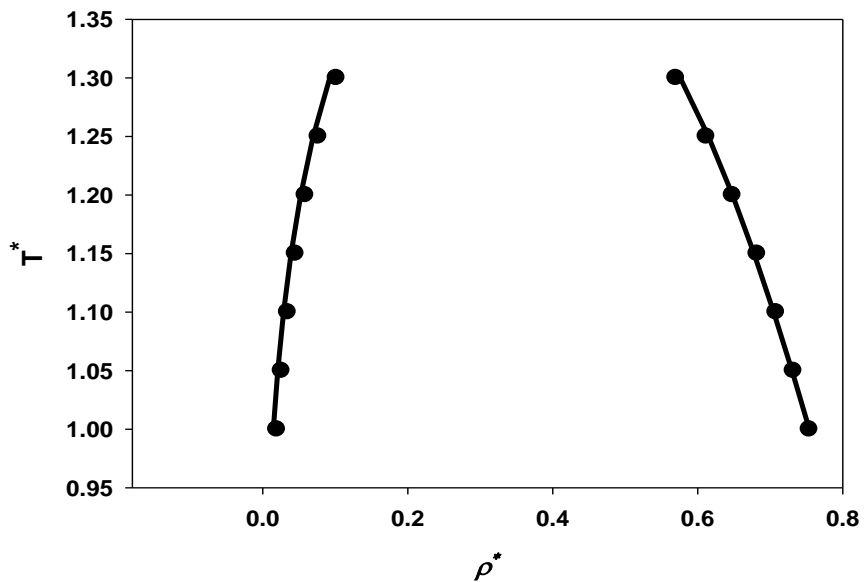


Figure 7.1 Reduced temperature vs. coexistence densities for the non-polarizable Stockmayer fluids with  $\mu^*=1$  and  $\alpha^*=0$ .

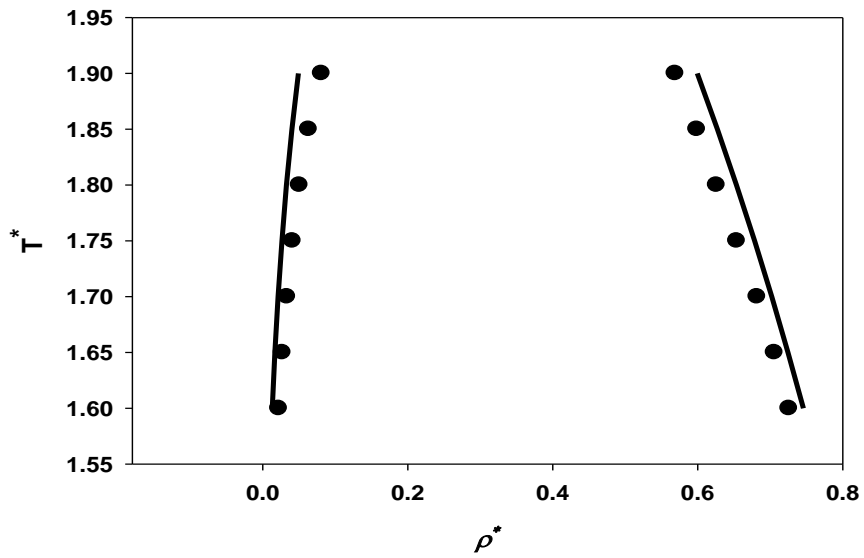


Figure 7.2 Reduced temperature vs. coexistence densities for the non-polarizable Stockmayer fluids with  $\mu^*=2$  and  $\alpha^*=0$ .

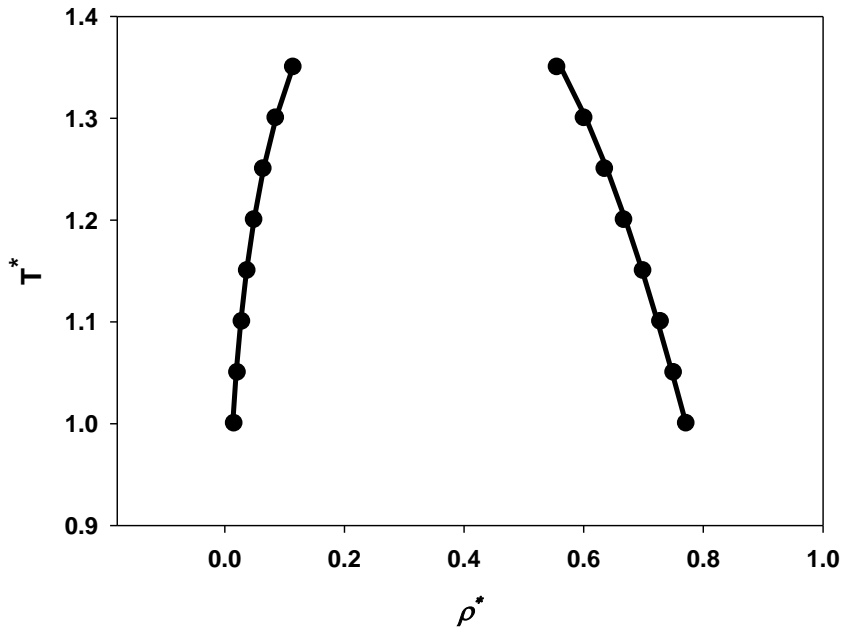


Figure 7.3 Reduced temperature vs. coexistence densities for the non-polarizable Stockmayer fluids with  $\mu^*=1$  and  $\alpha^*=0.03$ .

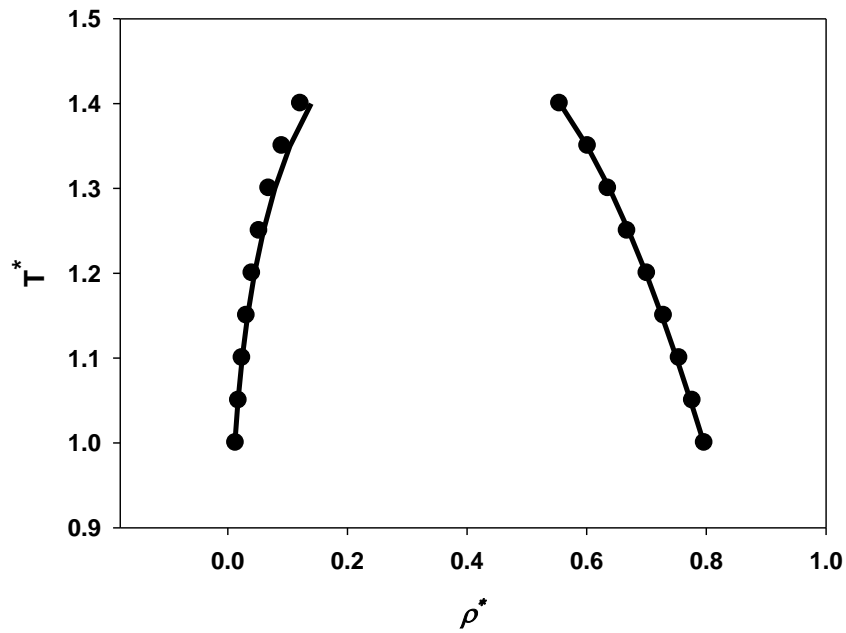


Figure 7.4 Reduced temperature vs. coexistence densities for the non- polarizable Stockmayer fluids with  $\mu^*=1$  and  $\alpha^*=0.06$ .

The coexistence pressure for the polarizable model with the SCMF is also compared to the simulation data. Figure 7.5 depicts  $\log_{10}(P^*)$  vs.  $1/T^*$  for  $\mu^*=1$  & 2 and  $\alpha^*=0.06$ . It is apparent from the figure that the polarizable model with SCMF compared well with the simulation data.

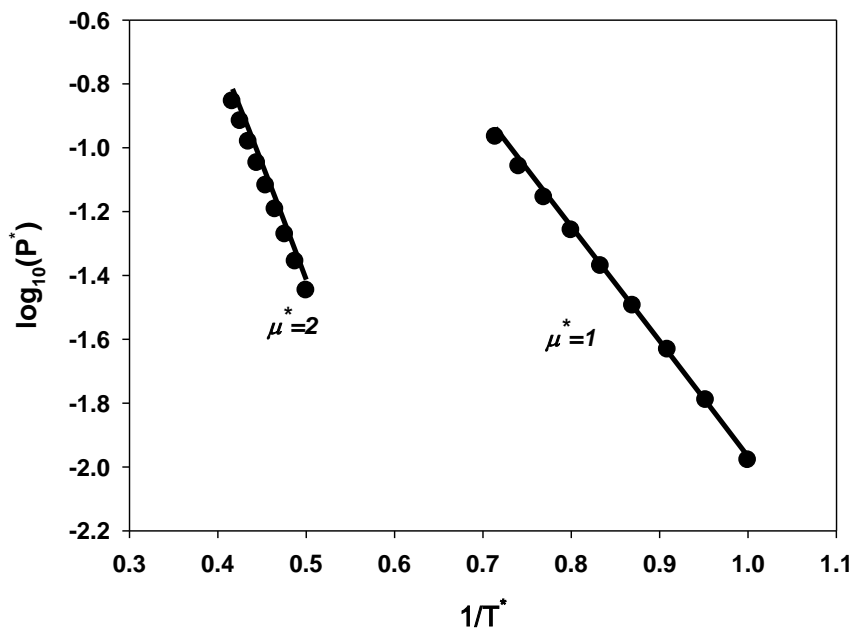


Figure 7.5 Vapour pressure vs. temperature for the polarizable Stockmayer fluids with  $\mu^*=1$  and  $\mu^*=2$ .

Although excellent comparisons were found as shown in the previous figures, there are some cases where the comparison with simulation data is not as good as in the previous cases. For instance, the polarizable model result of temperature vs. coexistence densities at  $\mu^*=2$  &  $\alpha^*=0.06$  is not in good agreement with the simulation data for the liquid density case, as shown in Figure 7.6 although the result of  $\log_{10}(P^*)$  vs.  $1/T^*$  for this case compared well with the simulation data (see Figure 7.5). The reason is most likely related to the accuracy of the dipolar term and not to the SCMF. This is because the result of the non-polarizable case of  $\mu^*=2$  was not good, as shown in Figure 7.2.

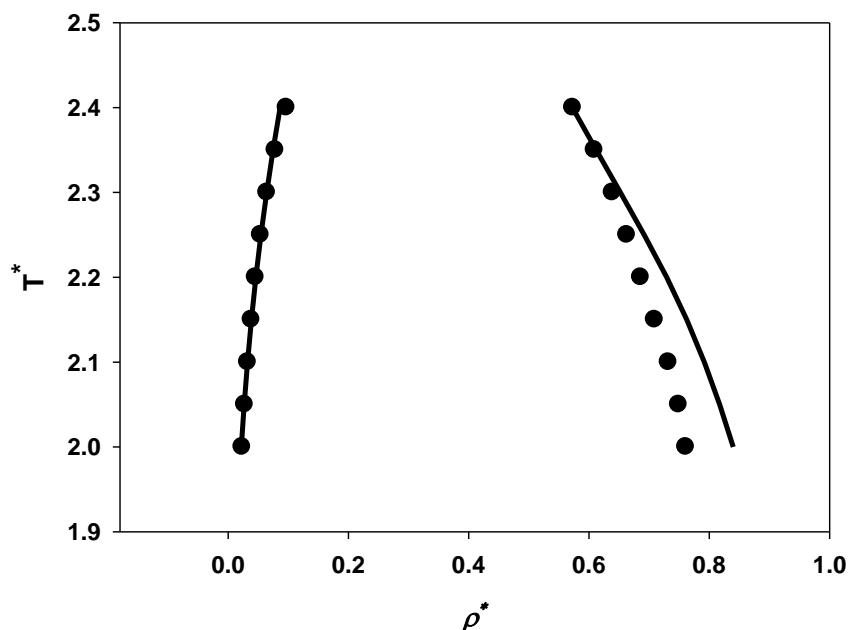


Figure 7.6 Reduced temperature vs. coexistence densities for the non- polarizable Stockmayer fluids with  $\mu^*=2$  and  $\alpha^*=0.06$ .

It should also be noted that the RPT has been compared with these simulation data by Kiyohara et al. (1997). The comparisons were in general not in good agreement with the simulation data. In their work, they used the same LJ equation and dipolar term as were used here. However, the coefficients of the pair and triple correlation functions were taken from Flytzani-Stephanopoulos et al. (1975). The result of the RPT for  $\mu^*=2$  &  $\alpha^*=0.06$  is given in Figure 7.7. The figure was taken from the work of Kiyohara et al. (1997). It is clear that the obtained curve by the RPT is not in good agreement with the simulation data. This is most likely related to the accuracy of the dipolar term which was improved in our case by the use of accurate coefficients of the pair and triple correlation function.

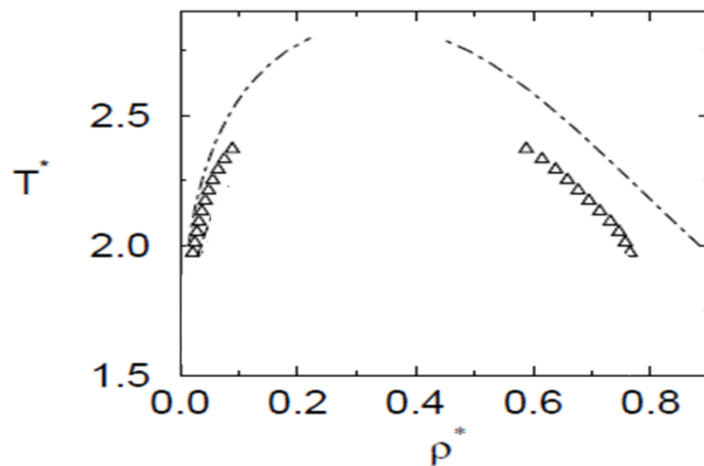


Figure 7.7 Reduced temperature vs. coexistence densities for the non- polarizable Stockmayer fluids with  $\mu^*=2$  and  $\alpha^*=0.06$ . (Figure taken from Kiyohara et al. (1997))

### 7.6.2 Comparison with energy and effective dipole moment

Kriebel and J. Winkelmann (1996) reported MD simulation data for polarizable Stockmayer fluids. In their work, the effective dipole moments and energy were reported at various polarizabilities and permanent dipole moments. The model used with the SCMF in the previous section is utilized here to calculate the effective dipole moment and the residual energy. Figure 7.8 gives a comparison of the residual internal energy as a function of density data with the polarizable model for various polarizabilities at  $T^*=3$ . It is apparent from the figure that the polarizable model compares well with the simulation data.

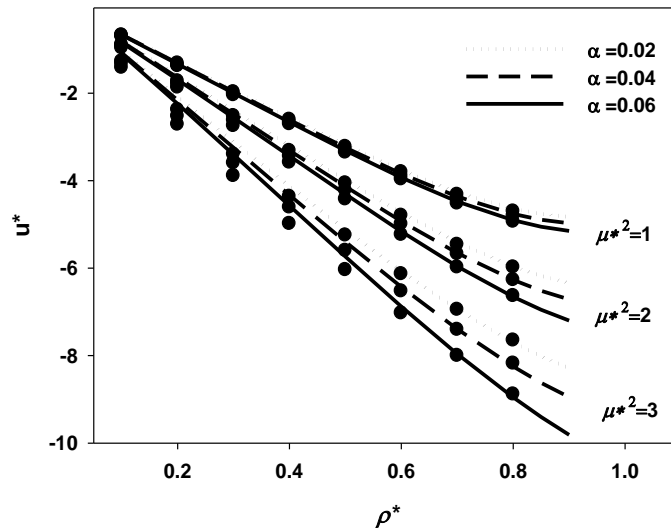


Figure 7.8 Residual internal energy as a function of density for different polarizable Stockmayer fluids for  $T^*=3$ .

For the effective dipole moment case, the calculated effective dipole moment from the polarizable model also compares well with the simulation data as shown in Figure 7.9 which shows the change of the effective dipole moment with density at various dipole moment and polarizabilities.

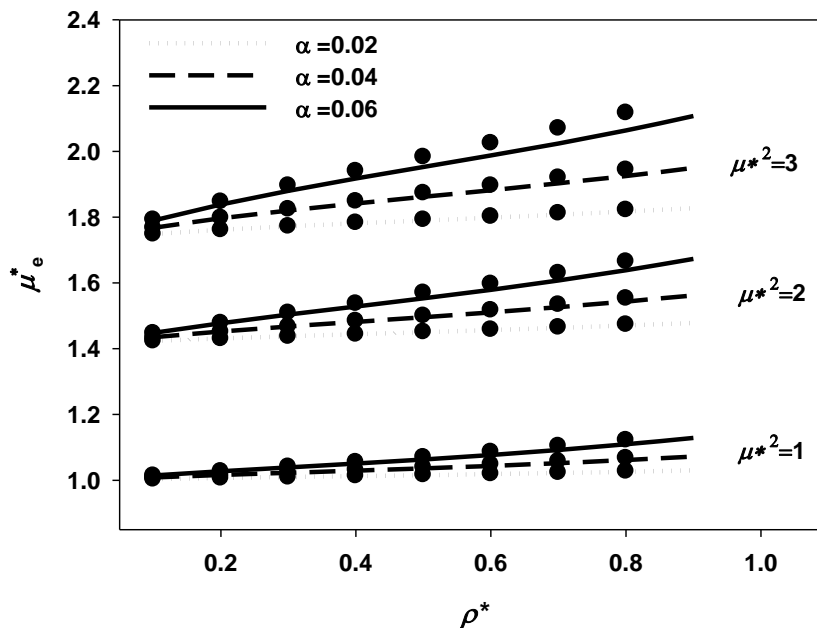


Figure 7.9 Effective dipole moment of different polarizable Stockmayer fluids versus density for  $T^*=3$ .

The previous comparisons to simulation data prove that the SCMF could take account of the polarizability very satisfactorily. Although the theory was presented here as a general theory for any type of polarizable systems, the above comparisons were limited to polarizable dipole-dipole systems. The reason for this is that simulation data is scarce for other higher polarizable multipolar systems. However, the evidence of applicability to higher polarizable multipole and ions is strong since higher polarizable multipole and ions have been investigated using integral equation theories and fairly good results have been obtained (Kusalik & Patey, 1988).

## 7.7 Application to real systems

The induction effect is more pronounced for higher dipole moment molecules. The study in this thesis was limited to water-alcohol-hydrocarbons systems. From the studies referred to in **Chapters 3 & 5**, it was clear that the prediction capability of SAFT with Chapman's term were excellent although the polarization was not taken into account. Even for Gross's term when the polarizability effect was considered, its effect was not that significant. Quadrupole-quadrupole interactions had to be added in order to achieve excellent prediction. This indicates that polarization doesn't play a significant role in alcohols. This is actually expected because the dipole moment of the functional group (C-OH) in alcohols is 1.7 D, which is not that big. Further, the effect of association, which was considered with Wertheim's association term, is more important for hydrogen-bonding components.

This does not imply that if the polarizations are considered, the model would perform poorly. However, it indicates that the polarizability effect would not be significant. To provide evidence that the model would not perform poorly, the polarization was incorporated into the simplified SAFT by the use of Chapman term. To simplify calculations, the self-energy term in the SCMF was ignored since it is much smaller than that of the effective term. Its effect would not be substantial for small dipole moment molecules. Figure 7.10 shows the polarizable simplified SAFT prediction of 1-butanol-heptane mixture at 40 °C and 60 °C. It is apparent that excellent prediction is obtained. The optimized polarizable simplified SAFT parameters of 1-butanol were as follows:  $m=3.9035$ ,  $v^{00}=16.791$ ,  $\epsilon/k=99.233$ ,  $\kappa^{AB}=0.081814$ ,  $\epsilon^{AB}/k=2371.8$ ,  $x_p=0.1281$  and the polarizability =  $8.79 \text{ \AA}^3$ .

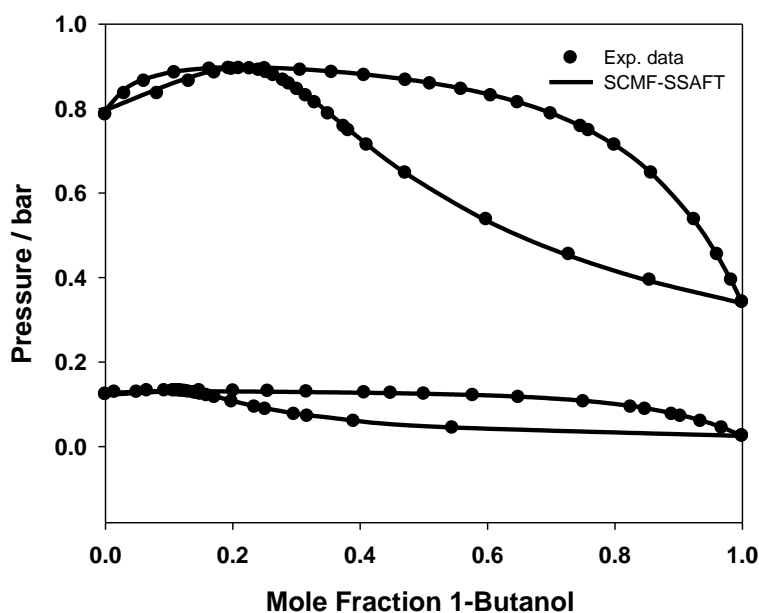


Figure 7.10 Prediction ( $k_{ij}=0$ ) of VLE of 1-butanol-heptane system at 40 °C and 60 °C.

Although the study was limited to water-alcohol-hydrocarbon systems, it is useful to test the capability of the SCMF with simplified SAFT for a higher dipole moment molecule for a non-associating compound. Butyraldehyde, which is an aldehyde compound, is selected since it has a relatively high dipole moment of 2.72 D. The adjusted parameters are found to be  $m=3.9035$ ,  $v^{00}=16.791$ ,  $\varepsilon/k=99.233$ ,  $\kappa^{AB}=0.081814$ ,  $\varepsilon^{AB}/k=2371.8$ ,  $xp=0.1281$  and the polarizability =  $8.79 \text{ \AA}^3$ . The mixture of butyraldehyde-heptane is tested at different temperatures of 45 °C and 70 °C. As shown in Figure 7.11, the predicted bubble pressure is in excellent agreement with the experimental data. Therefore, the polarizable SAFT works very well for systems that have high dipole moments.

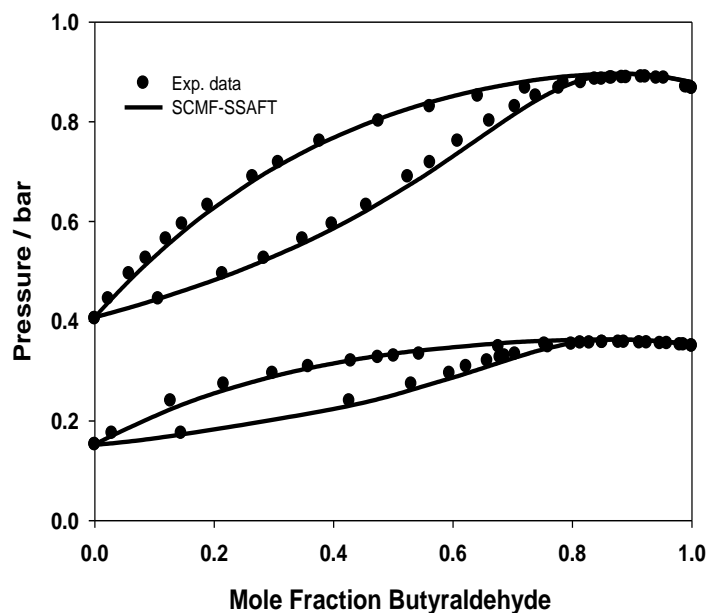


Figure 7.11 Prediction ( $k_{ij}=0$ ) of VLE of butyraldehyde-heptane system at 45 °C and 70 °C. Experimental data were taken from Eng & Sandler (1984).

## 7.8 Conclusions

In this chapter, a general polarizable polar theory was presented using the SCMF theory that was proposed originally by Carnie and Patey (1982) for integral equation theories. A general form was given of the SCMF to take account of any polarization interactions like dipole-dipole, dipole-quadrupole, dipole-octupole, dipole-ions, etc. in a straightforward manner. The SCMF was made applicable to any theory-based equation of state. It was also extended to mixtures. To validate the theory, a comparison was made with the simulation data. It was found that the SCMF compared with the simulation data very well. Finally, the SCMF was applied to real systems and through the simplified SAFT and was found able to predict VLE very well.

## CHAPTER 8

### CONCLUSIONS AND RECOMMENDATIONS

#### FOR FUTURE WORK

##### 8.1 Conclusions

In this thesis, the predictive capability of the statistical association fluid (SAFT) theory equation of state has been improved in predicting vapour-liquid equilibrium for water-alcohol-hydrocarbon mixtures without adjusting mixture experimental data. The adjustable SAFT pure parameters have been obtained based solely on pure vapour pressure and liquid density experimental data. The account of the dipole-dipole interactions was the main reason for giving improved predictions. The dipole-dipole interactions have been considered by three approaches available in the literature; namely, Chapman, Gross and Economou approaches. The main difference between these three dipolar terms is that the magnitude of the chemical potential of the dipole-dipole interactions was highest in Chapman's term and lowest in the Economou term. The three dipolar terms have been compared by studying vapour liquid equilibrium (VLE) for more than 50 mixtures of binary systems of water-alcohol hydrocarbon mixtures at different temperatures. The Chapman term was found to be superior to the other two dipolar terms and has shown excellent predictive capability for most of the studied systems. However, its predictive capability was poor for methanol-containing systems at low temperatures. The incorporation of the Gross term enabled the equation of state to predict the VLE of short-chain alcohol-alcohol mixtures with excellent results. It has also improved the prediction of bubble point pressure for other water-alcohol-hydrocarbon mixtures compared to the non-polar cases, which are known to give qualitative results.

In order to carry out effective evaluation of the predictive capability of dipolar SAFT in multiphase systems such as liquid-liquid equilibrium (LLE) and vapour-liquid-liquid equilibrium (VLLE), a new algorithm has been proposed to conduct multiphase phase and stability testing. The new algorithm is based on the Gupta et al method (1992), and it resolves the disadvantages

of the Gupta et. al method. For instance, the new algorithm didn't encounter difficulty when the phase fraction approached zero. Further, unlike the Gupta et al. approach, the new algorithm used the exact stability equations that were approximated by Gupta et al. The algorithm has been tested extensively with water-hydrocarbon systems and has been proven to perform efficiently for such systems. The algorithm was also tested for alcohol-alcohol as well as other mixtures of industrial interest such as water-ethylene glycol-CO<sub>2</sub>-hydrocarbons.

In this thesis, the proposed algorithm has been exploited to study the dipolar SAFT in multiphase systems for water-alcohol-hydrocarbon mixtures. The phase behaviour of LLE and VLLE was described by the use of dipolar Perturbed Chain SAFT (PC-SAFT) and Simplified SAFT (SSAFT). For the Chapman term, it was shown that the excellent predictive capability that was obtained in the VLE was not achieved in the LLE and VLLE with the same pure parameter sets. The PC-SAFT with the Jog and Chapman term (PC-SAFT-JC), which showed excellent predictive capability in the VLE, highly overestimates the upper critical solution temperature. However, if another set of pure parameters was utilized, good prediction could be achieved as shown for water-hydrocarbon and alcohol-hydrocarbon mixtures.

The excellent prediction that was obtained by the dipolar PC-SAFT using the Chapman term indicated that the other electrostatic interactions like quadrupole-quadrupole and polarization interactions are not important. For this reason, the work in this thesis extended to exploring the effect of other electrostatic interactions such as quadrupole-quadrupole interactions and the polarizability effect arising from induced dipole-dipole. The polarizability effect was considered by the use of the renormalization perturbation theory proposed by Wertheim while the quadrupole-quadrupole term was considered by the use of Gross's term. The work revealed that the incorporation of the polarizability effect with the aid of the Gross term alone didn't improve the PC-SAFT to the degree of being able to accurately predict VLE. However, when the quadrupole-quadrupole interactions were incorporated along with the polarizability effect, excellent predictive capability was achieved comparable to but less accurate than that of the PC-SAFT-JC. Then, the work explored the polarizability effect with the use of the Chapman term with the PC-SAFT. It was found that excellent prediction of VLE is still achieved. However, this

was slightly less accurate than that of the PC-SAFT-JC. In conclusion, the most accurate in prediction of VLE was achieved with the use of the PC-SAFT-JC equation of state.

The incorporation of various molecular interactions to a theory-based equation of state would result in a very complex equation of state. To conduct phase equilibrium calculations, the first derivatives from any Helmholtz free energy term that describe any kind of molecular interaction are required with respect to mole fraction and density. In the present study, an accurate numerical method called complex-step approximation has been presented to compute the required first derivatives for theory-based equations of state in phase equilibrium calculations. The accuracy of first derivatives is comparable to those obtained analytically up to at least 9 significant digits. Besides being accurate, the complex-step approximation is very simple to use. The method has been tested with very complicated theory-based equations of state and its use has been shown to result in calculations equivalent in terms of accuracy to those obtained analytically.

In the present study, a general treatment of polar-polarizable mixtures has been developed for theory-based equations of state to take account of any kind of polarization arising from polar molecules including ion-induced interactions. The proposed method has been developed based on the self-consistent mean field (SCMF) theory that was proposed originally by Carnie and Patey (1982) for integral equation theories. In this work, the SCMF has been extended to mixtures and incorporated into theory-based equations of state. The extended theory-based equation of state has then been compared to available molecular simulation data from the literature of polarizable Stockmayer particles. It has been shown that the SCMF compares very well to the simulation data. The comparison has been conducted for coexistence phase behaviour of reduced dipole moment equal to 1 and 2, and of reduced polarizabilities equal to 0.03 and 0.06. The computed effective dipole moment and the residual internal energy vs. reduced density from the SCMF was also compared to those obtained from simulation data at reduced square permanent dipole moment equal to 1, 2 and 3 and reduced polarizabilities equal to 0.02, 0.04 and 0.06. The comparison showed that the SCMF is in excellent agreement with the simulation data. The SCMF has been incorporated into the SAFT to compute VLE for real

mixtures. The SMCF-SAFT has shown excellent prediction capability without the need to use mixture experimental data to adjust any parameters.

## 8.2 Recommendations for future work

The availability of an accurate dipolar term is very important since the influence of dipole-dipole interactions are the most significant among other electrostatic interactions. In this study, the comparison of the dipolar terms revealed that Chapman's term is generally superior to the Gross and Economou terms. However, it should be noted that the comparison was based on water and alcohols which don't have large dipole moment values. The Chapman term is based on the mean spherical approximation which doesn't have good accuracy at large dipole moment values. Hence, the superiority of the Chapman term might not apply at large dipole moments. Therefore, further study is recommended to extend the comparisons to higher dipole moments. Conclusions at higher dipole moments would make it possible to choose an accurate candidate for a theory-based equation of state such as SAFT.

The prediction capability of the theory-based equation of state was limited to multiphase equilibrium such as VLE, LLE and VLLE. Further work is recommended to evaluate the prediction capability of the dipolar SAFT for thermo-physical properties; particularly for mixtures. In addition, it would be interesting to explore the role of other electrostatic interactions in the calculation of these properties; particularly because the computation of thermo-physical properties is normally conducted by adjusting the VLE data; then it uses the adjusted parameters to compute thermo-physical properties. In this thesis, the excellent prediction of VLE was achieved physically by putting more emphasis on understanding the intermolecular behaviour of the mixture.

Although a general treatment of polar-polarizable mixtures was presented in this thesis, evaluation was limited to induced dipole-dipole models due to the lack of simulation data for other polarization interactions. Nevertheless, the study could be extended directly to real mixtures for other induced interactions which were not considered in this thesis such as induced

dipole-quadrupole and dipole-octupole. This of course needs the availability of permanent polar models which could be taken from the literature. Furthermore, the study of polar-polarizable mixtures using the self-consistent mean field theory could be extended to other mixtures that are more polarizable than those considered in this study. Another interesting extension that could be explored is the incorporation of the self-consistent mean field theory to electrolyte solutions.

Finally, any improvement on the theory-based equations of state would result in more complex terms. In this thesis, complex-step approximation was suggested to compute phase equilibrium calculations which are based on first derivatives. To study the thermo physical properties and critical states of mixtures, the second and third derivatives are required. Complex step approximation would be of great help if the so-called multi-step complex approximation is used. The multi-step complex step approximation doesn't have the subtractive cancellation error. Therefore, use of the multi-step approximation with theory-based of equations of state is recommended, to simplify the calculations.

## REFERENCES

- Abdel-Ghani, R.M., 1995. EOS mixing rules for multi-phase behaviour. *Master Thesis, University of Calgary* .
- Alder, B.J., Young, D.A. & Mark, M.A., 1972. Studies in Molecular Dynamics. X. Corrections to the Augmented van der Waals Theory for the Square Well Fluid. *Journal of Chemical Physics*, 56, pp.3013-20.
- Alekseeva, M.V. & Moiseenko, M.F., 1982. Eksperimentalnoe issledovanie i rascheti ravnovesiya zhidkost-par v sisteme n-propilovij spirt---hexan---n-dezilovij spirt (in Russian). *Khimiya i Termodinamika Rastvorov (Chemistry and Thermodynamics of Solutions)*, 5, p.179.
- Al-Saifi, N.M., Hamad, E.Z. & Englezos, P., 2008. Prediction of vapor-liquid equilibrium in water-alcohol-hydrocarbon systems with the dipolar perturbed-chain SAFT equation of state. *Fluid Phase Equilibria*, 271, pp.82-93.
- Arce, A., Blanco, A., Soto, A. & Tojo, J., 1995. Isobaric vapor-liquid equilibria of methanol + 1-octanol and ethanol + 1-octanol. *Journal of Chemical and Engineering Data*, 40, pp.1011-14.
- Aslam, N. & Sunol, A.K., 2006. Reliable computation of all the density roots of the statistical associating fluid theory equation of state through global fixed-point homotopy. *Industrial and Engineering Chemistry Research*, 45, pp.3303-10.
- Baker, L.E., Pierce, A.C. & Luks, K.D., 1981. Gibbs energy analysis of phase equilibria. *SPE/DOE Second Joint Symposium on Enhanced Oil Recovery*.
- Barker, J.A. & Henderson, D., 1967. Perturbation Theory and Equation of State for Fluids: The Square-Well Potential. *THE JOURNAL OF CHEMICAL PHYSICS*, 47(8), pp.2856-61.
- Barr-David, F. & Dodge, B.F., 1959. Vapor-Liquid Equilibrium at High Pressures. The Systems Ethanol-Water and 2-Propanol-Water. *Journal of Chemical and Engineering Data*, 4(2), pp.107-21.
- Bernatova, S., Linek, J. & Wichterle, I., 1992. Vapour-liquid equilibrium in the butyl alcohol -n-decane system at 85, 100 and 115°C. *Fluid Phase Equilibria*, 74, pp.127-32.
- Berro, C., 1987. *International DATA Series, Selected Data on Mixtures, Series A*, 1, p.73.
- Berro, C. & Peneloux, A., 1984. Excess Gibbs energies and excess volumes of 1-butanol-n-heptane and 2-methyl-1-propanol-n-heptane binary systems. *Journal of Chemical and Engineering Data*, 29, pp.206-10.

Berro, C., Rogalski, M. & Peneloux, A., 1982. A new ebulliometric technique. Vapour-liquid equilibria in the binary systems ethanol-n-heptane and ethanol-n-nonane. *Fluid Phase Equilibria*, 8(1), pp.55-73.

Berro, C., Rogalski, M. & Peneloux, A., 1982. Excess Gibbs energies and excess volumes of 1-butanol-n-hexane and 2-methyl-1-propanol-n-hexane binary systems. *Journal of Chemical and Engineering Data*, 27, pp.352-55.

Berro, C., Weclawski, J. & Neau, E., 1986. *International DATA Series, Selected Data on Mixtures, Series A*, 3, p.221.

Bishnoi, P.R., Gupta, A.K., Englezos, P. & Kalogerakis, N.E., 1989. Multiphase equilibrium flash calculations for systems containing gas hydrates. *Fluid Phase Equilibria*, 53, pp.97-104.

Blas, F.J. & Vega, L.F., 1997. Thermodynamic behavior of Homonuclear and Heteronuclear Lennard-Jones Chains with Association Sites from Simulation and Theory. *Molecular Physics*, 92, pp. 135-150.

Boublikova, L. & Lu, B.C., 1969. Isothermal Vapor-Liquid Equilibria for the Ethanol-n-Octane System. *International Journal of Applied Chemistry*, 19, pp.89-92.

Boudjema, R., Cox, M.G., Forbes, A.B. & Harris, P.M., 2003. Automatic Differentiation: Techniques and their Application in Metrology. *NPL Report CMSC 26/03, National Measurement Directorate*.

Caillol, J.M. et al., 1987. A theoretical study of a polar-polarizable model for liquid ammonia. *Molecular Physics*, 62(5), pp.1225-38.

Campbell, S.W., Wilsak, R.A. & Thodos, G., 1987. *The Journal of Chemical Thermodynamics*, 19, p.449.

Campbell, S.W., Wilsak, R.A. & Thodos, G., 1987. (Vapor + Liquid) Equilibrium Behavior of (n-Pentane + Ethanol) at 372.7, 397.7 and 422.6 K. *The Journal of Chemical Thermodynamics*, 19, p.449.

Carlson, E.C., 1996. Don't Gamble with Physical Properties for Simulations. *Chemical engineering progress*, (October), pp.35-46.

Carnahan, N.F. & Starling, K.E., 1969. Equation of State of non-attracting Rigid Spheres. *Journal of Chemical Physics*, 51, pp.635-36.

Carnie, S.L. & Patey, G.N., 1982. Fluids of polarizable hard spheres with dipoles and tetrahedral quadrupoles Integral equation results with application to liquid water. *Molecular Physics*, 47(5), pp.1129-51.

- Castier, M., Rasmussen, P. & Fredenslund, A., 1989. Calculation of simultaneous chemical and phase equilibria in nonideal systems. *Chemical Engineering Science*, 44(2), pp.237-48.
- Chapman, W.G., Gubbins, K.E., Jackson, G. & Radosz, M., 1989. SAFT: Equation- of-State Solution Model for Associating Fluids. *Fluid Phase Equilibria*, 52, pp.31-38.
- Chapman, W.G., Gubbins, K.E., Jackson, G. & Radosz, M., 1990. New reference equation of state for associating liquids. *Industrial and Engineering Chemistry Research*, 29, p.1709.
- Chapman, W.G., Jackson, G. & Gubbins, K.E., 1988. Phase equilibria of associating fluids - Chain molecules with multiple bonding sites. *Molecular Physics*, 65, p.1057.
- Chen, C.-C., 1986. Representation of solid-liquid equilibrium of aqueous electrolyte. 27, p.457-474.
- Chen, C.-C., 2002. An industry perspective on polymer process modelling. *CAST Communications, AIChE*.
- Chen, S.S. & Kreglewski, A., 1977. Applications of the augmented van der Waals theory of fluids. Part I. *Ber. Bunsenges. Phys. Chem.*, 81, p.1048-1052.
- Chen, S.S. & Kreglewski, A., 1977. Applications of the augmented van der Waals theory of fluids. Part I. *Berichte Der Bunsen-Gesellschaft Physical Chemistry*, 81, p.1048.
- Churakov, S.V. & Gottschalk, M., 2003. Perturbation Theory based Equation of State for Polar Molecular Fluids: I. Pure Fluids. *Geochimica et Cosmochimica Acta*, 67, pp. 2397-2414.
- Clough, S., Beers, Y., Klein, G.P. & Rothman, L.S., 1973. Dipole Moment of Water from Stark Measurements of H<sub>2</sub>O, HDO, and D<sub>2</sub>O. *Journal of Chemical Physics*, 59, pp.2254-59.
- Crowe, C.M. & Nishio, M., 1975. Convergence promotion in the simulation of chemical processes—the general dominant eigenvalue method. *American Institute of Chemical Engineers Journal*, 21(3), pp.528-33.
- Daubert, T.E., Danner, R.P., Sibul, H.M. & Stebbins, C.C., 1989. *Physical and Thermodynamic Properties of Pure Chemicals: Data Compilation*. Washington, DC: Taylor & Francis.
- Deiters, U.K. & Schneider, G.M., 1986. HIGH PRESSURE PHASE EQUILIBRIA: EXPERIMENTAL METHODS. *Fluid Phase Equilibria*, 29, pp.145-60.
- Dominik, A., Chapman, W.G., Kleiner, M. & Sadowski, G., 2005. Modelling of polar systems with the PC-SAFT equation of state: Investigation of the performance of two polar terms. *Industrial & Engineering Chemistry Research*, 44, pp.6928-38.
- Elliott, J. & Lira, C.T., 1999. *Introductory Chemical Engineering Thermodynamics*. Prentice Hall International Series in the Physical and Chemical Engineering Sciences.

Eng, R. & Sandler, S.I., 1984. Vapor-liquid equilibria for three aldehyde/hydrocarbon mixtures. *Journal of Chemical & Engineering Data*, 29, pp.156-61.

Erbar, J.H., 1973. Three Phase Equilibrium Calculations. In *Proceedings to 52nd Annual National Gas Processors Association Meeting.*, 1973.

Flory, P.J., 1941. Thermodynamics of High Polymer Solutions. *J. Chem. Phys.*, pp.660-61.

Flytzani-Stephanopoulos, M., Gubbins, K.E. & Gray, C.G., 1975. Thermodynamics of mixtures of non-spherical molecules. *Molecular Physics*, 30(6), pp.1649-76.

Freshwater, D.C. & Pike, K.A., 1967. Vapor-liquid equilibrium data for systems of acetone-methanol-isopropanol. *Journal of Chemical and Engineering Data*, 12(2), pp.179-83.

Fu, Y.H. & Sandler, S.I., 1995. A simplified SAFT equation of state for associating compounds and mixtures. *Industrial and Engineering Chemistry Research*, 34, pp.1897-909.

Gallier, P.W., Britt, H.I., Evans, L.B. & Chen, C.-C., 1981. ASPEN: advanced system for process engineering. 1, pp.43-49.

Gautam, R. & Seider, W.D., 1979. Computation of phase and chemical equilibrium: Part I. Local and constrained minima in Gibbs free energy. *American Institute of Chemical Engineers Journal*, 25, pp.991-99.

Geiseler, G. et al., 1967. *Z. Physical Chemistry (Zeitschrift fur Physikalische Chemie)*, 56, p.288

Gierycz, P., Gregorowicz, J. & Malanowski, S., 1988. Vapour pressures and excess Gibbs energies of (butan-1-ol + n-octane or n-decane) at 373.15 and 383.15 K. *The Journal of Chemical Thermodynamics*, 20(4), pp.385-88.

Gil-Villegas, A. et al., 1997. Statistical Associating Fluid Theory for Chain Molecules with Attractive Potentials of Variable Range. *Journal of Chemical Physics*, 106(10), pp.4168-86.

Gmehling, J., Onken, U. & Weidlich, U., 1977. *Vapor-Liquid Equilibrium Data Collection, Chemistry Data Series, DECHEMA, Frank*, 1.

Gokel, G.W., 2004. *Dean's Handbook of Organic Chemistry*. 2nd ed. McGraw-Hill.

Goral, M., Skrzecz, A., Bok, A. & Maczynski, A., 2004. Recommended Vapor-Liquid Equilibrium Data. Part 3. Binary Alkanol - Aromatic Hydrocarbon Systems. *Journal of Physical and Chemical Reference Data*, 33, p.959.

Gracia, M. et al., 1992. Vapour pressures of (butan-1-ol + hexane) at temperatures between 283.10 and 323.12 K. *The Journal of Chemical Thermodynamics*, 24, pp.463-71.

- Gray, C.G., Joslin, C.G., Venkatasubramanian, V. & Gubbins, K.E., 1985. Induction effects in fluid mixtures of dipolar-quadrupolar polarizable molecules. *Molecular Physics*, 54(5), pp.1129-48.
- Gregory, J.K. et al., 1997. The Water Dipole Moment in Water Clusters. *Science*, 275, pp.814-17.
- Gross, J., 2005. An equation-of-state contribution for polar components: Quadrupolar molecules. *American Institute of Chemical Engineers Journal*, 51, p.2556.
- Gross, J. & Sadowski, G., 2001. Perturbed-chain SAFT: An equation of state based on a perturbation theory for chain molecules. *Industrial and Engineering Chemistry Research*, 40, pp.1244-60.
- Gross, J. & Sadowski, G., 2002. Application of the Perturbed-Chain SAFT Equation of State to Associating Systems. *Industrial and Engineering Chemistry Research*, 41, pp.5510-15.
- Gross, J. & Vrabc, J., 2006. An equation of state contribution for polar components: Dipolar molecules. *American Institute of Chemical Engineers Journal*, 52, p.1194.
- Gros, H.P., Zabaloy, M.S. & Brignole, E.A., 1996. High-Pressure Vapor–Liquid Equilibria for Propane + 2-Butanol, Propylene + 2-Butanol, and Propane + 2-Butanol + 2-Propanol. *Journal of Chemical and Engineering Data*, 41(2), pp.335-38.
- Gubbins, K.E. & Twu, C.H., 1978a. Thermodynamics of polyatomic fluid mixtures—I theory. *Chemical Engineering Science*, 33, pp.863-78.
- Gupta, A.K., 1990. Steady State Simulation of Chemical Processes. *Ph.D. Thesis, Department of Chemical and Petroleum Engineering, University of Calgary, Calgary, Canada.*
- Gupta, A.K., Bishnoi, P.R. & Kalogerakis, N., 1990. Simultaneous multiphase isothermal/isenthalpic flash and stability calculations for reacting/non-reacting systems. *Gas Separation and Purification*, 4(4), pp.215-22.
- Gupta, A.K., Bishnoi, P.R. & Kalogerakis, N., 1991. A method for the simultaneous phase equilibria and stability calculations for multiphase reacting and non-reacting systems. *Fluid Phase Equilibria*, 63(1-2), pp.65-89.
- Han, G. & Rangaiah, G.P., 1998. A Method for Multiphase Equilibrium Calculations. *Computers and Chemical Engineering*, 22, pp.897-911.
- Hanson, D.O. & Van Winkle, M., 1967. Alteration of the relative volatility of hexane-1-hexene by oxygenated and chlorinated solvents. *Journal of Chemical and Engineering Data*, 12(3), pp.319-25.

- Heidemann, R.A., 1974. Three phase equilibria using equations of state. *American Institute of Chemical Engineers Journal*, 20(5), pp.847-55.
- Heidemann, R.A., 1983. Computation of high pressure phase equilibria. *Fluid Phase Equilibria*, 14, pp.55-78.
- Holderbaum, T., Utzig, A. & Gmehling, J., 1991. Vapour—liquid equilibria for the system butane/ethanol at 25.3, 50.6 and 72.5°C. *Fluid Phase Equilibria*, 63(1-2), pp.219-26.
- Holscher, I.F., Schneider, G.M. & Ott, J.B., 1986. Liquid-Liquid Phase Equilibria Of Binary Mixtures Of Methanol With Hexane, Nonane And Decane At Pressures Up To 150 Mpa. *Fluid Phase Equilibria*, 27, pp.153-69.
- Honggang, Z. & McCabe, C., 2006. Phase behavior of dipolar fluids from a modified statistical associating fluid theory for potentials of variable range. *Journal of Chemical Physics*, 125, p.104504.
- HOYE, J.S. & STELL, G., 1980. Dielectric theory for polar molecules with fluctuating polarizability. *Journal of chemical physics*, 73, p.461.
- Hradetzky, G. & Lempe, D.A., 1991. Phase equilibria in binary and higher systems methanol + hydrocarbon(s) Part I. Experimental determination of liquid-liquid equilibrium data and their representation using the NRTL equation. *Fluid Phase Equilibria*, 69, pp.285-301.
- Huang, S.H. & Radosz, M., 1990. Equation of State for Small, Large, Polydisperse and Associating Molecules. *Industrial and Engineering Chemistry Research*, 29, p.2284.
- Huang, S.H. & Radosz, M., 1991. Equation of state for small, large, polydisperse, and associating molecules: extension to fluid mixtures. *Industrial and Engineering Chemistry Research*, 30(8), pp.1994-2005.
- Huggins, M.L., 1941. Solution of Long Chain Compounds. *J. Chem. Phys*, p. 440.
- Iglesias-Silva, G.A. et al., 2003. An algebraic method that includes Gibbs minimization for performing phase equilibrium calculations for any number of components or phases. *Fluid Phase Equilibria*, 210, pp.229-45.
- Jackson, G., Chapman, W.G. & Gubbins, K.E., 1988. Phase Equilibria of Associating Fluids. Spherical Molecules with Multiple Bonding Sites. *Molecular Physics*, 65, pp.1-31.
- Janaszewski, B., Oracz, P., Goral, M. & Warycha, S., 1982. *Fluid Phase Equilibria*, 9, p.295.
- Jog, P. & Chapman, W.G., 1999. Application of Wertheim's Thermodynamic Perturbation Theory to Dipolar Hard Sphere Chains. *Molecular Physics*, 97, pp.307-19.

Jog, P.K., Sauer, S.G., Blasius, J. & Chapman, W.G., 2001. Application of Dipolar Chain Theory to the Phase Behavior of Polar Fluids and Mixtures. *Industrial & Engineering Chemistry Research*, 40, pp.4641-48.

Johnson, K., Muller, E.A. & Gubbins, K.E., 1994. Equation of state for Lennard-Jones chains. *The Journal of Physical Chemistry*, 98, pp.6413-19.

Johnson, J., Zollweg, J. & Gubbins, K.E., 1993. The Lennard-Jones equation of state revisited. *Molecular Physics*, 78(3), pp.591-618.

Joslin, C.G., Gray, C.G. & Gubbins, K.E., 1985. Renormalized perturbation theory for dipolar and quadrupolar polarizable liquids. *Molecular Physics*, 54, pp.1117-28.

Karakatsani, E.K. & Economou, I.G., 2006. Perturbed Chain-Statistical Associating Fluid Theory Extended to Dipolar and Quadrupolar Molecular Fluids. *Journal of Physical Chemistry B*, 110, p.9252.

Karakatsani, K. & Economou, I.G., 2007. Phase Equilibrium Calculations for Multi-Component Polar Fluid Mixtures with tPC-PSAFT. *Fluid Phase Equilibria*, 261, pp.265-71.

Karakatsani, E.K., Spyriouni, T. & Economou, I.G., 2005. Extended SAFT Equations of State for Dipolar Fluids. *American Institute of Chemical Engineers Journal*, 51, p.2328.

Kinoshita, M. & Takamatsu, T., 1986. A powerful solution algorithm for single-stage flash problems. *Computers and Chemical Engineering*, 10(4), pp.353-60.

Kister, H.Z., 2002. Can We Believe Simulation Results? *Chemical Engineering Progress*, (October), pp.52-56.

Kiyohara, K., Gubbins, K.E. & Panagiotopoulos, A., 1997. Phase coexistence properties of polarizable Stockmayer fluids. *Journal of Chemical Physics*, 106, p.3338.

Kleiner, M. & Gross, J., 2006. An equation of state contribution for polar components: Polarizable dipoles. *American Institute of Chemical Engineers Journal*, 52, p.1951.

Kleiner, M. & Gross, J., 2006. An equation of state contribution for polar components: Polarizable dipoles. *AICHE J.*, 52(5), p.1951-1961.

Kobayashi, R. & Katz, D.L., 1953. Vapor-Liquid Equilibria for Binary Hydrocarbon-Water Systems. *Industrial and Engineering Chemistry Research*, 45(3), pp.440-51.

Kontogeorgis, G.M., Voutsas, E.C., Yakoumis, I.V. & Tassios, D.P., 1996. An Equation of State for Associating Fluids. *Industrial and Engineering Chemistry Research*, 35, p.4310.

- Kraska, T. & Gubbins, K.E., 1996. Phase Equilibria Calculations with a Modified SAFT Equation of State. 1. Pure Alkanes, Alkanols, and Water. *Industrial & Engineering Chemistry Research*, 35, pp.4727-37.
- Kriebel, C. & Winkelmann, J., 1996. Thermodynamic properties of polarizable Stockmayer fluids: perturbation theory and simulation. *Molecular Physics*, 88(2), pp.559-78.
- Kurihara, K., Minoura, T., Takeda, K. & Kojima, K., 1995. Isothermal vapor–liquid equilibria for methanol+ethanol+water, methanol+water and ethanol+water. *Journal of Chemical and Engineering Data*, 40, pp.679-84.
- Kusalik, P.G. & Patey, G.N., 1988. On the molecular theory of aqueous electrolyte solutions. I. The solution of the RHNC approximation for models at finite concentration. *Journal of Chemical physics*, 88(12), pp.7715-38.
- Lancia, A., Musmarra, D. & Pepe, F., 1996. Vapor-Liquid Equilibria for Mixtures of Ethylene Glycol, Propylene Glycol, and Water between 98° and 122°C. *Journal of Chemical Engineering of Japan*, 29, pp.449-55.
- Larsen, B., Rasaiah, J.C. & Stell, G., 1977. Thermodynamic Perturbation Theory for Multipolar and Ionic Liquids. *Molecular Physics*, 33, p.987.
- Larsen, B., Rasaiah, J.C. & Stell, G., 1977. Thermodynamic perturbation theory for multipolar and ionic liquids. *Molecular Physics*, 33, pp.987-1027.
- Lee, K.-H., Lombard, M. & Sandler, S.I., 1985. The Generalized Van der Waals Partition Function. II. Application to the Square-Well Fluid. *Fluid Phase Equilibria*, 21, pp.177-96.
- Leu, A.D., Chen, C.J. & Robinson, D.B., 1990. Vapor-Liquid equilibrium in selected binary systems. *American Institute of Chemical Engineers Symposium Series*, 271, p.11.
- Li, X. & Englezos, P., 2003. Vapor–Liquid Equilibrium of Systems Containing Alcohols Using the Statistical Associating Fluid Theory Equation of State. *Industrial and Engineering Chemistry Research*, 42(20), pp.4953-61.
- Lindberg, G.W. & Tassios, D., 1971. Effect of organic and inorganic salts on relative volatility of nonaqueous systems. *Journal of Chemical and Engineering Data*, 16, pp.52-55.
- Lisal, M., Aim, K., Mecke, M. & Fischer, J., 2004. Revised equation of state for two-center Lennard–Jones fluids. *International Journal of Thermophysics*, 25, pp.159-73.
- Lucia, A. & Luo, Q., 2001. Binary refrigerant-oil phase equilibrium using the simplified SAFT equation. *Advances in Environmental Research*, 6, pp.123-34.
- Lucia, A., Padmanabhan, L. & Venkataraman, S., 2000. Multiphase equilibrium flash calculations. *Computers and Chemical Engineering*, 24, p.2557–2569.

- Lyness, J.N., 1967. Numerical Algorithms Based on the Theory of Complex Variable. In *Proceedings to A.C.M. (Association for Computing Machinery) National Meeting.*, 1967.
- Lyness, J.N. & Moler, C.B., 1967. Numerical Differentiation of Analytic Functions. *The SIAM Journal on Numerical Analysis* , 4(2), pp.202-10.
- Macconi, M., Morini, B. & Porcelli, M., 2009. Trust-region quadratic methods for nonlinear systems of mixed equalities and inequalities. *Applied Numerical Mathematics*, 59(5), pp.859-76.
- Maciel, M.R.W. & Francesconi, A.Z., 1988. Excess Gibbs free energies of (n-hexane + propan-1-ol) at 338.15 and 348.15 K and of (n-hexane + propan-2-ol) at 323.15, 338.15 and 348.15 K. *The Journal of Chemical Thermodynamics*, 20, pp.539-44.
- Maczynski, A., Wisniewska-Gocłowska, B. & Goral, M., 2004. Recommended Liquid–Liquid Equilibrium Data. Part 1. Binary Alkane–Water Systems. *Journal of Physical and Chemical Reference Data*, 33(2), pp.549-77.
- Mansoori, G.A., Carnahan, N.F., Starling, K.E. & Leland, T.W., 1971. Equilibrium Thermodynamic Properties of the Mixture of Hard Spheres. 54, pp.1523-25.
- Martins, J.R.R.A., Sturdza, P. & Alonso, J., 2003. The Complex-Step Derivative Approximation. *ACM Transactions on Mathematical Software*, 29(3), pp.245-62.
- Matsuda, H. & Ochi, K., 2004. Liquid–liquid equilibrium data for binary alcohol + n-alkane (C10–C16) systems: methanol + decane, ethanol + tetradecane, and ethanol + hexadecane. *Fluid Phase Equilibria* , 224 , p.31–37.
- McDonald, I.R., 1974. Application of the thermodynamic perturbation theory to polar and polarizable fluids. *Journal of Physical Chemistry*, 7, pp.1225-36.
- Mecke, M., Muller, A., Winkelmann, J. & Fischer, J., 1997. An equation of state for two-center Lennard–Jones fluids. *International Journal of Thermophysics*, 18, pp.683-98.
- Michelsen, M.L., 1982. The isothermal flash problem. Part I. Stability. *Fluid Phase Equilibria*, 9, pp.1-19.
- Michelsen, M.L., 1982. The isothermal flash problem. Part II: phase split calculation. *Fluid Phase Equilibria*, 9, pp.21-40.
- Moelwyn-Hughes, E.A. & Thorpe, P.L., 1964. The Physical and Thermodynamic Properties of Some Associated Solutions. I. Dielectric Constants and Heats of Mixing. *Proceedings of the Royal Society of London. Series A, Mathematical and Physical Sciences*, 11 Feb. pp.423-36.
- Morini, B. & Porcelli, M., 2010. TRESNEI, a Matlab trust-region solver for systems of nonlinear equalities and inequalities, Computational Optimization and Applications. *Computational Optimization and Applications*, (DOI: 10.1007/s10589-010-9327-5).

Muller, E.A. & Gubbins, K.E., 2001. Molecular-based equations of state for associating fluids: A review of SAFT and related approaches. *Industrial and Engineering Chemistry Research*, 40, p.2193.

Muller, A., Winkelmann, J. & Fischer, J., 1996. Backbone family of equations of state: 1. Nonpolar and polar pure fluids. *American Institute of Chemical Engineers Journal*, 42, pp.1116-26.

Nagashima, A., Yoshii, S., Matsuda, H. & Ochi, K., 2004. Measurement and Correlation of Excess Molar Enthalpies for Ethylene Glycol + Alkanol Systems at the Temperatures (298.15, 308.15, and 323.15) K. *Journal of Chemical and Engineering Data*, 49(2), pp.286-90.

Nezbeda, I. & Pavliek, J., 1996. Application of primitive models of association: A simple theoretical equation of state of water. *Fluid Phase Equilibria*, 116, p.530.

Ng, H.J., Chen, C.J. & Robinson, D.B., 1986. RR-96 Vapor liquid equilibrium and condensing curves in the vicinity of the critical point for a typical gas condensate. Gas Processors Association (GPA) Research Report.

Nghiem, L.X. & Li, Y., 1984. Computation of Multiphase Equilibrium Phenomena With An Equation of State. *Fluid Phase Equilibria*, 17, pp.77-95.

NguyenHuynh, D., Passarello, J.P., Tobaly, P. & de Hemptinne, J.C., 2008. Application of GC-SAFT EOS to polar systems using a segment approach. *Fluid Phase Equilibria*, 264, p.62-75.

Oracz, P. & Kolasinka, G., 1987. Vapour-Liquid Equilibria--III. Total Vapour Pressure Measurements for Binary Mixtures of Methanol, Ethanol, 1-Propanol and 1-Butanol With Benzene, Toluene and P-Xylene At 313.15 K. *Fluid Phase Equilibria*, 35, pp.253-78.

Orge, B. et al., 1997. Mixing properties of(methanol, ethanol, or 1-propanol) with (n-pentane, n-hexane, n-heptane and n-octane) at 298.15 K. *Fluid Phase Equilibria*, 133, pp.213-27.

OShea, S.J. & Stokes, R.H., 1986. Activity coefficients and excess partial molar enthalpies for (ethanol + hexane) from 283 to 318 K. *The Journal of Chemical Thermodynamics*, 18, p.691.

Pan, H. & Firoozabadi, A., 1998. Complex Multiphase Equilibrium Calculations by Direct Minimization of Gibbs Free Energy Using Simulated Annealing. *SPE Reservoir Evaluation and Engineering*, pp.36-42.

Patel, N.C. & Teja, A.S., 1982. A new cubic equation of state for fluids and fluid mixtures. *Chemical Engineering Science*, 37, pp. 463-473.

Pemberton, R.C. & Mash, C.J., 1978. Thermodynamic properties of aqueous non-electrolyte mixtures II. Vapour pressures and excess Gibbs energies for water + ethanol at 303.15 to 363.15 K determined by an accurate static method. *The Journal of Chemical Thermodynamics*, 10, pp.867-88.

- Peng, D.Y. & Robinson, D.B., 1976. A New Two-constant Equation of State. *Industrial & Engineering Chemistry Fundamentals*, 15, pp.58-64.
- Prausnitz, J., Lichtenthaler, R. & Azevedo, E., 1999. *Molecular Thermodynamics of Fluid-Phase Equilibria*. Third Edition ed.
- Raal, J.D. & Muhlbauer, A.L., 1997. *Phase equilibria: measurement and computation*. Raylor & Francis.
- Rabinowitz, P., 1970. *Numerical Methods for Nonlinear Algebraic Equations*. Routledge. Ch 7.
- Reimers, J.L., Bhethanabotla, V.R. & Campbell, S.W., 1992. Total Pressure Measurements for n-Pentane - Methanol - Ethanol at 303.15 K. *Journal of Chemical and Engineering Data*, 37, p.127.
- Ronc, M. & Ratcliff, G.A., 1976. Measurement of vapor-liquid equilibria using a semi-continuous total pressure static equilibrium still. *The Canadian Journal of Chemical Engineering*, 54, p.326.
- Rushbrook, G.S., Stell, G. & Hoye, J.S., 1973. Theory of polar liquids I. Dipolar hard spheres. *Molecular Physics*, 26(5), pp.1199-215.
- Saager, B. & Fischer, J., 1992. Construction and application of physically based equations of state : Part II. The dipolar and quadrupolar contributions to the Helmholtz energy. *Fluid Phase Equilibria*, 72, p.67.
- Saager, B., Fischer, J. & Neumann, M., 1991. Reaction Field Simulations of Monatomic and Diatomic Dipolar Fluids. *Molecular Simulation*, 6(1-3), pp.27-49.
- Sandler, S.I., ed., 1994. *Modles for Thermodynamic and Phase Equilibria Calculations*. New York: Marcel Dekker.
- Sandler, S.I., Orbey, H. & Lee, B.-I., 1993. Equation of State. In S.I. Sandler, ed. *Models for Thermodynamic and Phase Equilibria Calculations*. New York: Marcel Dekker, Inc. pp.87-186.
- Sauer, S. & Chapman, W.G., 2003. A Parametric Study of Dipolar Chain Theory with Applications to Ketone Mixtures. *Industrial & Engineering Chemistry Research*, 42, pp.5687-96.
- Schmelzer, J., Lieberwirth, I., Krug, M. & Pfestorf, R., 1983. Vapour-liquid equilibria and heats of mixing in alkane-1-alcohol systems. I. Vapour-liquid equilibria in 1-alcohol-undecane systems. *Fluid Phase Equilibria*, 11, pp.187-200.
- Sengers, J.V., Kayser, R.F., Peters, C.J. & White, H.J., 2000. *Equations of State of Fluids and Fluid Mixtures*. Elsevier Science.

- Seo, J., Lee, J. & Kim, H., 2000. Isothermal vapor–liquid equilibria for ethanol and n-pentane system at the near critical region. *Fluid Phase Equilibria*, 172, pp.211-19.
- Shirono, K. & Daiguji, H., 2006. Dipole moments of water molecules confined in Na-LSX zeolites, Molecular dynamics simulations including polarization of water. *Chemical Physics Letters*, 417, pp.251-55.
- Singh, J. & Benson, G.C., 1968. Measurement of the vapor pressure of methanol-n-decanol and ethanol-n-decanol mixtures. *The Canadian Journal of Chemical Engineering*, 46, p.1249.
- Singh, J. & Benson, G.C., 1968. Vapor–liquid equilibrium studies of n-propanol–n-decanol mixtures. *The Canadian Journal of Chemical Engineering*, 46(12), pp.2065-69.
- Singh, J., Pflug, H.D. & Benson, G.C., 1969. Excess thermodynamic properties of isopropanol–n-decanol mixtures. *The Canadian Journal of Chemical Engineering*, 47(4), pp.543-46.
- Smith, B.D. & Srivastava, R., 1986. *Thermodynamic Data for Pure Compounds, Halogenated Hydrocarbons and Alcohols, Physical Science Data*. New York: Elsevier Science.
- Soares, M.E., Medina, A.G., McDermott, C. & Ashton, N., 1982. Three phase flash calculations using free energy minimisation. *Chemical Engineering Science*, 37(4), pp.521-28.
- Soave, G., 1972. Equilibrium Constants from a Modified Redlich-Kwong Equation of State. *Chemical Engineering Science*, 27, pp.1197-203.
- Song, W.X. & Larson, M.A., 1991. Phase equilibrium calculation by using large-scale optimization technique. *Chemical Engineering Science*, 46(10), pp.2513-23.
- Squire, W. & Trapp, G., 1998. Using Complex Variables to Estimate Derivatives of Real Functions. *SIAM Review*, 40(1), pp.110-12.
- Tai, T.B., Ramalho, R.S. & Kaliaguine, S., 1972. Application of wilson's equation to determination of vapor-liquid equilibrium data and heats of mixing for non-ideal solutions. *The Canadian Journal of Chemical Engineering*, 50, p.771.
- Tamouza, S., Passarello, J., Tobaly, P. & de Hemptinne, J., 2005. Application to binary mixtures of a group contribution SAFT EOS (GC-SAFT). *Fluid Phase Equilibria*, 228-229, pp.409-19.
- Teh, Y.S. & Rangaiah, G.P., 2002. A study of equation-solving and gibbs free energy minimization methods for phase equilibrium calculations. *Trans IChemE*, 80(October Part I), pp.745-59.
- Treble, M.A. & Bishnoi, P.R., 1988. Extension of the Treble-Bishnoi Equation of State to fluid Mixtures. *Fluid Phase Equilibria*, 40, pp.1-21.

Tumakaka, F. & Sadowski, G., 2004. Application of the Perturbed-Chain SAFT equation of state to polar systems. *Fluid Phase Equilibria*, 217, p.233.

Twu, C.H. & Gubbins, K.E., 1978b. Thermodynamics of polyatomic fluid mixtures—II : Polar, quadrupolar and octopolar molecules. *Chemical Engineering Science*, 33, pp.879-87.

Van Ness, H.C. & Abbott, M.M., 1997. *International DATA Series, Selected Data on Mixtures, Series A*, 1, p.1.

Van Ness, H.C., Soczek, C.A., Peloquin, G.L. & Machado, R.L., 1967. Thermodynamic excess properties of three alcohol-hydrocarbon systems. *Journal of Chemical and Engineering Data*, 12, pp.217-24.

Van Ness, H.C., Soczek, C.A., Peloquin, G.L. & Machado, R.L., 1967. Thermodynamic excess properties of three alcohol-hydrocarbon systems. *Journal of Chemical and Engineering Data*, 12(2), pp.217-24.

Vega, L.F., Llovel, F. & Blas, F.J., 2009. Capturing the Solubility Minima of n-Alkanes in Water by Soft-SAFT. *The Journal of Physical Chemistry B*, 113, p.7621–7630.

Venkatasubramanian, V., Gubbins, K.E., Gray, C.G. & Joslin, C.G., 1984. Induction effects in polar-polarizable liquid mixtures. 52(6), pp.1411-29.

Vimalchand, P., Donohue, M.D. & Celmins, I., 1985. Thermodynamics of multipolar molecules , The perturbed-Anisotropic-Chain theory. In K.C. Chao & R.L. Robinson, eds. *Equations of state*. American Chemical Society. pp.297-313.

Voutsas, E.C., Boulougouris, G.C., Economou, I.G. & Tassios, D.P., 2000. Water/hydrocarbon phase equilibria using the thermodynamic perturbation theory. *Industrial & Engineering Chemistry Research*, 39, pp.797-804.

Wanger, W. & Prub, A., 2002. The IAPWS Formulation 1995 for the Thermodynamic Properties of Ordinary Water Substance for General and Scientific Use. *Journal of Physical and Chemical Reference Data*, 31, p.387.

Weeks, J.D., Chandler, D. & Andersen, H.C., 1971. Role of Repulsive Forces in Determining the Equilibrium Structure of Simple Liquids. *THE JOURNAL OF CHEMICAL PHYSICS*, 54(12), pp.5237-47.

Wertheim, M.S., 1984a. Fluids with Highly Directional Attractive Forces. I. Statistical Thermodynamics. *Journal of statistical physics*, 35, p.19.

Wertheim, M.S., 1984b. Fluids with Highly Directional Attractive Forces. II. Thermodynamic Perturbation Theory and Integral Equations. *journal of statistical physics*, 35, p.35.

- Wertheim, M.S., 1986a. Fluids with Highly Directional Attractive Forces. III. Multiple Attraction Sites. *journal of statistical physics*, 42, p.459.
- Wertheim, M.S., 1986b. Fluids with Highly Directional Attractive Forces. IV. Equilibrium Polymerization. *journal of statistical physics*, 42, p.477.
- Wieczorek, S.A. & Stecki, J., 1978. Vapour pressures and thermodynamic properties of hexan-1-ol + n-hexane between 298.230 and 342.824 K. *The Journal of Chemical Thermodynamics*, 10, pp.177-86.
- Wilsak, R.A., Campbell, S.W. & Thodos, G., 1987. Vapor-Liquid Equilibria Measurements for the n-Pentane-Methanol System at 372.7, 397.7 and 422.6 K. *Fluid Phase Equilibria*, 33, p.157.
- Winkelmann, J., 1981. Perturbation theory of dipolar hard spheres: the vapour-liquid equilibrium of strongly polar substances. *Fluid Phase Equilibria*, 7, pp.207-17.
- Wolff, H. & Goetz, R., 1976. The association of various deuterated ethanols in n-hexane (using vapour pressure measurements). *Z. Physical Chemistry (Zeitschrift fur Physikalische Chemie)*, 100, p.25.
- Wolff, H. & Hoeppe, H.E., 1968. Determination of hydrogen bond association of methanol in n-hexane by vapour pressure measurements. *Berichte Der Bunsen-Gesellschaft Physical Chemistry*, 72, p.710.
- Wu, J.S. & Bishnoi, P.R., 1986. An algorithm for three-phase equilibrium calculations. *Computers and Chemical Engineering*, 10(3), pp.269-76.
- Xu, G., Brennecke, J.F. & Stadtherr, M.A., 2002. Reliable Computation of Phase Stability and Equilibrium from the SAFT Equation of State. *Industrial and Engineering Chemistry Research*, 41, pp.938-52.
- Yarrison, M. & Chapman, W.G., 2004. A systematic study of methanol + n-alkane vapor-liquid and liquid-liquid equilibria using the CK-SAFT and PC-SAFT equations of state. *Fluid Phase Equilibria*, 226, pp.195-205.
- Yaws, C.L., 2003. *Handbook of thermodynamics and physical properties of chemical compounds*. Knovel.
- Yuan-H, F. & Sandler, S.I., 1995. A Simplified SAFT Equation of State for Associating Compounds and Mixtures. *Industrial and Engineering Chemistry Research*, 34(5), pp.1897-909.
- Zielkiewicz, J., 1991. (Vapour + liquid) equilibria in (propan-1-ol + n-hexane + n-heptane) at the temperature 313.15 K. *The Journal of Chemical Thermodynamics*, 23, pp.605-12.
- Zielkiewicz, J., 1992. (Vapour + liquid) equilibria in (propan-1-ol + heptane + octane) at the temperature 313.15 K. *The Journal of Chemical Thermodynamics*, 24, p.455.

Zielkiewicz, J., 1993. (Vapor + liquid) equilibria in (heptane + ethanol + propan-1-ol) at the temperature 313.15 K. *The Journal of Chemical Thermodynamics*, 25, pp.1077-82.

Zielkiewicz, J., 1994. (Vapor + liquid) equilibria in (heptane + propan-2-ol or butan-1-ol or 2-methylpropan-1-ol or 2-methylpropan-2-ol or pentan-1-ol) at the temperature 313.15 K. *The Journal of Chemical Thermodynamics*, 26, pp.919-23.

Zwanzig, R.W., 1954. High-Temperature Equation of State by a Perturbation Method. I. Nonpolar Gases. *THE JOURNAL OF CHEMICAL PHYSICS*, 22(8), pp.1420-26.

## APPENDIX A

### ADJUSTABLE PARAMETERS OF PC-SAFT

The adjustable parameters of PC-SAFT are given in Table A.1. For water and ethylene glycol, the adjustable parameters were given in **Chapter 3**.

Table A.1 PC-SAFT Parameters.

Compound	M	m	$\sigma$	$\varepsilon/\kappa$	$k^{AB}$	$\varepsilon^{AB}/\kappa$	Q	$\mu$	Reference
	[g/mol]		[Å]	[K]		[K]	[DA]	[D]	
methane	16.043	1.000	3.704	150.030					(Gross & Sadowski, 2002)
propane	44.096	2.002	3.618	208.110					(Gross & Sadowski, 2002)
butane	58.123	2.332	3.709	222.880					(Gross & Sadowski, 2002)
pentane	72.146	2.690	3.773	231.200					(Gross & Sadowski, 2002)
hexane	86.177	3.058	3.798	236.770					(Gross & Sadowski, 2002)
octane	114.231	3.818	3.837	242.780					(Gross & Sadowski, 2002)
carbon dioxide	44.010	1.513	3.187	163.330			4.4		(Gross, 2005)
water	18.015	1.226	2.792	203.000	0.072	2406.700		1.85	
ethylene glycol	62.068	3.404	2.844	178.370	0.135	2152.400		1.7	

## APPENDIX B

### PHASE EQUILIBRIUM CALCULATIONS

To perform phase equilibrium calculations, the fugacity coefficient is obtained from (Prausnitz et al., 1999):

$$\ln \varphi_k = \frac{\mu_k^{res}(T, v)}{kT} - \ln Z$$

B-1

and

$$\frac{\mu_k^{res}(T, v)}{kT} = a^{res} + (Z - 1) + \left( \frac{\partial a^{res}}{\partial x_k} \right)_{T, v, x_{i \neq k}} - \sum_{j=1}^N \left[ x_j \left( \frac{\partial a^{res}}{\partial x_j} \right)_{T, v, x_{i \neq j}} \right]$$

B-2

The compressibility factor ( $Z$ ) is obtained by differentiating the Helmholtz free energy with respect to density:

$$Z = 1 + \rho \left( \frac{\partial a^{res}}{\partial \rho} \right)_{T, N}$$

B-3

As seen from the above equations, it is necessary to differentiate the residual Helmholtz energy with respect to mole fraction and density to conduct phase equilibrium calculations.